MASSACHUSETTS INSTITUTE OF TECHNOLOGY

LINCOLN LABORATORY

MILLSTONE HILL THOMSON SCATTER RESULTS FOR 1968

J. V. EVANS

Group 21

TECHNICAL REPORT 499

23 JANUARY 1973

LEXINGTON MASSACHUSETTS

The work reported in this document was performed at Lincoln Laboratory, a center for research operated by Massachusetts Institute of Technology. The work is sponsored by the Office of the Chief of Research and Development, Department of the Army; it is supported by the Advanced Ballistic Missile Defense Agency under Air Force Contract F19628-73-C-0002.

ABSTRACT

This report summarizes the results for the electron density distribution, electron and ion temperatures in the F-region obtained during 1968 using the Millstone Hill (42.6°N, 71.5°W) Thomson (incoherent) scatter radar system. These data, for the height interval approximately 200 to 800 km, were gathered over 24-hour observing periods, roughly twice per calendar month. The time required to obtain a complete electron density and temperature profile over this height interval was usually 30 minutes.

During 1968 the apparatus employed to measure the frequency spectrum of the reflected signals vs altitude, which in turn yields the estimates of the electron and ion temperatures, was rebuilt permitting the measurements at all altitudes to be made in real time, and with greater accuracy than heretofore. In addition, the new spectrum analyzer permitted the first measurements at Millstone Hill of the vertical drift of the plasma. These results, which are difficult to condense into summary form, are not included in the report.

The density and temperature results show that the separate clear patterns of summer and winter diurnal behavior, recognized at sunspot minimum, can still be discerned at sunspot maximum on all but very disturbed days. A number of disturbance patterns observed previously were again detected in 1968, albeit on fewer occasions than in 1967. Apparently, by chance, the days selected for observation in 1968 contained fewer instances of magnetic disturbance than in 1967.

The average heat flux from the magnetosphere has been investigated. While there appears to be a clear dependence on solar flux (as defined by the 10.7-cm radio emission), there remains a summer-to-winter variation of 5 to 7 that cannot be easily explained.

Accepted for the Air Force
Joseph J. Whelan, USAF
Acting Chief, Lincoln Laboratory Liaison Office

CONTENTS

MILLSTONE HILL THOMSON SCATTER RESULTS FOR 1968

I. INTRODUCTION

Thomson (incoherent) scatter radar measurements of F-region electron densities and temperatures were made at Millstone Hill, Westford, Massachusetts (42.6°N, 71.5°W), approximately twice per month throughout 1968 for periods usually of 24 hours. This report summarizes the results obtained and discusses them in relation to the behavior observed in previous years (Table I). Earlier reports in this series[1-5] present the results of synoptic studies carried out in the years 1963 through 1967. Results obtained during some of the months in these years are discussed in greater detail in a number of journal articles as referenced in Table I.

TABLE I

PUBLICATIONS CONCERNING THE MILLSTONE HILL UHF (68-cm Wavelength) THOMSON SCATTER RESULTS

Year	Months Covered	Publication
1963	February 1963 to January 1964	Ref. 1
	March, July, August, September	Ref. 6
	April, July, November	Ref. 7
1964	January through December	Ref. 2
	April, July, November	Ref. 8
1965	January through December	Ref. 3
	June, August, September	Ref. 9
	June	Ref. 10
	January, April, July	Ref. 11
1966	January through December	Ref. 4
	January, March, July, September	Ref. 12
1967	January through December	Ref. 5
	February, June, October, December	Ref. 12

In addition to the measurements reported here of F-region observations made with the vertically directed UHF radar system, a number of measurements were conducted in 1968 of the E, F1, and F2 regions employing the L-band radar with beam directed obliquely. These measurements were aimed at determining the ion composition in the F1 region[13,14] and the horizontal drift in the E and F regions.[15] In as much as these results have already been reported, they are not included in this paper.

Section II provides a summary of the equipment, observing and data-processing procedures employed during 1968. These were changed during the middle of the year to yield more reliable results and eliminate the need for non-real-time processing of magnetic tape records of the IF signals. Section III presents the results for electron density, electron and ion temperatures and Section IV provides a summary.

II. EQUIPMENT, OBSERVING AND DATA PROCESSING PROCEDURES

A. Equipment

The UHF incoherent scatter radar equipment has been described previously.[1] During 1968 the spectrum analyzer portion of the receiver was replaced by one of newer design that was interfaced directly into the SDS 9300 computer. These changes are fully documented in Ref. 16 but will be summarized briefly here.

In the earliest observations conducted at Millstone Hill[1,2], the spectrum of the signals from a given height was determined by gating a portion of the IF signals, in length equal to the transmitter pulse, into a bank of twenty-four narrowband crystal filters. The filter outputs were rectified and the voltages integrated using analog RC integrators. To calibrate the analyzer, a second gate applied a sample of noise, selected from near the end of the timebase, to the filters, and the rectified noise voltages were stored in a second set of integrators. This scheme suffered because of gain differences and drifts in the integrators, and because it required about an hour to explore the signals returned from all heights. Also, with the limited number of integrators available, it was possible to explore readily only one half of the signal spectrum, thereby precluding the possibility of measuring ionospheric drifts.

In 1965 a magnetic tape recording system was constructed[3] that permitted the signals to be recorded for later non-real-time processing. This arrangement reduced the time required to complete a series of measurements to 30 minutes (at the expense of many hours of later post-processing of the tape records). In addition to this change, the spectrum analyzer was rebuilt to distribute 48 filters across the entire spectrum. To cope with this increase, it was arranged that the integrators would store only the difference between the signal and noise voltage samples. This change eliminated problems introduced by differences in the gains of the integrators that hitherto stored the signal and the noise samples. Unfortunately, though not recognized at the time, the spectrum one obtains by integrating the difference between the signal and the noise samples depends upon the predector signal-to-noise ratio.[3] As a result, the interpretation of the spectra became uncertain.

The problems inherent with the tape recorder and analyzer employed from mid-1965 were soon recognized, and beginning in 1966 efforts made to improve the system. One ambitious approach that was attempted but was abandoned as being too costly and requiring too much development would have provided complete computer-processing through the use of a number of parallel multiplier units.[16] Finally, in 1967, construction began of a new spectrum analyzer that obviated most of the difficulties of the earlier one. This was placed in operation in July 1968 (Ref. 16).

In the new spectrum analyzer, the integration of the echoes is carried out digitally by the SDS 9300 computer, thereby eliminating all problems due to gain differences and drift. In addition, the signals are no longer gated from the time base, but instead are continuously applied to a bank of 5-pole crystal filters each of which is matched to the length of the pulse employed (0.5 or 1.0 msec).

Each of the (two) filter banks available employs 24 filters spanning ±11.5 kHz about the radar frequency with 1 kHz spacing. The voltages at the filter outputs are sampled at 0.5-msec intervals so that a spectrum may be obtained every 75 km of altitude. Since the filters must be sampled sequentially (at intervals of 20 μsec), a tapped delay-line is used to drive the filters in a manner that provides exact compensation for the delays between samples. Thus, although it takes 480 μsec to scan through all filters, the outputs correspond to the same real altitude.

B. Observing Procedure

During 1968 we attempted to make observations twice per month for a period of 24 hours. Table II lists the dates and times for which measurements were successfully carried out and reduced. Included in Table II is the mean of the planetary magnetic index K_p over each period of observation.

As noted above, the observing procedures were changed in 1965 to reduce the amount of time required to obtain a complete electron density and temperature profile from 1 hour to 30 minutes. This was accomplished by recording the IF signals for later non-real-time processing. The recording and playback system, discussed extensively in Ref. 3, was employed until the end of June 1968.

In addition to this change, the spectrum analyzer was modified in June 1965 to permit both halves of the signal spectrum to be explored. As already noted, this was carried out in a way which, though not recognized at the time, caused some loss of information. As a result, the values obtained for ion temperature between January and June 1968 are unreliable between about 300 and 500 km and, therefore, are not included in this report. These changes and means of minimizing the unwanted effects they introduced in the results are discussed in Ref. 3 and will not be repeated here.

Beginning in July 1968, the new spectrum analyzer was placed in operation. Several of the first 24-hour runs made with this device could not be analyzed owing to a programming error which caused the results to be incompletely recorded. Other day's data were later lost when it proved impossible to read the data tapes owing to the presence of either "write-" or "read-errors." Thus, Table II lists only days for which results were secured.

Following the introduction of the new spectrum analyzer, special efforts were made to detect the vertical drift of the ionization above $h_{max}F2$ (Ref. 17). For this reason, some observations were conducted in which the measurements made using the 1-msec pulses ("C mode") were repeated four times in each cycle.[16,17] This raised the time to complete a cycle of measurement to 45 minutes.

In the normal operating mode, measurements were made using 0.1-, 0.5-, and 1.0-msec pulses in sequence; the complete cycle occupying 30 minutes. These runs are termed "regular" in Table II to distinguish them from those emphasizing the determination of "drift." Usually 24 hours of each type of measurement were carried out in each calendar month.

The value of N_{max} to be employed in the data-reduction was made available in the form of a measurement of the F-region critical frequency f_oF2 in MHz at the start of each cycle.* This measurement was made by the radar operator, who then typed the value into the computer which stored it along with all the other information on magnetic tape. To make the measurement, the C-4 ionosonde was modified to permit it to be turned on and monitored remotely, as well as have its frequency controlled by a remote frequency synthesizer. Thus, the operator would turn on the sounder and advance the frequency of the synthesizer until the F2 ordinary return was just perceived at great range. The synthesizer dials then gave the required value of f_oF2.

This procedure was intended to eliminate instances where incoherent scatter data were gathered, but could not be reduced owing to lack of ionosonde measurements.

---

* $N_{max} = 1.24 \times 10^4 (f_oF2)^2$ el/cm^3 when f_oF2 is expressed in MHz.

TABLE II

INCOHERENT SCATTER OBSERVATIONS – 1968

Begin			End			Mean K_p	Obs†	Comments
Date	C*	EST	Date	C*	EST			
16 January		1030	17 January		1030	3+	A	Disturbed
23 January		1130	24 January		1100	2+	A	
13 February		1630	14 February	Q	1600	1+	A	Quiet
27 February	q	1130	28 February	D	1200	3_o	A	Disturbed
26 March		1200	27 March		1200	3–	A	Disturbed
16 April		1000	17 April		1130	2_o	A	
25 April	q	1300	26 April	Q	1300	1+	A	Quiet
23 May	q	0730	24 May	Q	0700	1–	A	Quiet
20 June		1200	21 June	Q	1200	1+	A	Quiet
18 July		1630	19 July		0800	2–	Reg	
15 August	D	1000	16 August	D	0900	4–	Reg	Disturbed
27 August	q	0830	28 August	Q	0830	1_o	Drift‡	Quiet
29 August	Q	0800	30 August	Q	0800	1–	Drift	Disturbed
3 September		1200	4 September		1200	3+	Drift‡	Disturbed
11 September		1300	12 September		1300	1+	Drift‡	Quiet
12 September		1500	13 September		1500	4_o	Reg	Disturbed
26 September		0900	27 September		0900	1_o	Drift‡	Quiet
3 October		1530	4 October		1730	1_o	Reg	Quiet
8 October		1100	9 October		1300	2–	Drift‡	
22 October		0800	23 October		0800	0+	Reg	Quiet
29 October		1000	30 October		1000	4–	Drift‡	Disturbed
14 November	Q	1630	15 November	Q	1030	1+	Reg	
19 November	Q	1200	19 November	Q	1800	1–	Drift	Quiet
25 November		1000	26 November		1000	2_o	Reg	
29 November	Q	0900	30 November	Q	0900	1–	Drift	Quiet
12 December		1200	13 December	q	1300	1_o	Drift‡	Quiet
17 December	Q	0900	18 December		0900	1_o	Reg	Quiet
30 December		1000	31 December		1030	2_o	Reg	

* Condition:

Q One of five quietest days in month

q One of ten quietest days in month

D One of five most disturbed days in month

† Observations:

A – Data gathered and analyzed as described in Lincoln Laboratory Report TR-474.

Reg } Data gathered and analyzed as described in Lincoln Laboratory Report TR-477.
Drift } Reg = Regular; Drift = Drift Measurement.

‡ These data have been independently reduced and published by Carpenter and Bowhill.[18]

C. Data Reduction

The measurements made prior to July 1968 were reduced in the manner described in Ref. 3 with the exception that computer-drawn "power" profiles were produced[5] in place of those previously obtained by a graphical overlay method. It was, however, still necessary to correct these profiles for the altitude variation of the scattering cross section of the electrons introduced by changes in the electron-to-ion temperature ratio T_e/T_i with height. This correction was performed by hand.[5]

Beginning in July 1968, the results were gathered in a manner that placed together all the quantities of interest on a single data tape so that complete machine reduction became possible. The computer programs employed are described in Ref. 16. Basically, the electron density profiles were obtained in a way that, (1) combined measurements made with the three pulse lengths, (2) removed spurious echoes due to satellites, (3) adjusted the absolute value to yield the correct value of $N_{max}F2$ as measured on the ionosonde, and (4) removed the dependence on altitude variations of T_e/T_i, and (5) on Debye length. This profile was available as a graph plotted by a Calcomp plotter (e.g., Fig. 1), and on a print-out as $\log_{10}N_e$ vs altitude.[16] Estimates of T_e and T_i were also provided on plots and on the print-out. The values of T_e were corrected for the effects of the changing Debye length with altitude.[16] (Previously this correction had also been made by hand.) Figure 1 shows results for one complete cycle. Table III contrasts the manner in which the measurements were made and reduced in each year since 1963.

For seven of the "drifts" observations (indicated by the daggers in Table II), the data have been independently reduced at the University of Illinois by Carpenter and Bowhill[18] in a manner similar to that employed for the earlier results, i.e., using graphical methods and hand calculations. We have compared these reductions with those obtained at Millstone and found generally good agreement. The Millstone reductions are presented in the report in order to preserve consistency.

TABLE III

OBSERVING PROGRAM AS A FUNCTION OF YEAR

Year	Length of Each Observing Period (hours)	Number of Observing Periods Per Month	Time Taken to Measure One Profile (hours)	Number of Profiles Obtained Per Month	Reduction Method Employed
1963	30	4	1.5	80	Mean hourly profiles constructed for each calendar month (Ref. 1).
1964	30	2	1.0	60	As in 1963
1965	48	1	0.5	96	As in 1963
1966	24	2	0.5	96	Each profile analyzed separately (Ref. 3).
1967	24	2	0.5	96	As in 1966
1968	24	2	0.5 or 0.75	96 or 64	As in 1965 until July when complete machine reduction began (Ref. 16).

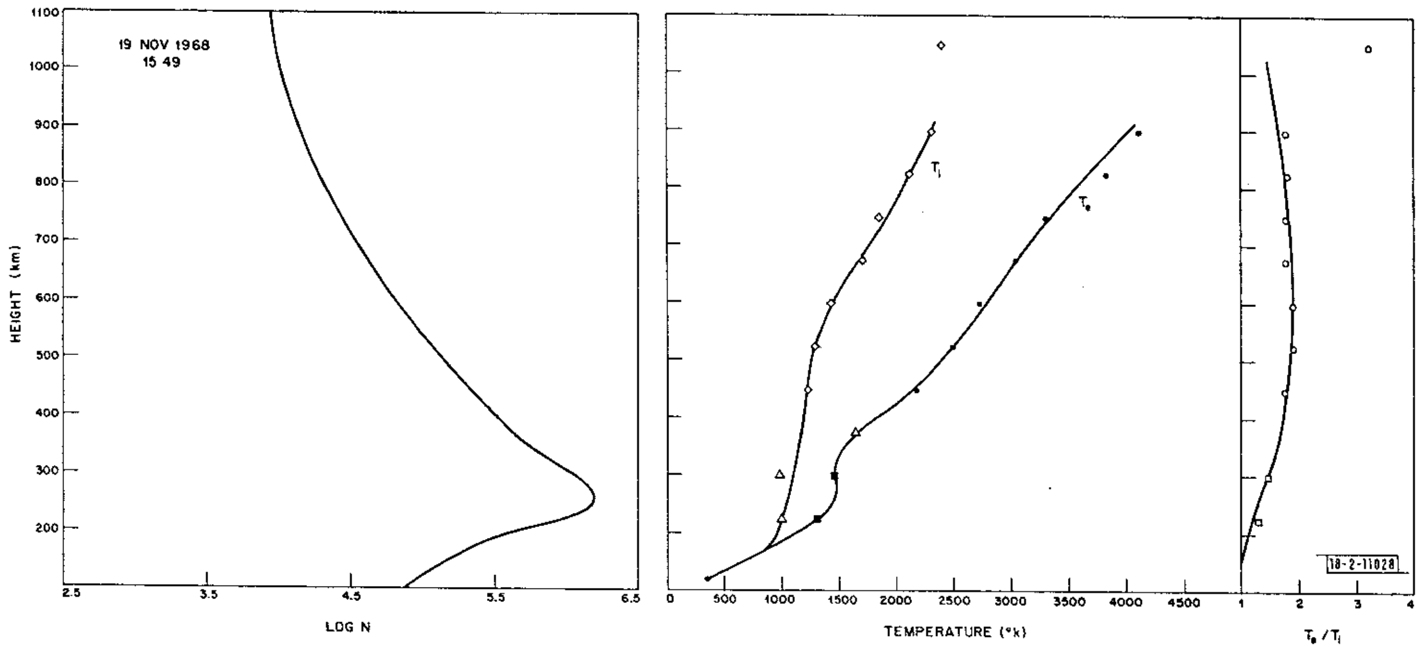

Fig. 1. Computer-drawn plot of the electron density (continuous curve), electron and ion temperatures and their ratios (points) as a function of height for measurements made over a 30 minute interval commencing at 1549 GMT (1049 EST) on 19 November 1968. Also shown are the hand-drawn curves adopted in analyzing these data.

The measurement of the vertical drift velocity[16,17] that became possible with the introduction of the new frequency synthesizer has posed some problems of data presentation that have not been resolved adequately at this time. Owing to the large variability in the sign and magnitude of the drift velocity as functions of height and time, as well as the large experimental uncertainty in the measurements (especially at high altitudes[17]), no simple means of data presentation has yet been devised comparable to the contour diagrams that have routinely been used to present N_e, T_e, and T_i as functions of height and time. Accordingly, these results are not presented here, but will be made available in tabular form to interested users on request.

III. RESULTS

A. Electron Density

Contours of electron density (expressed as plasma frequency in 0.5-MHz intervals) obtained during the period January-June 1968 are presented in Figs. 2(a) through (i), while those obtained in the balance of the year are presented as Figs. 3(a) through (s). In Fig. 3, the contours are labeled by the corresponding value of $\log_{10}N_e$, and are in steps of 0.2.

We have discussed in previous reports[2-5] the principal types of diurnal behavior observed at Millstone. Quiet days exhibit a characteristic "winter" or "summer" variation. There is a fairly abrupt transition between the two in the equinoxes. For the results presented here, the "winter" pattern prevails up to 16-17 April [Fig. 2(f)] and after 3-4 October [Fig. 3(i)].

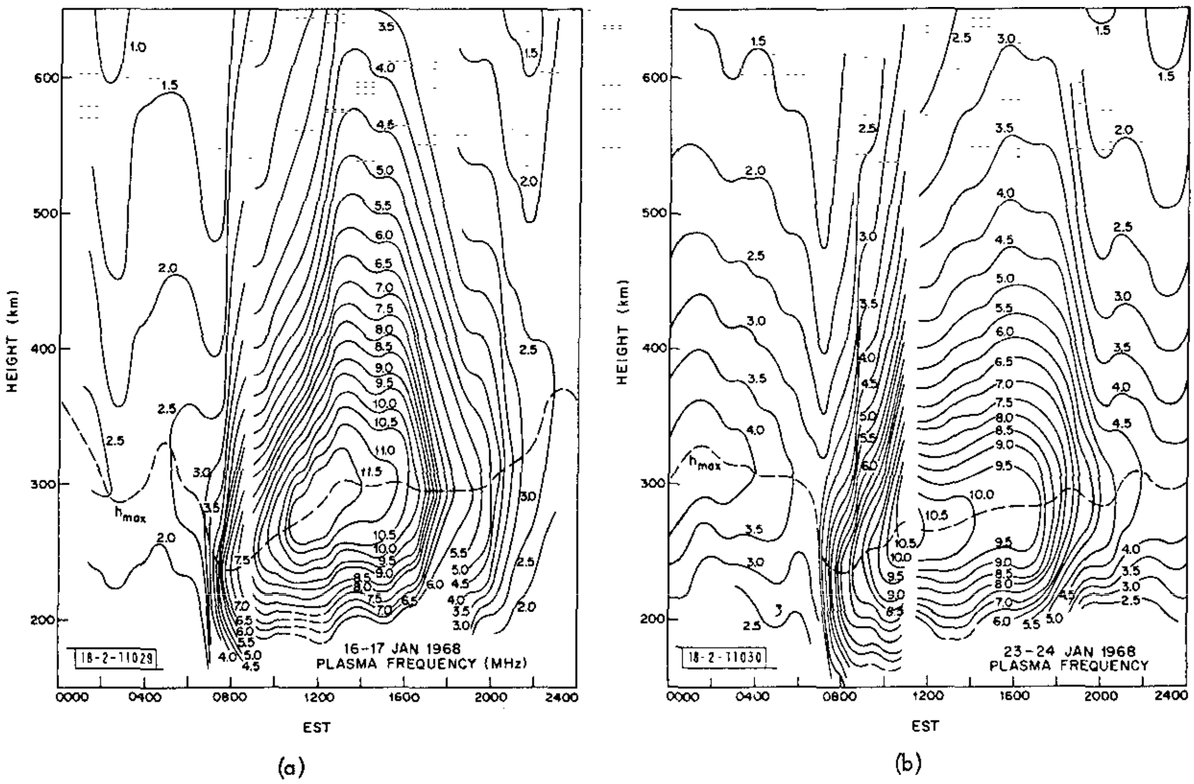

Fig. 2(a-i). Contour diagrams of constant plasma frequency (in 0.5 MHz steps) as functions of height and time gathered during the first six months of 1968.

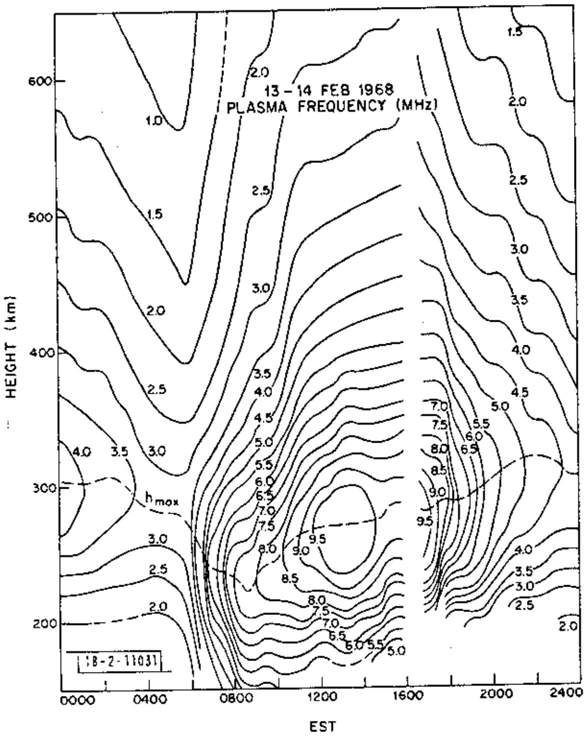

(c)

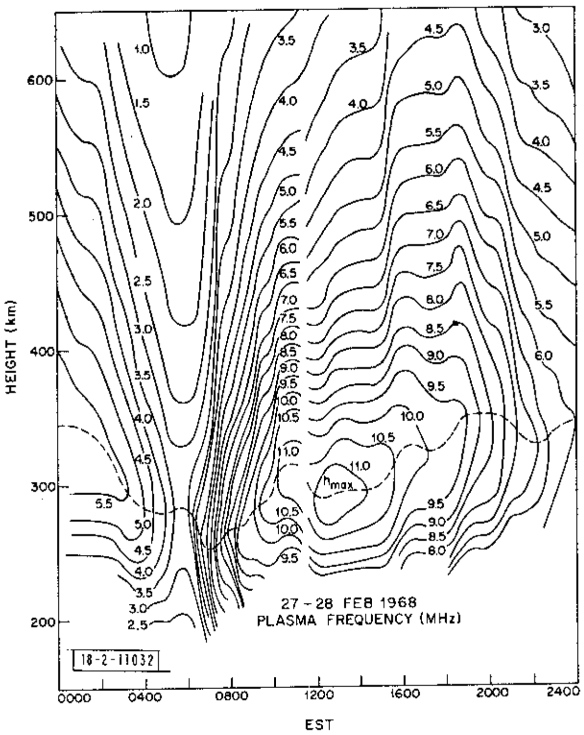

(d)

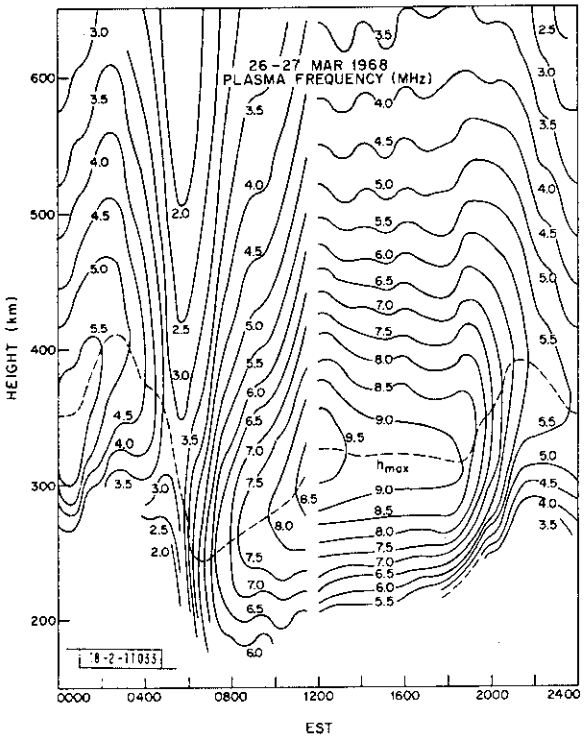

(e)

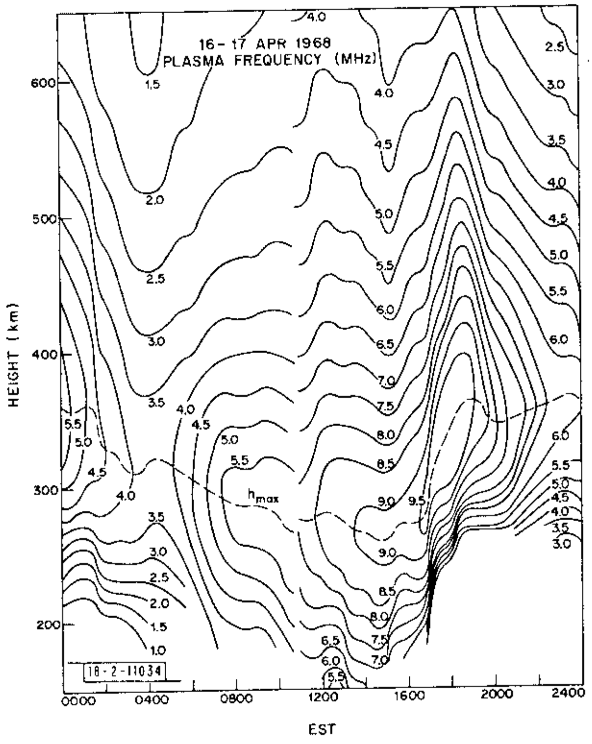

(f)

Fig. 2(a–i). Continued.

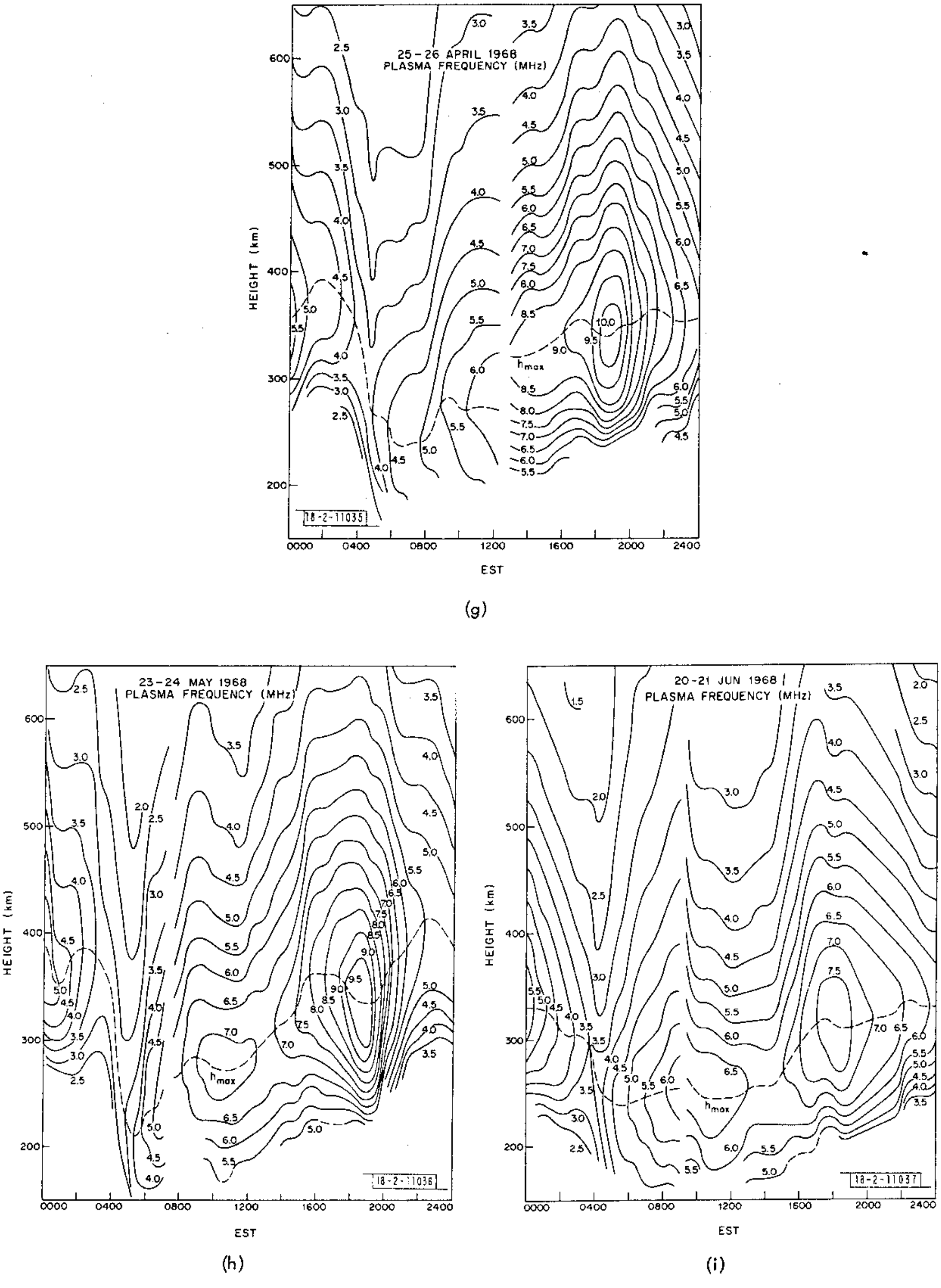

Fig. 2(a–i). Continued.

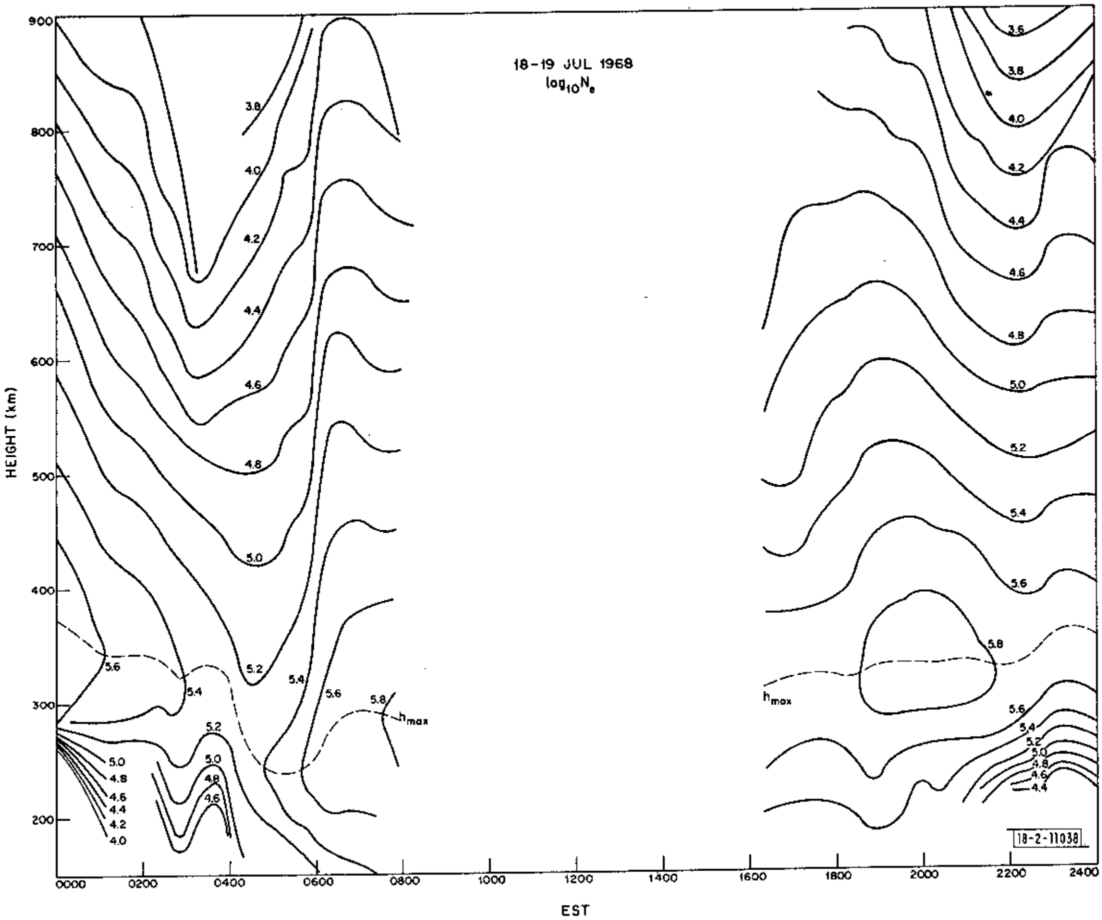

(a)

Fig. 3(a-s). Contour diagrams of constant $\log_{10}$ electron density (in $\log_{10}N_e = 0.2$ steps) as functions of height and time gathered during the last six months of 1968.

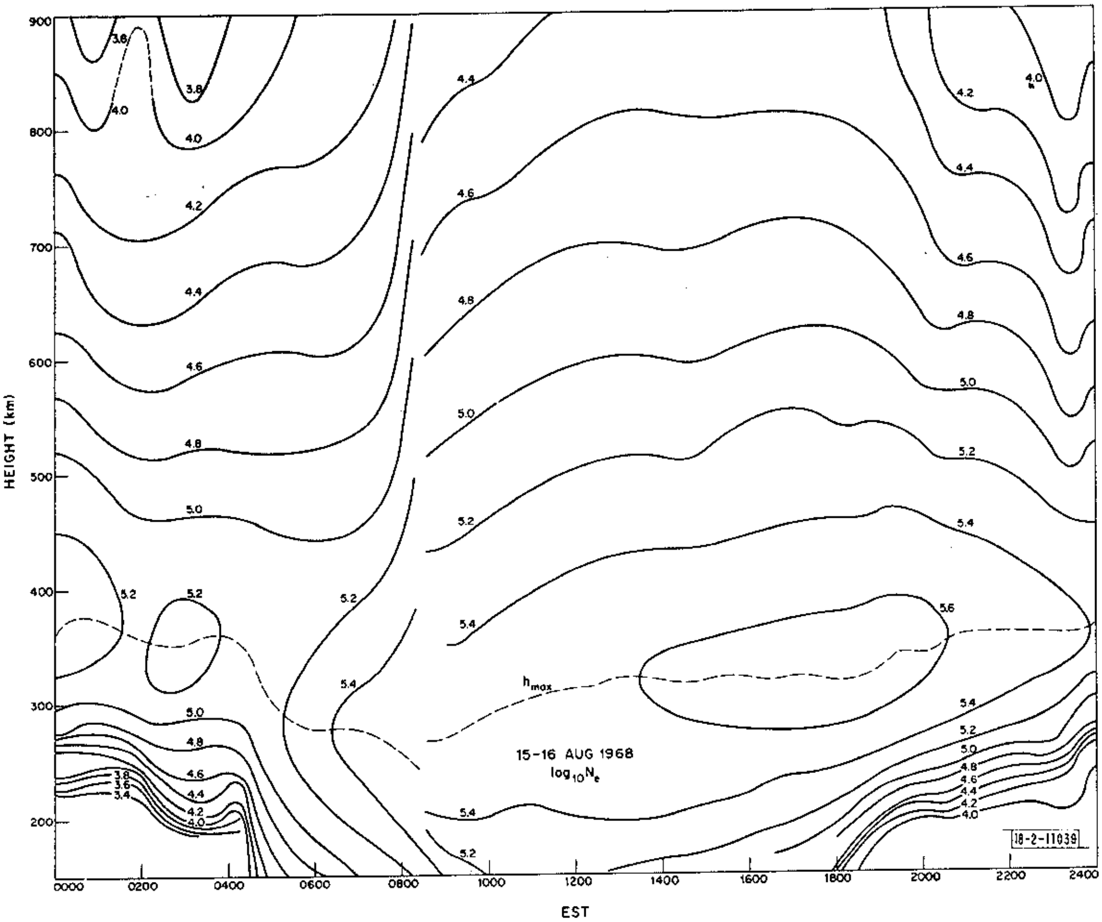

(b)

Fig. 3(a-s). Continued.

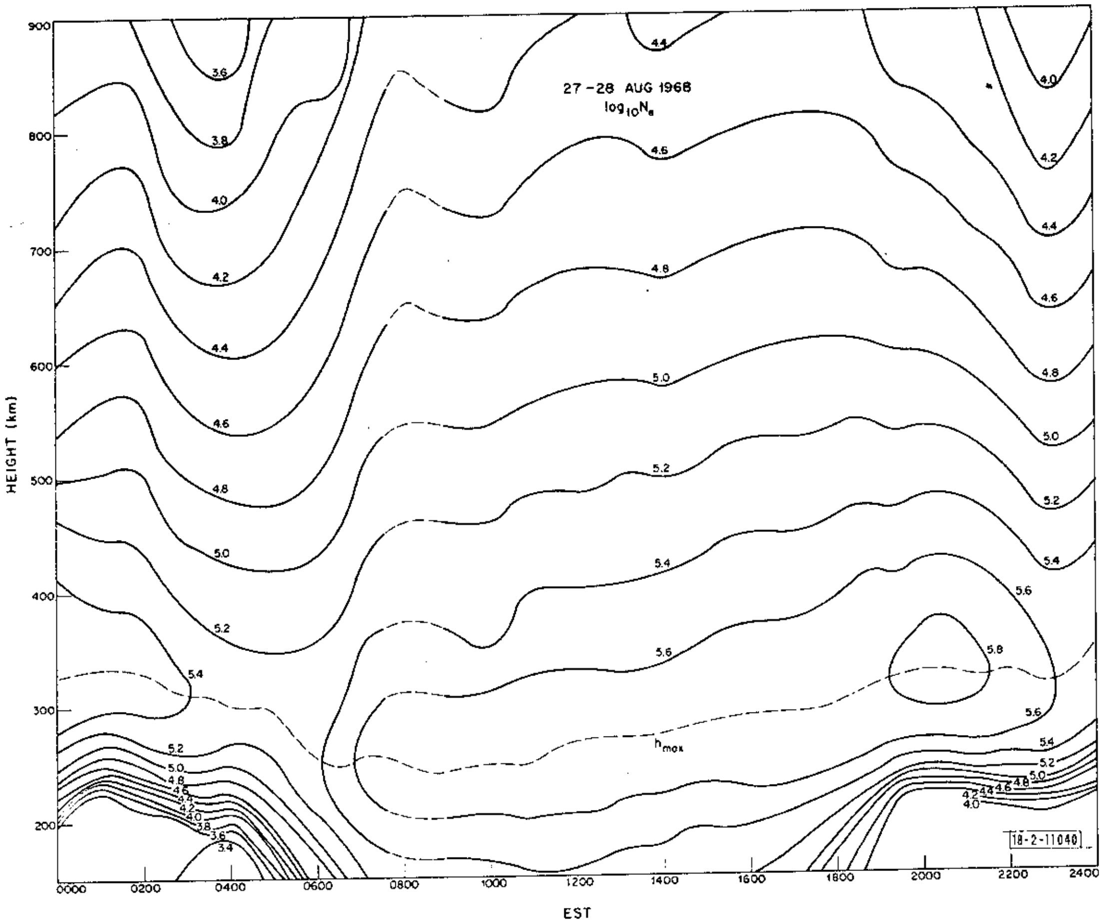

(c)

Fig. 3(a–s). Continued.

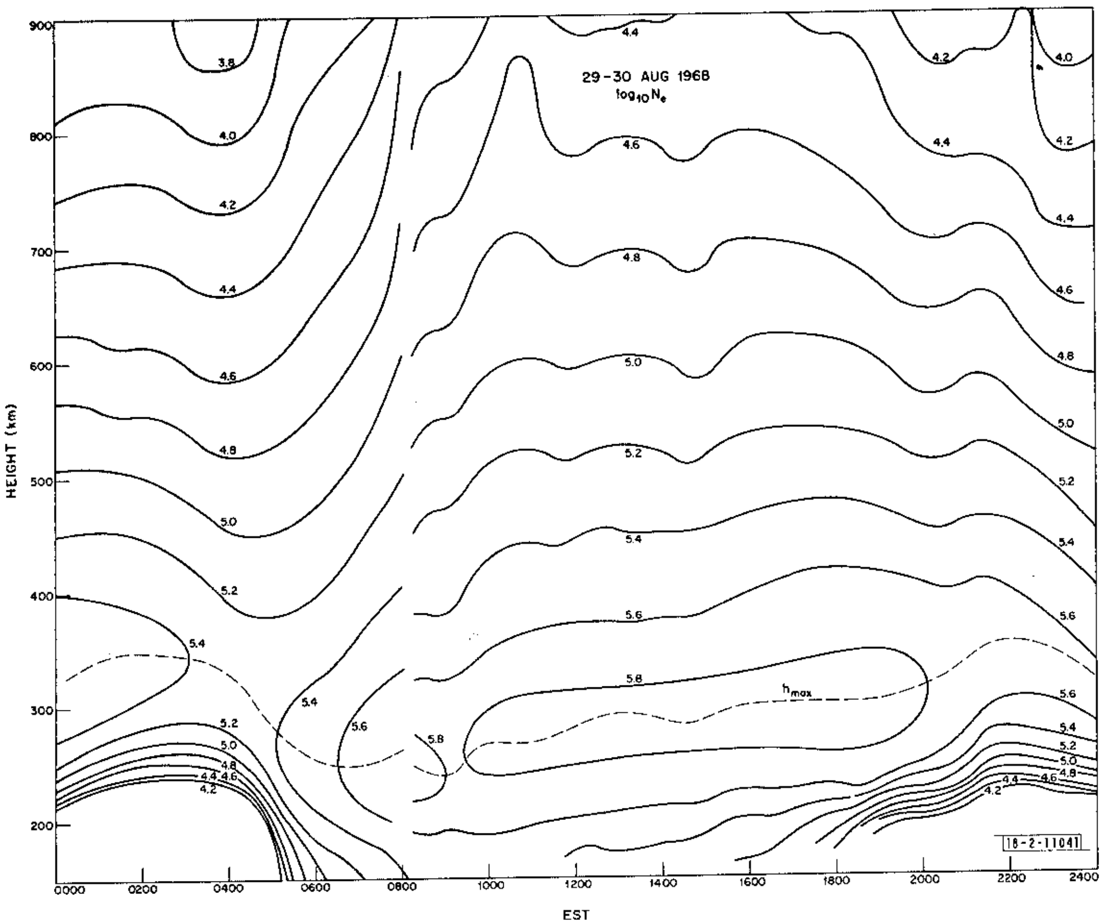

(d)

Fig. 3(a-s). Continued.

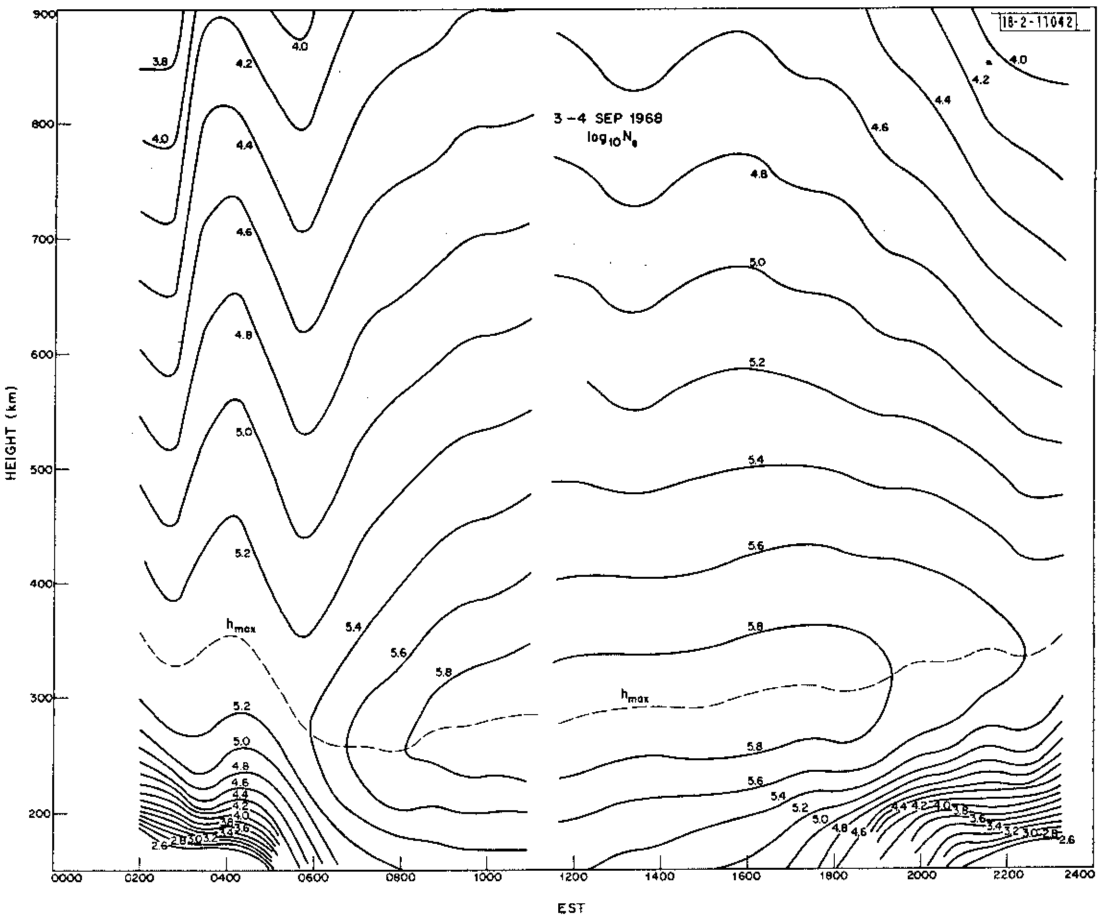

(e)

Fig. 3(a–s). Continued.

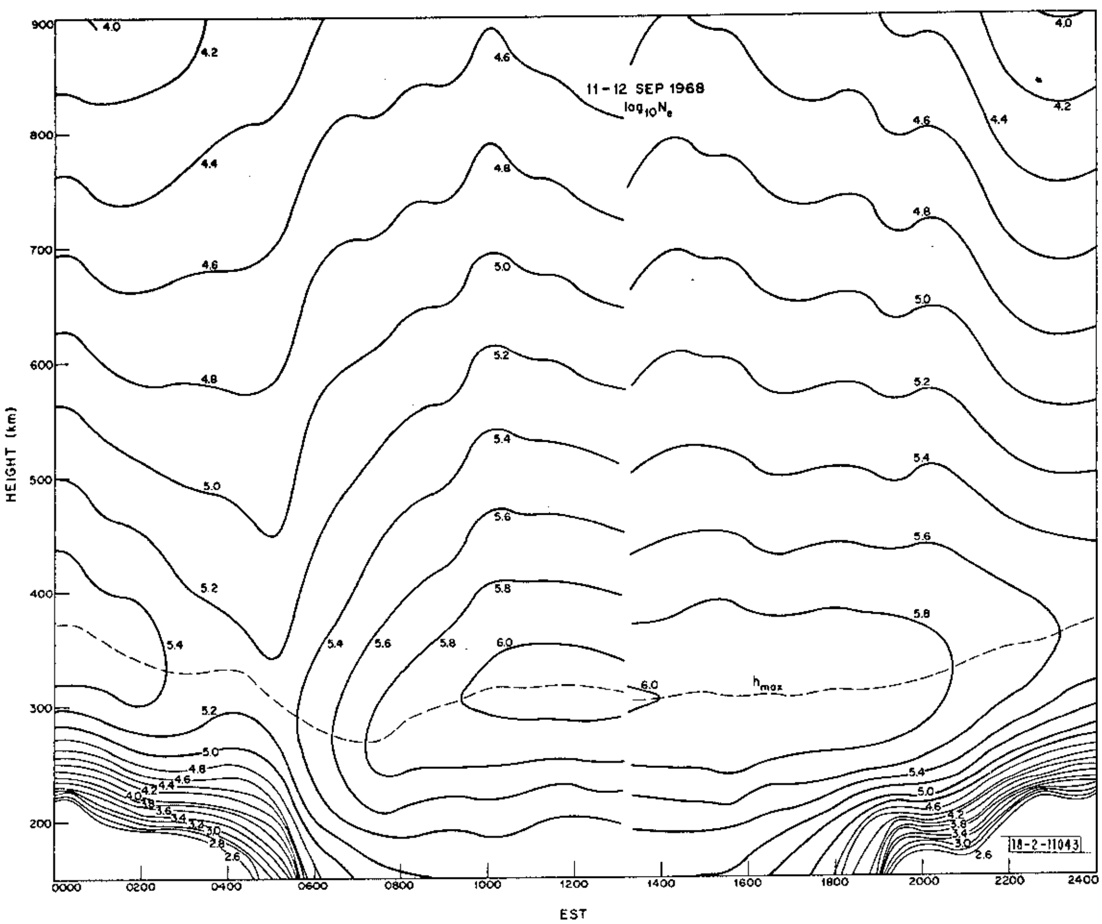

(f)

Fig. 3(a–s). Continued.

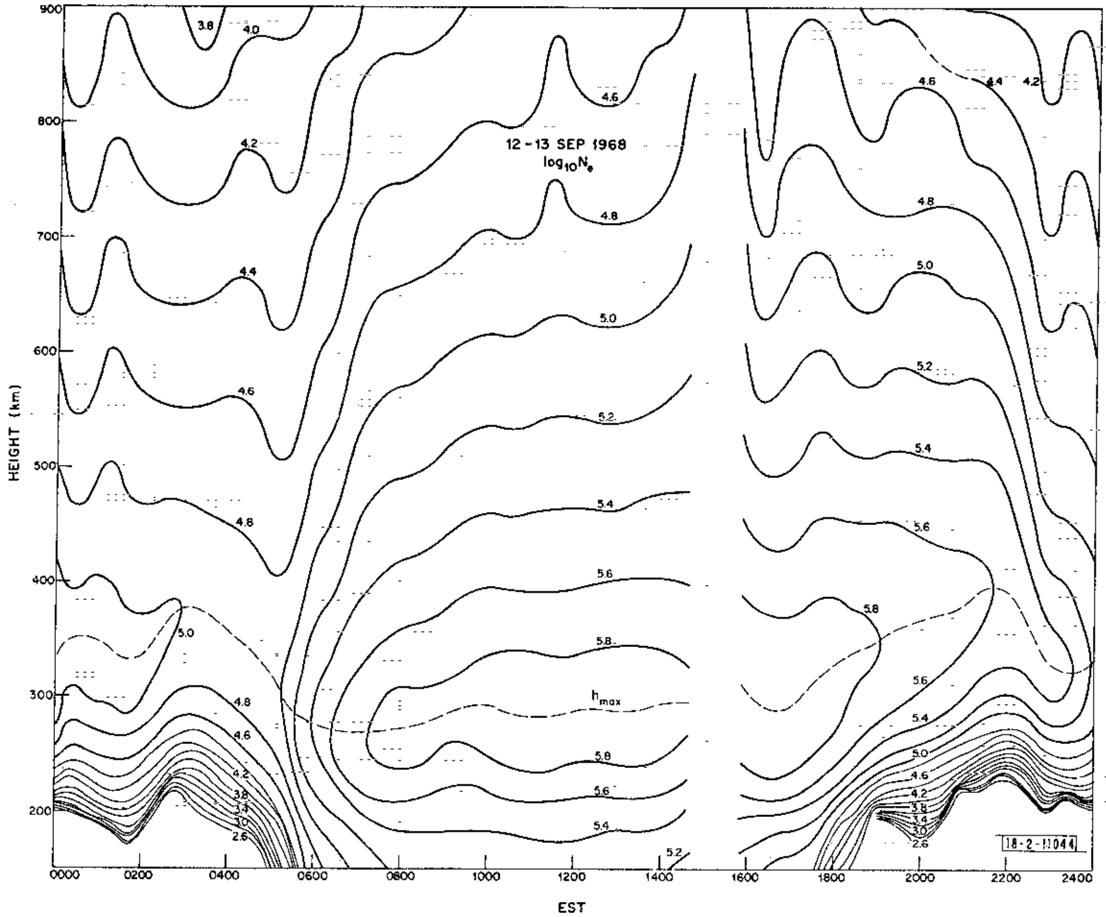

(g)

Fig. 3(a–s). Continued.

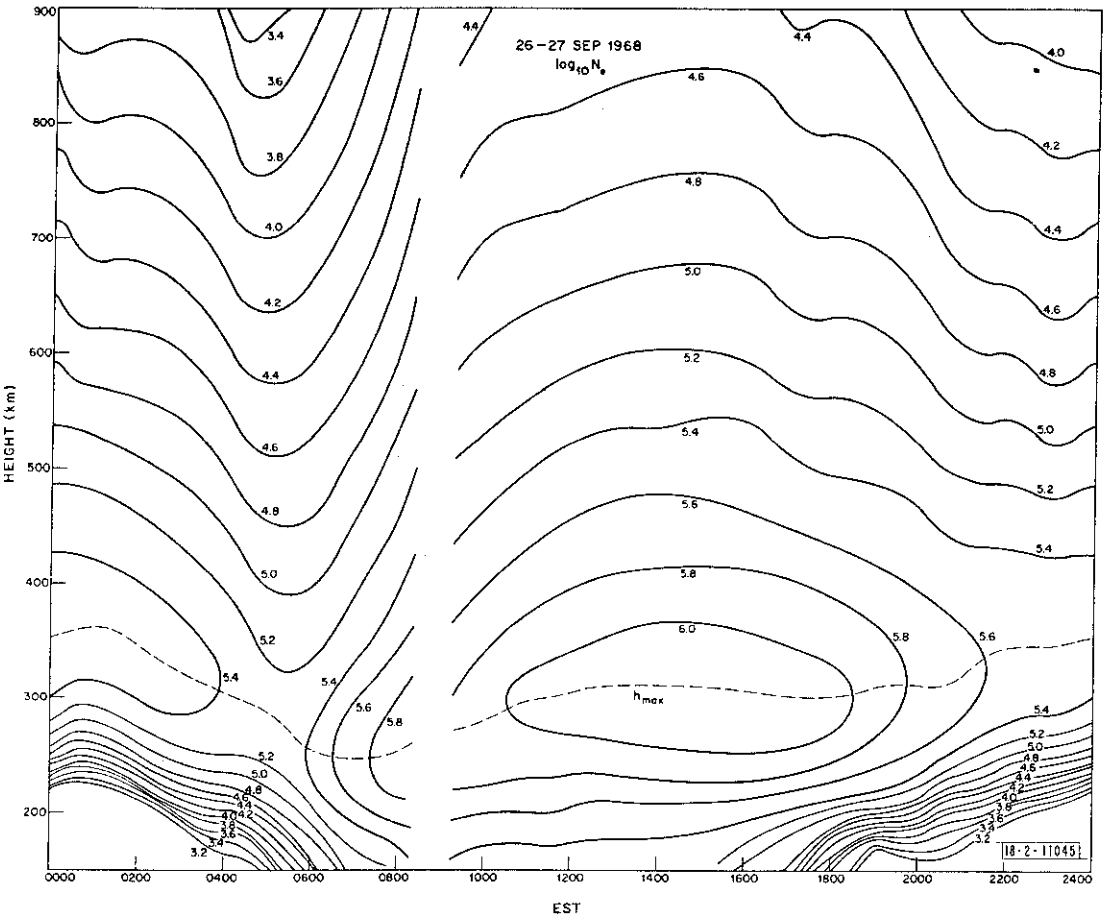

(h)

Fig. 3(a-s). Continued.

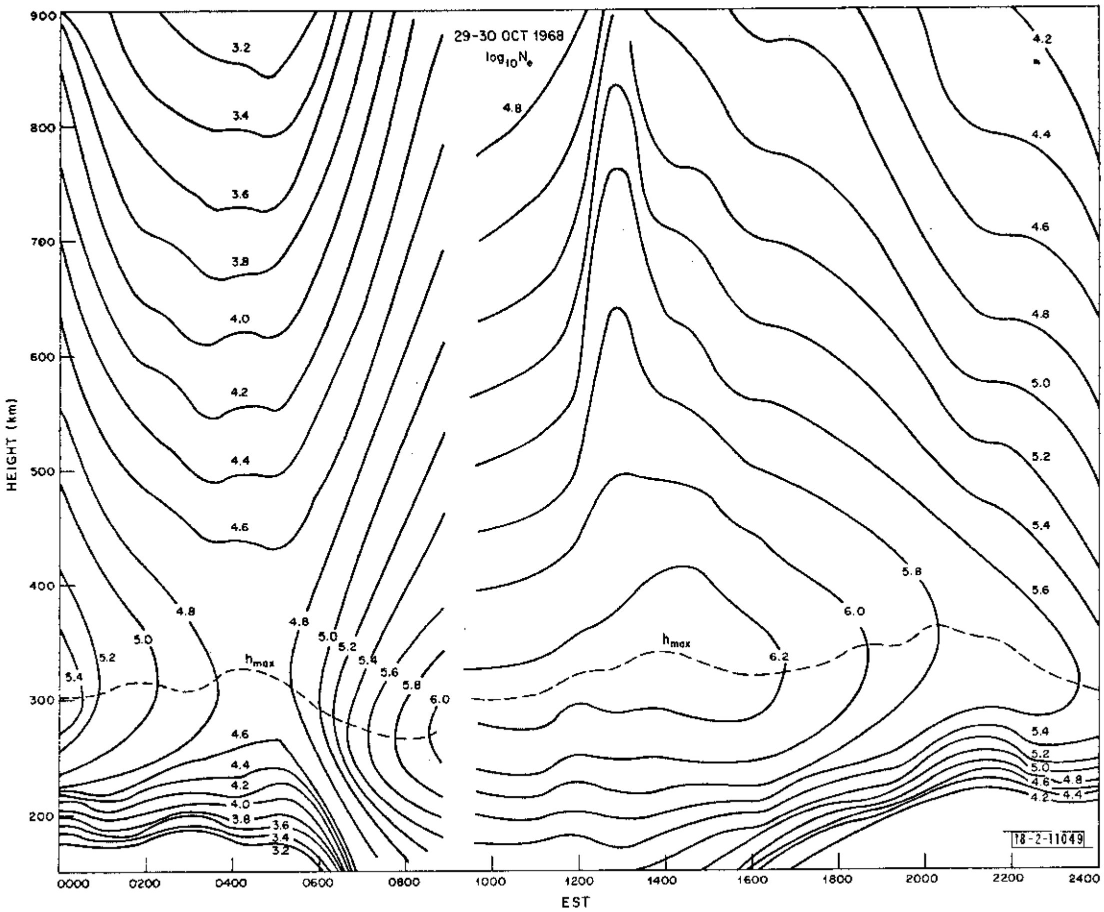

(l)

Fig. 3(a–s). Continued.

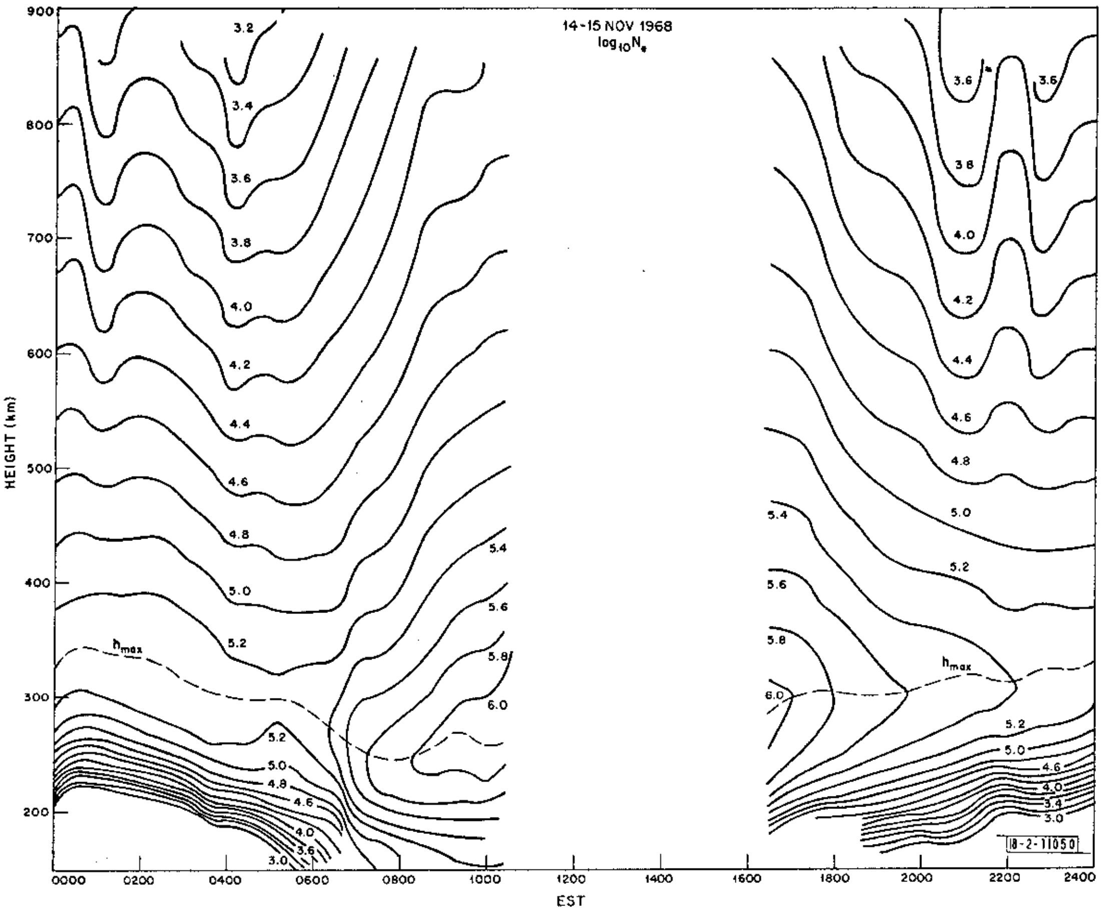

(m)

Fig. 3(a-s). Continued.

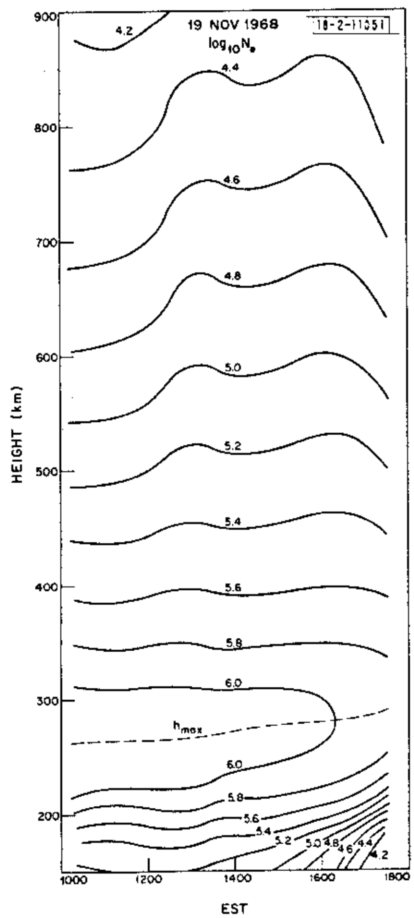

(n)

Fig. 3(a-s). Continued.

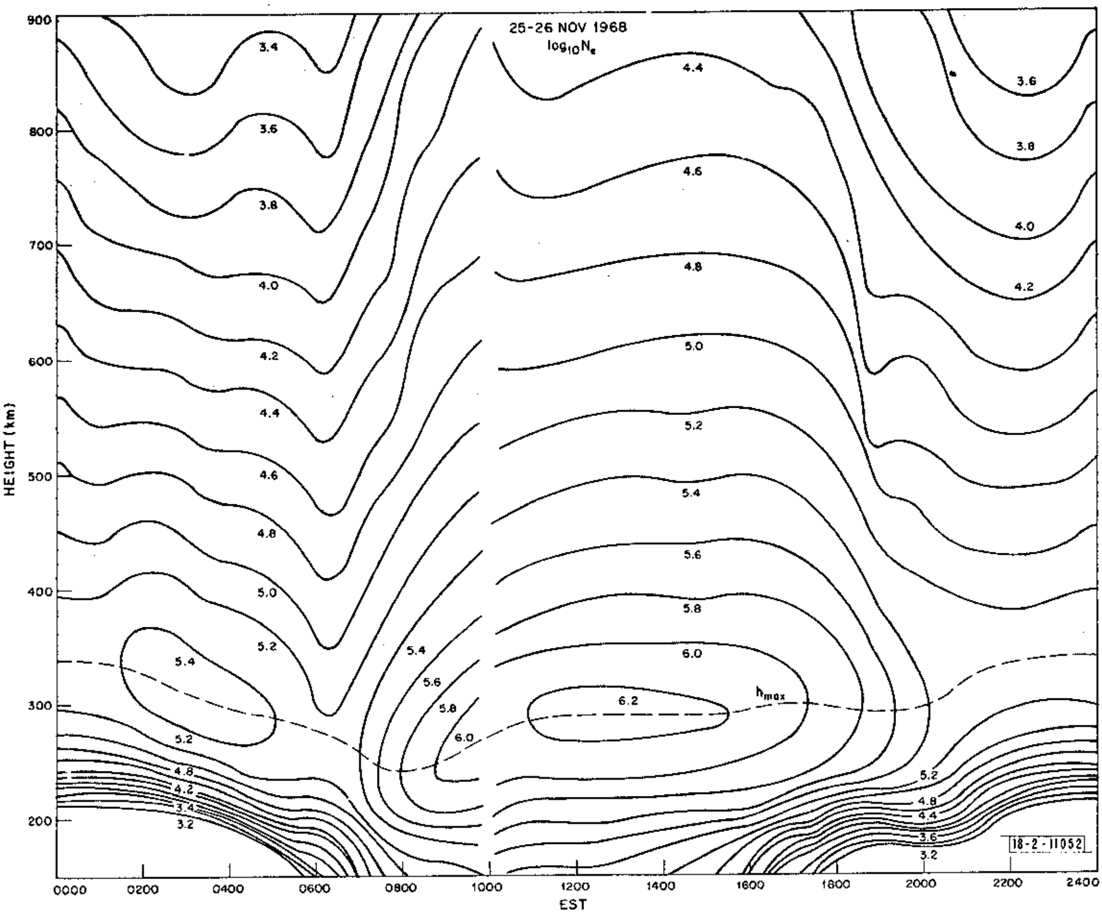

(o)

Fig. 3(a-s). Continued.

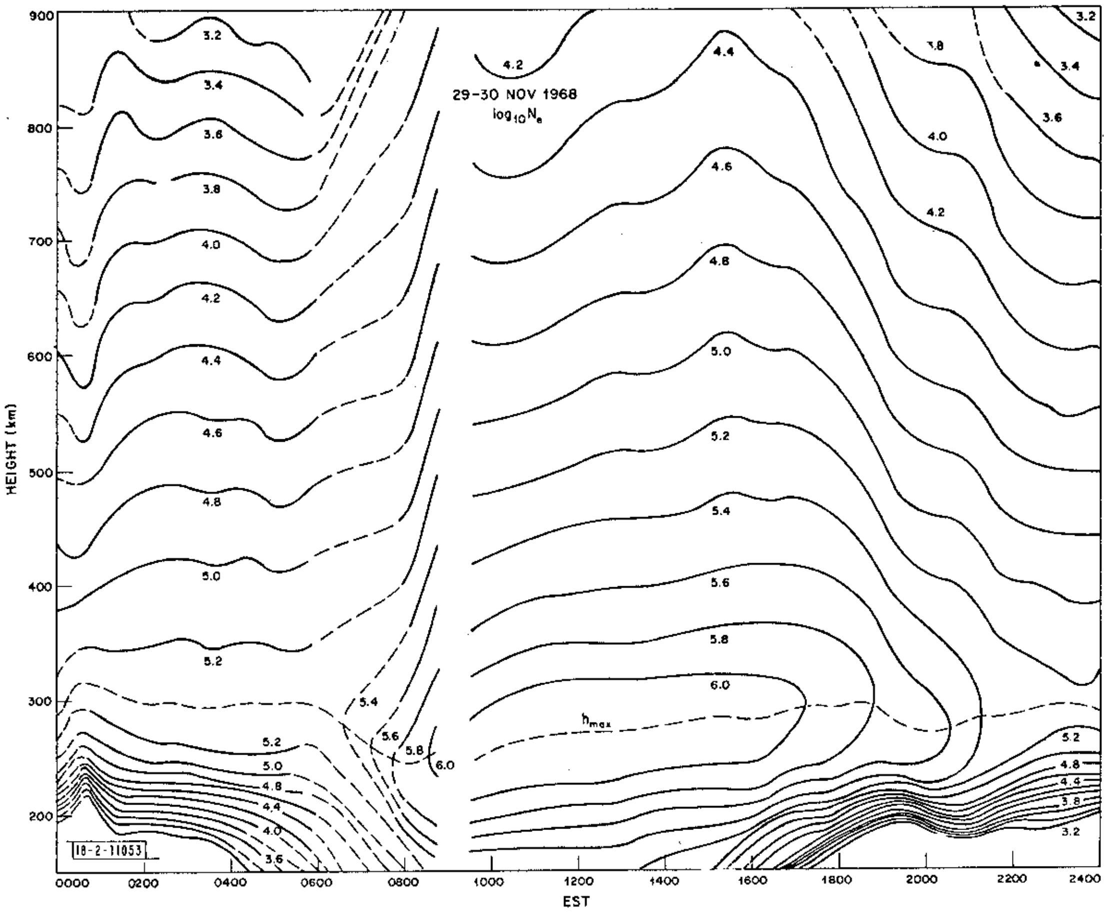

(p)

Fig. 3(a–s). Continued.

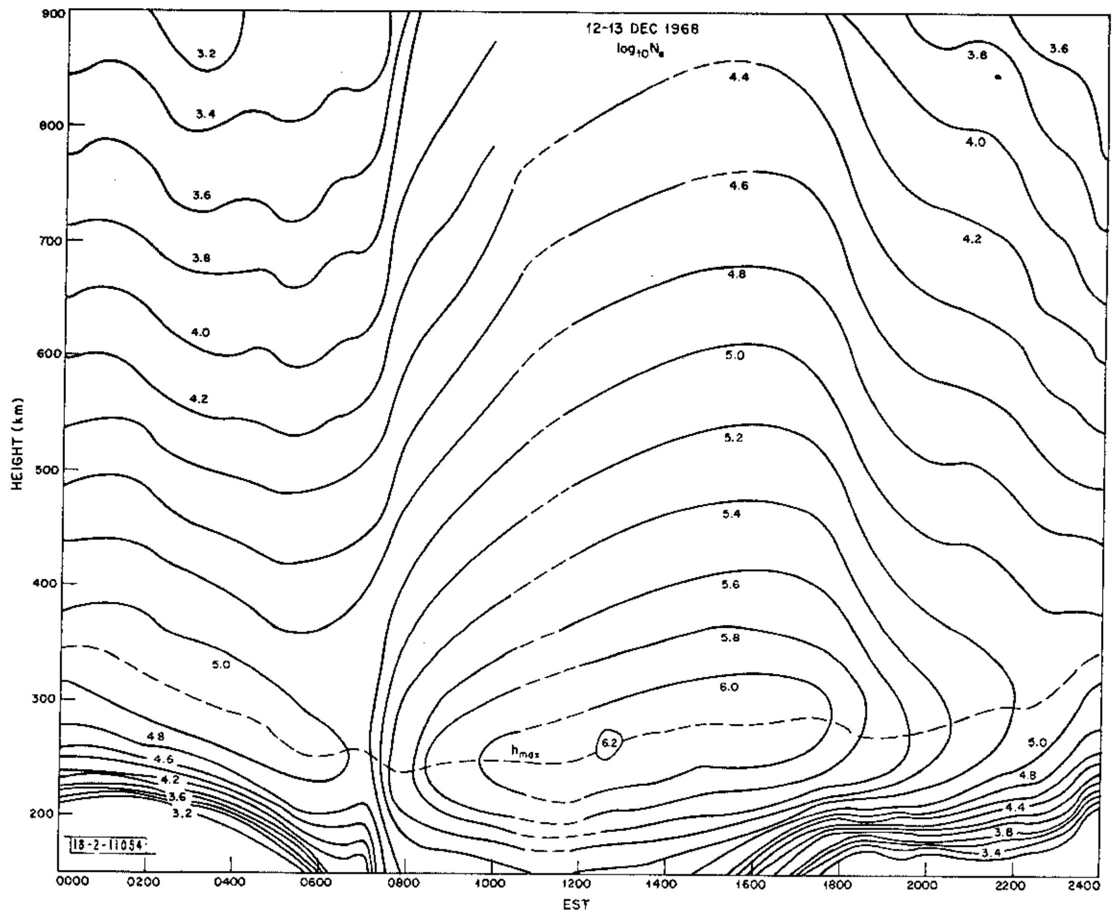

(q)

Fig. 3(a–s). Continued.

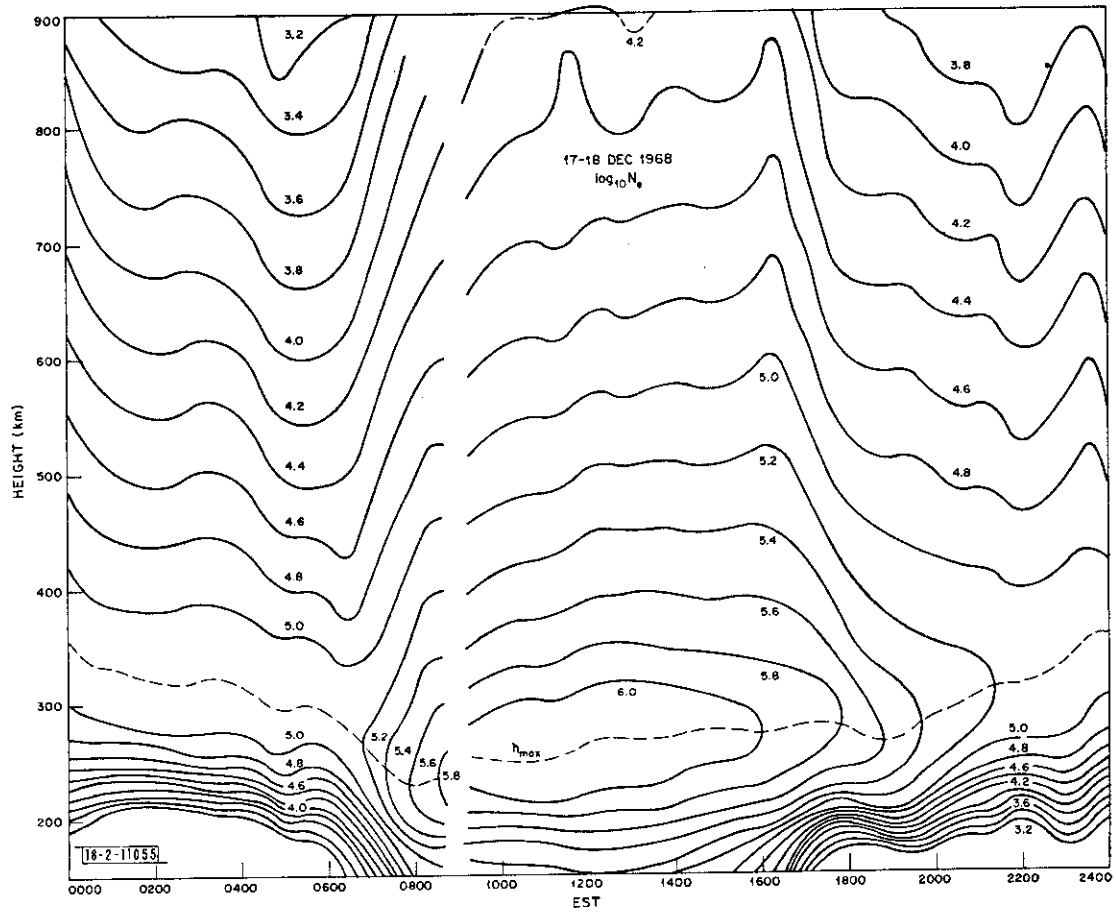

(r)

Fig. 3(a–s). Continued.

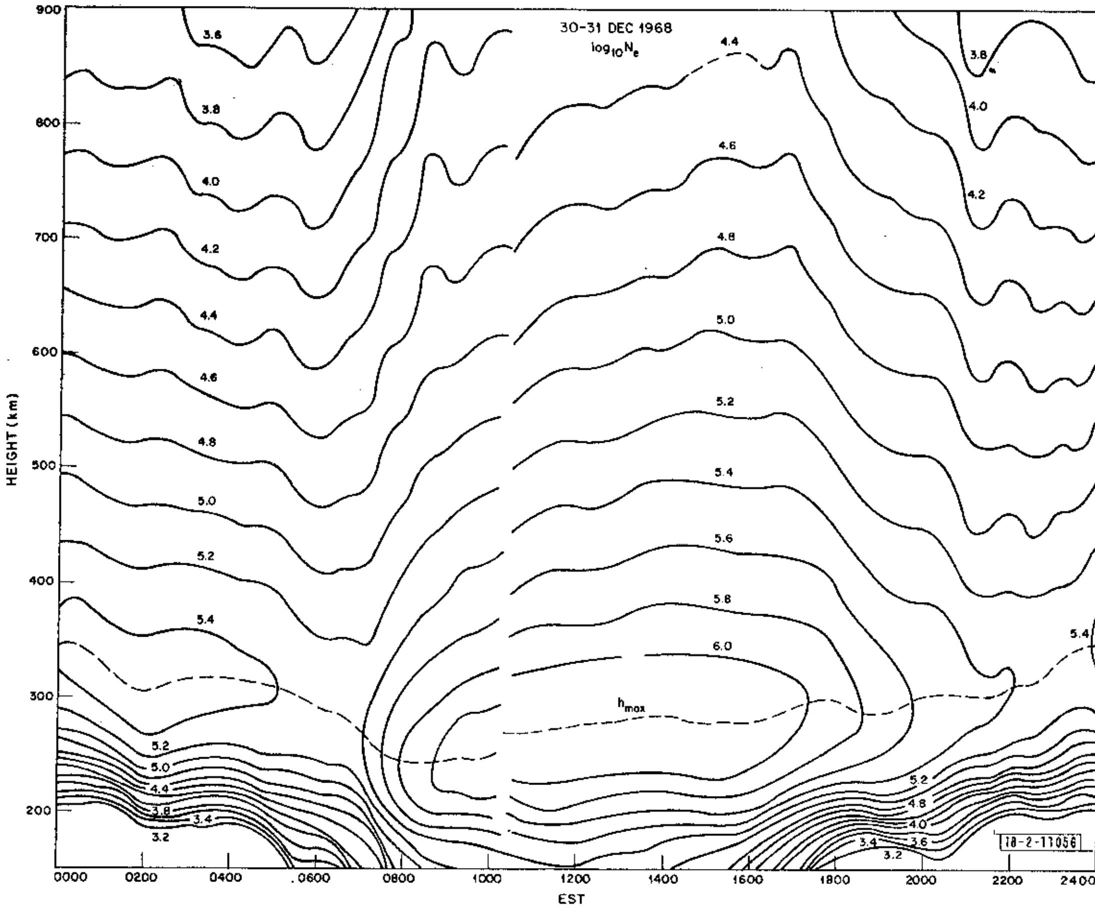

(s)

Fig. 3(a–s). Continued.

The winter behavior is characterized by a single daytime peak in f_oF2 centered near noon or somewhat after. At sunspot minimum, there is usually a second smaller peak in the density in the early morning hours (0200-0400) that is anomalous. This feature seems largely absent at sunspot maximum as many of the days presented here do not exhibit it [cf., Figs. 3(i) through (k), 3(p) through (r)]. A number of nights do show an early morning increase, e.g., 25-26 November [Fig. 3(o)] and 30-31 December [Fig. 3(s)]; this is less pronounced than seen at sunspot minimum, and it is noteworthy that these nights tend to be magnetically disturbed (Table I).

The summer behavior is characterized by lower daytime values of f_oF2 and larger nighttime values than in winter. There is, therefore, less diurnal variation, and the peak density is usually encountered at local ground sunset, e.g., 16-17 and 25-26 April 1972 [Figs. 2(f), 2(g)]. On many days in the summer, N_{max} reaches a second weaker maximum before noon giving rise to a shallow midday minimum, the so-called "bite-out." Examples of this behavior are to be found for 23-24 May and 20-21 June [Figs. 2(h), 2(i)]. We have discussed elsewhere[11,12] the probable causes of these variations and will not repeat them here.

A number of characteristic deviations from these patterns have been recognized that are associated with magnetically disturbed conditions. One type of variation that has been seen, on many occasions, is an increase in the daytime density above normal, which is followed by abnormally low nighttime values. These increases are found to occur up to 18 hours after a magnetic storm's sudden commencement, usually in the late afternoon or early evening. These "positive-phase" portions of the storm have been examined separately employing the results gathered on 29-30 October 1968 [Fig. 3(l)] and in July 1969 (Ref. 19). From the drift information obtained, it appears that some of the increases are caused by southward directed thermospheric winds, while others are related to horizontal motions caused by penetration of magnetospheric electric fields inside the plasmasphere.[20] This last class of event has a preferred time of occurrence near 1700 LT and is associated with marked increases of the local magnetic field. No clear instances of this type of disturbance appear to have been observed in 1968. Irregular increases, extending over much of the day, seem to be caused by thermospheric winds and 29-30 October is thought to be an example of such an event.[19]

Abnormally low nighttime densities have been encountered near sunspot maximum during magnetically disturbed conditions and attributed to the motion of the mid-latitude trough of low ionization over the station.[5,12] This does not seem to have occurred often during 1968 and possibly the behavior on 17 January 1968 [Fig. 2(a)] represents the only case.

F-region densities, somewhat lower than normal, are frequently encountered during magnetic storms (negative phase) on the day (or days) following the positive increase. Usually $h_{max}F2$ is lower on these days and the F1 layer more pronounced than usual. On occasion the F1 peak becomes larger than the F2 peak (G condition). The only instance of this behavior recorded in 1968 appears to be on 27 March [Fig. 2(e)].

B. Electron Temperature

Contours of constant electron temperature at 200°K intervals are presented in Figs. 4(a) through (i) and 5(a) through (s). We have discussed previously[2-5] the characteristic temperature behavior for summer and winter observed at Millstone. The summer months usually exhibit the simplest pattern. In these months, the electron temperature usually increases monotonically with altitude at all times (indicating the presence of a source of heat in the magnetosphere).

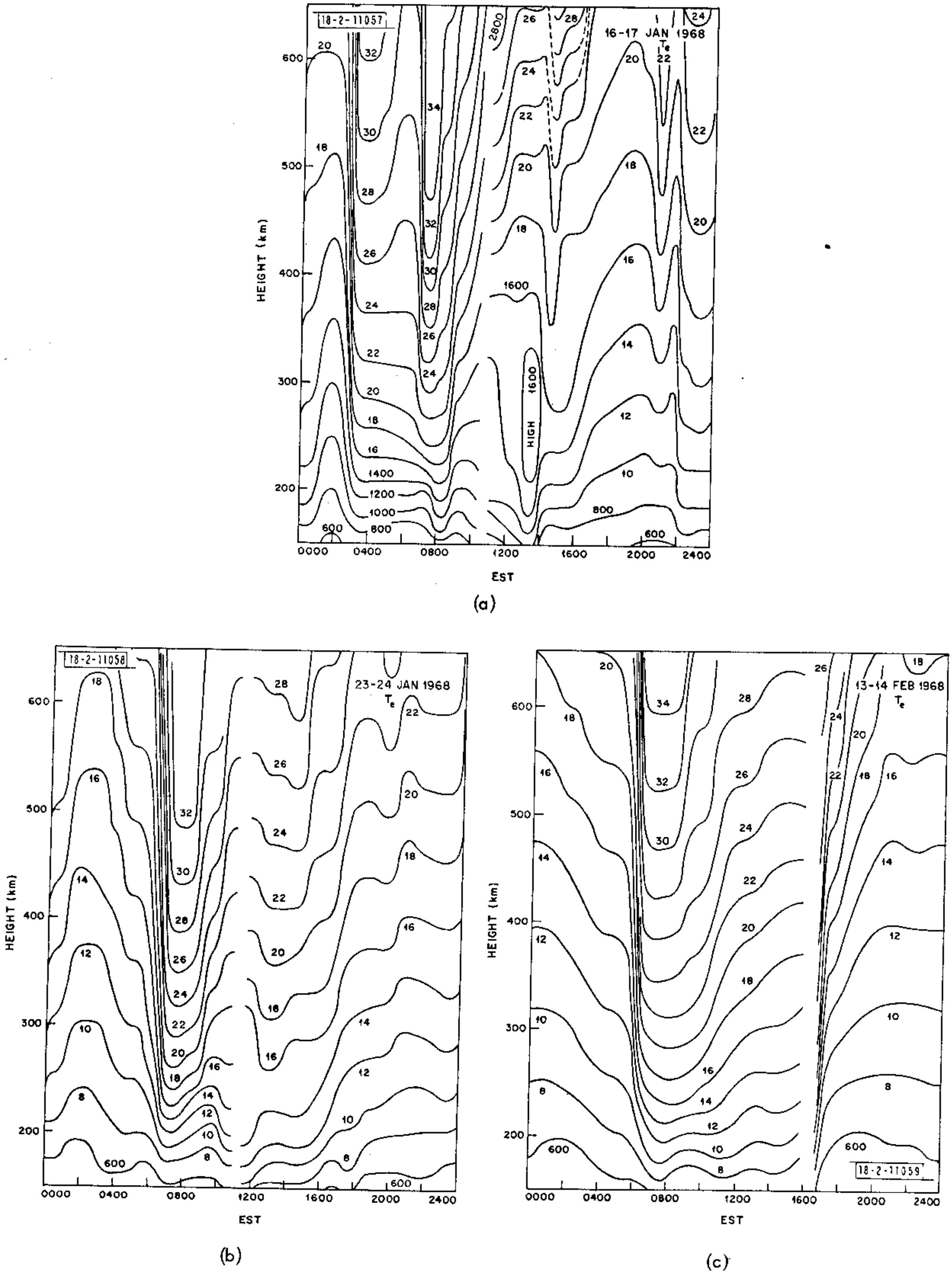

Fig. 4(a–i). Contour diagrams of constant electron temperature (in 200°K steps) as functions of height and time gathered during the first six months of 1968.

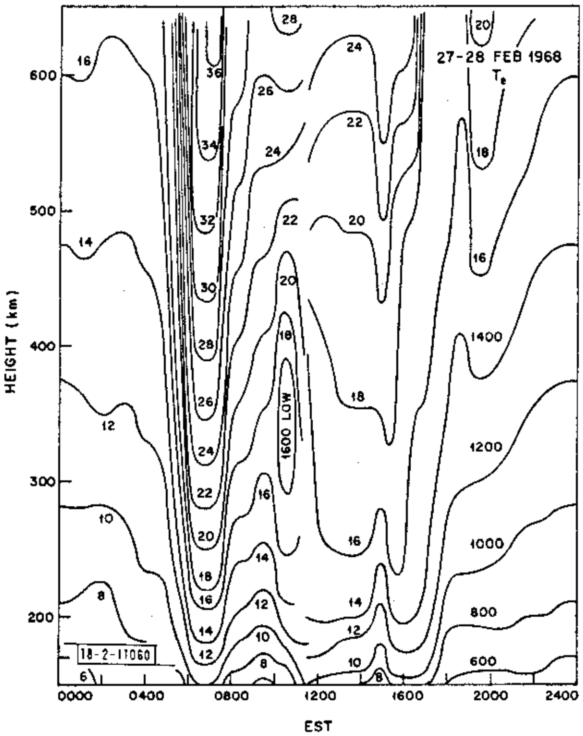

(d)

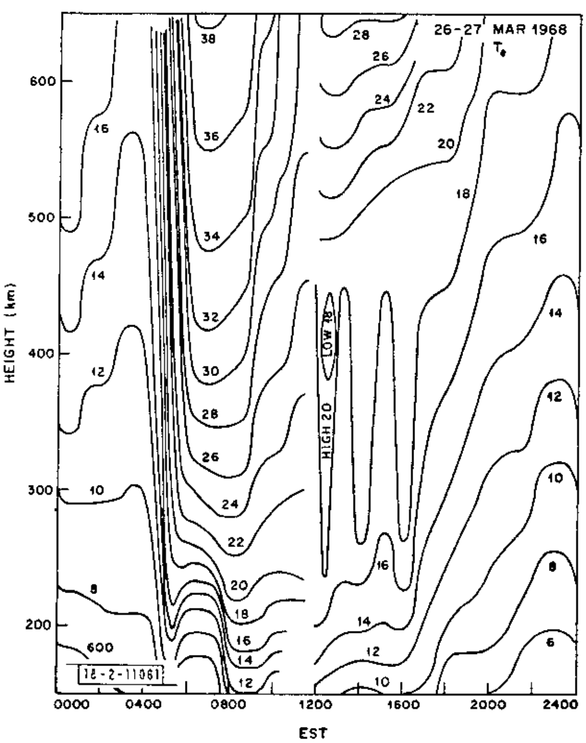

(e)

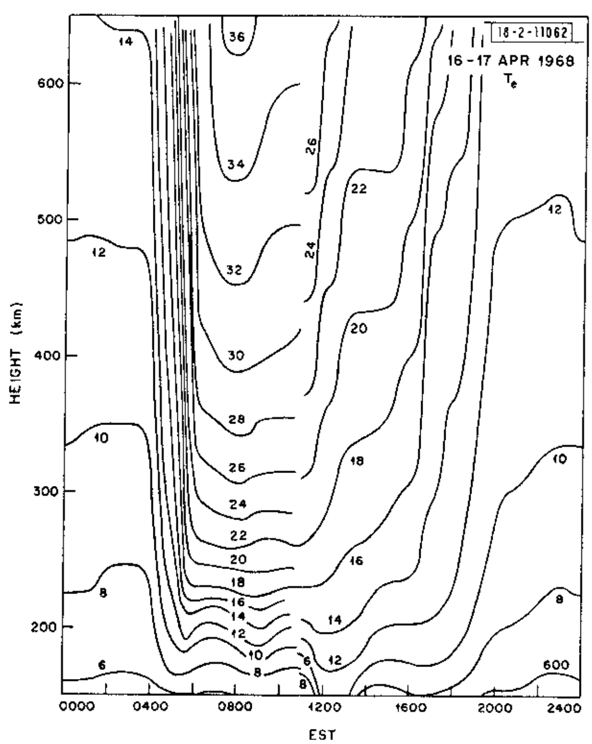

(f)

Fig. 4(a-i). Continued.

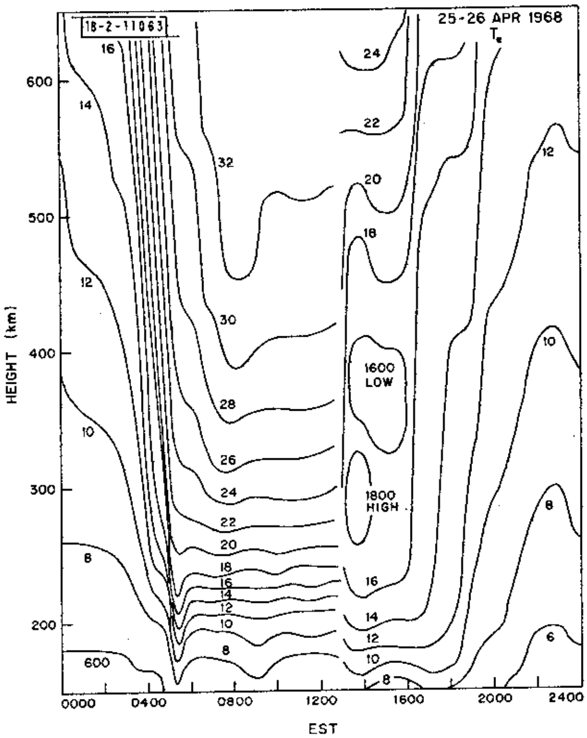

(g)

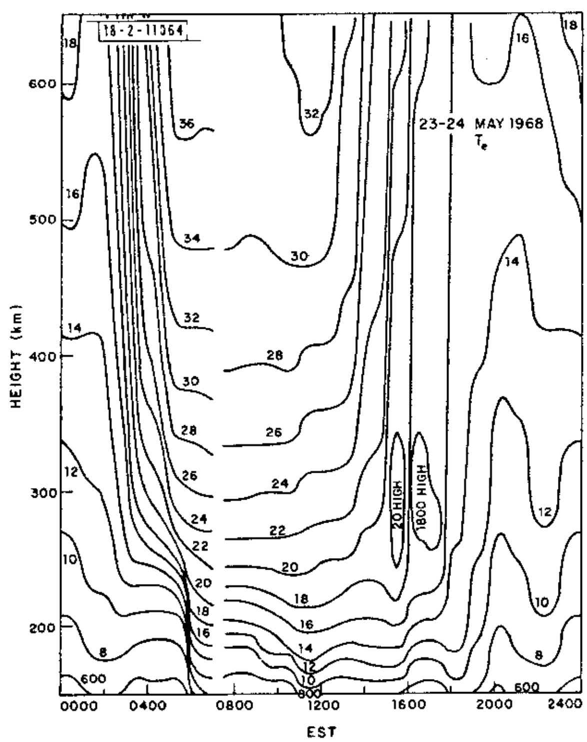

(h)

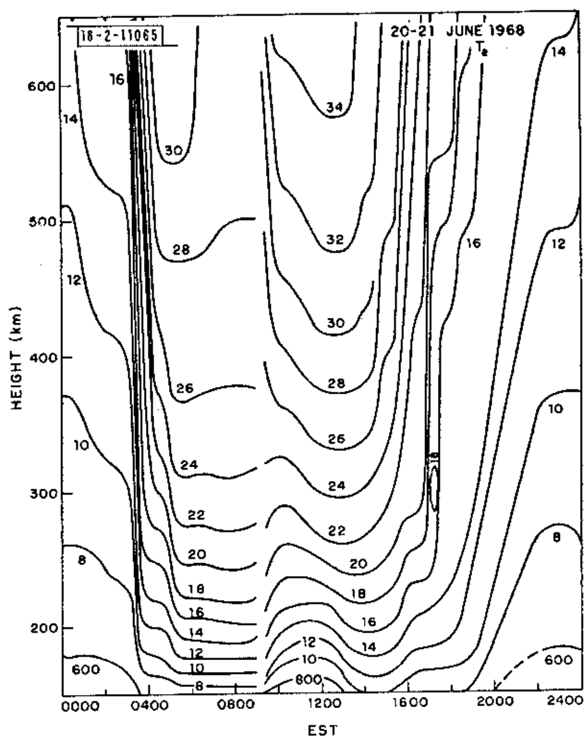

(i)

Fig. 4(a-i). Continued.

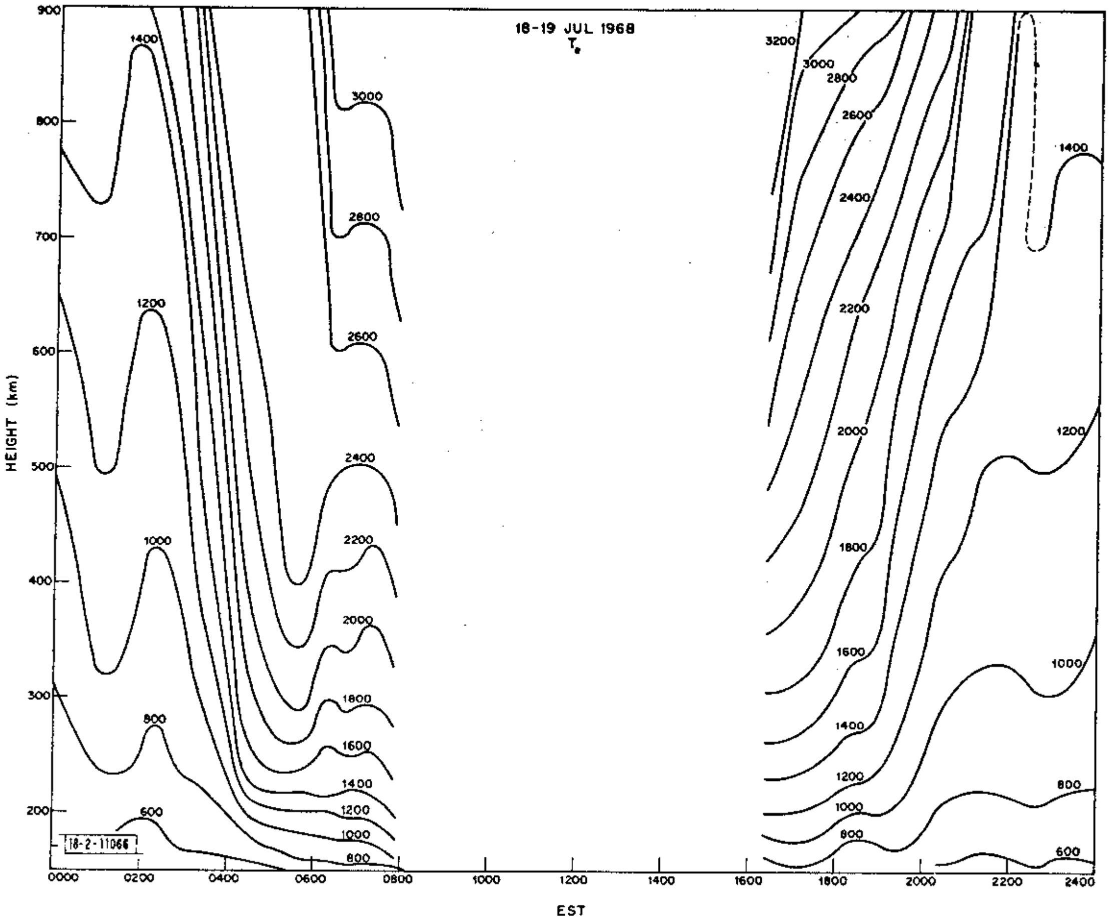

(a)

Fig. 5(a–s). Contour diagrams of constant electron temperature (in 200°K steps) as functions of height and time gathered during the last six months of 1968.

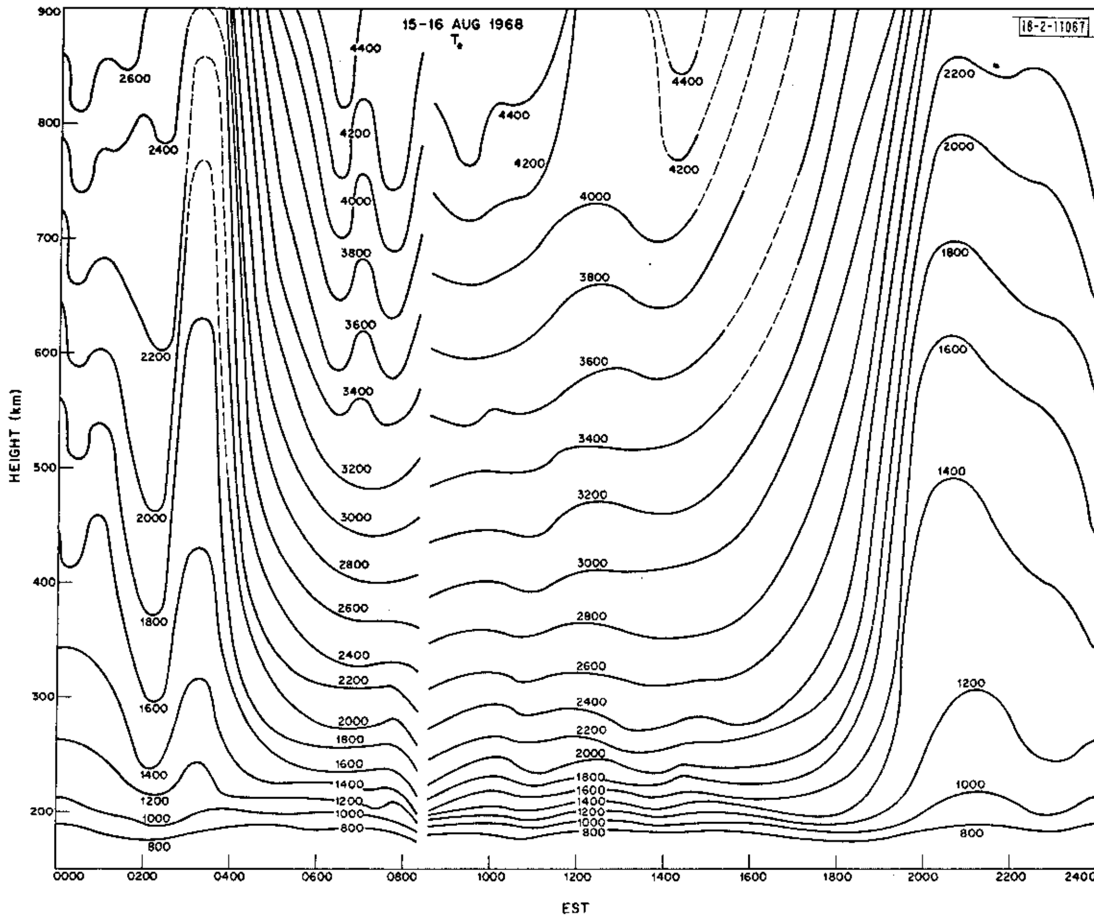

(b)

Fig. 5(a-s). Continued.

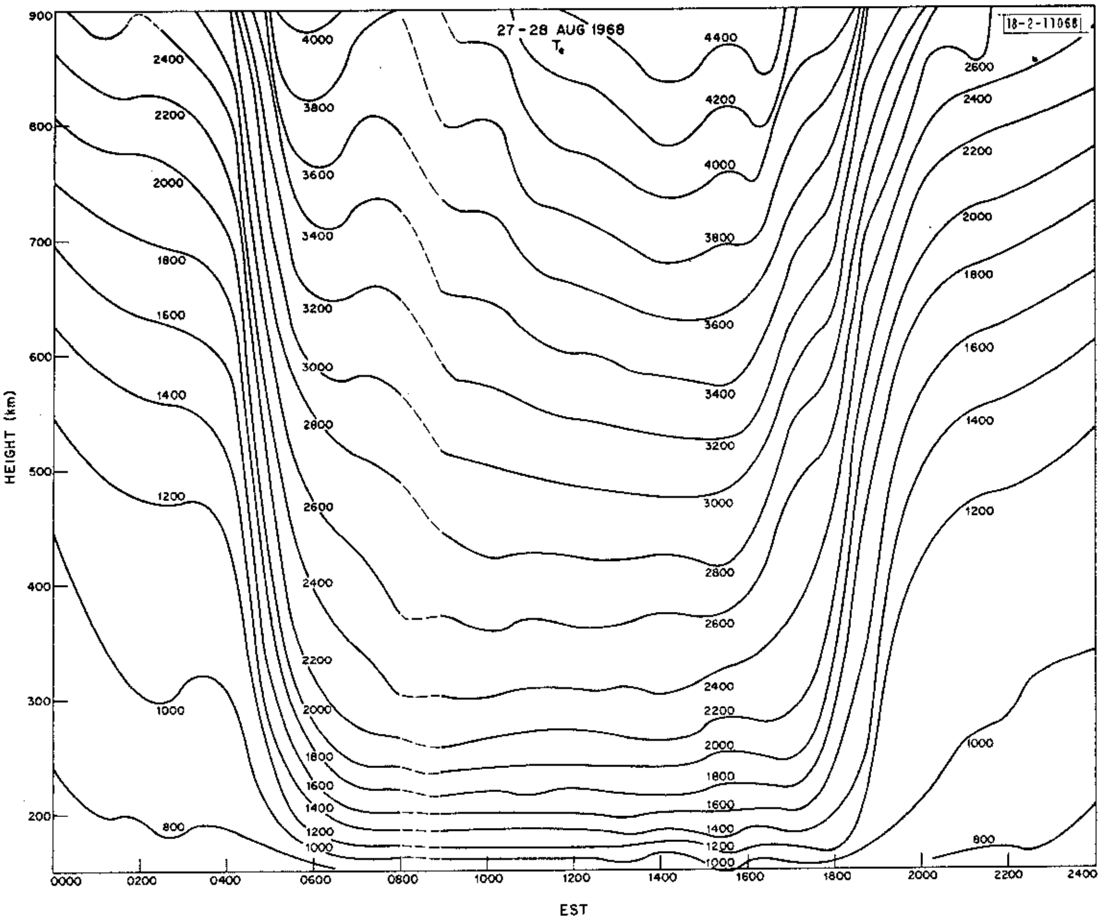

(c)

Fig. 5(a–s). Continued.

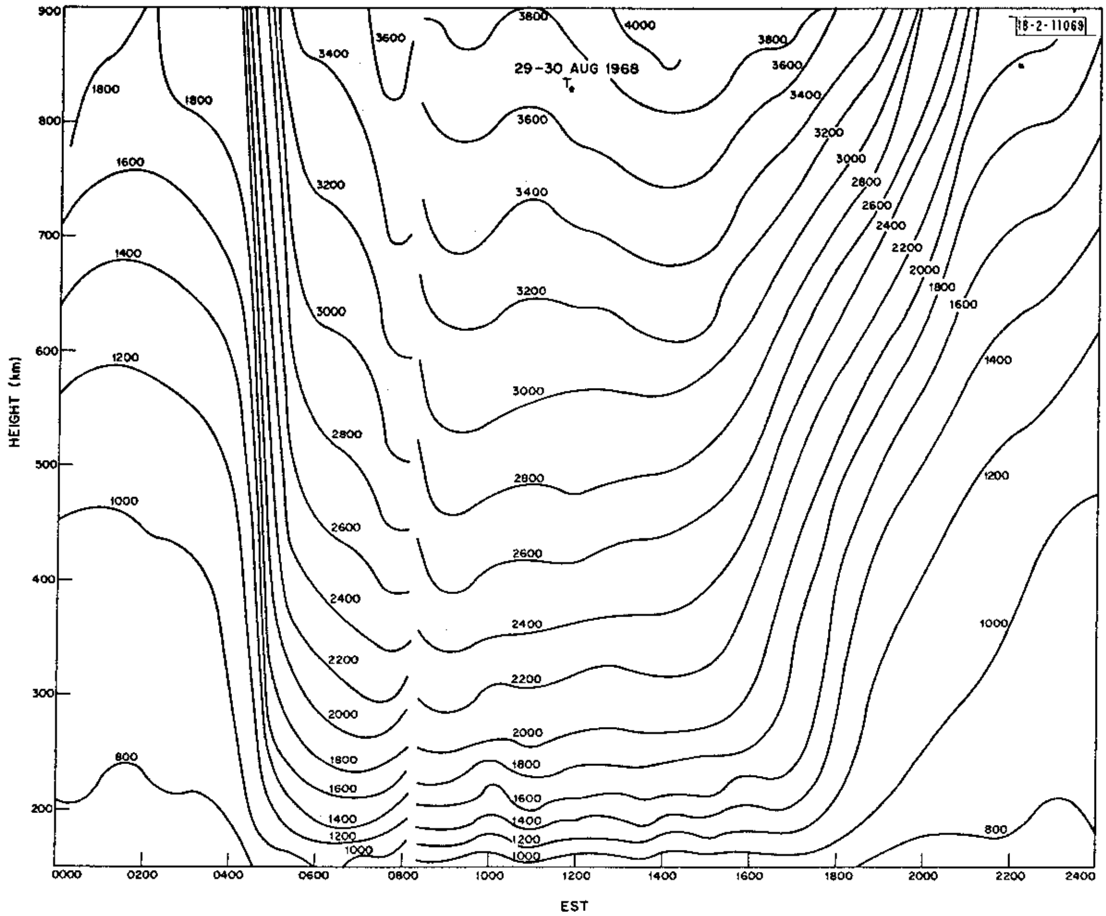

(d)

Fig. 5(a–s). Continued.

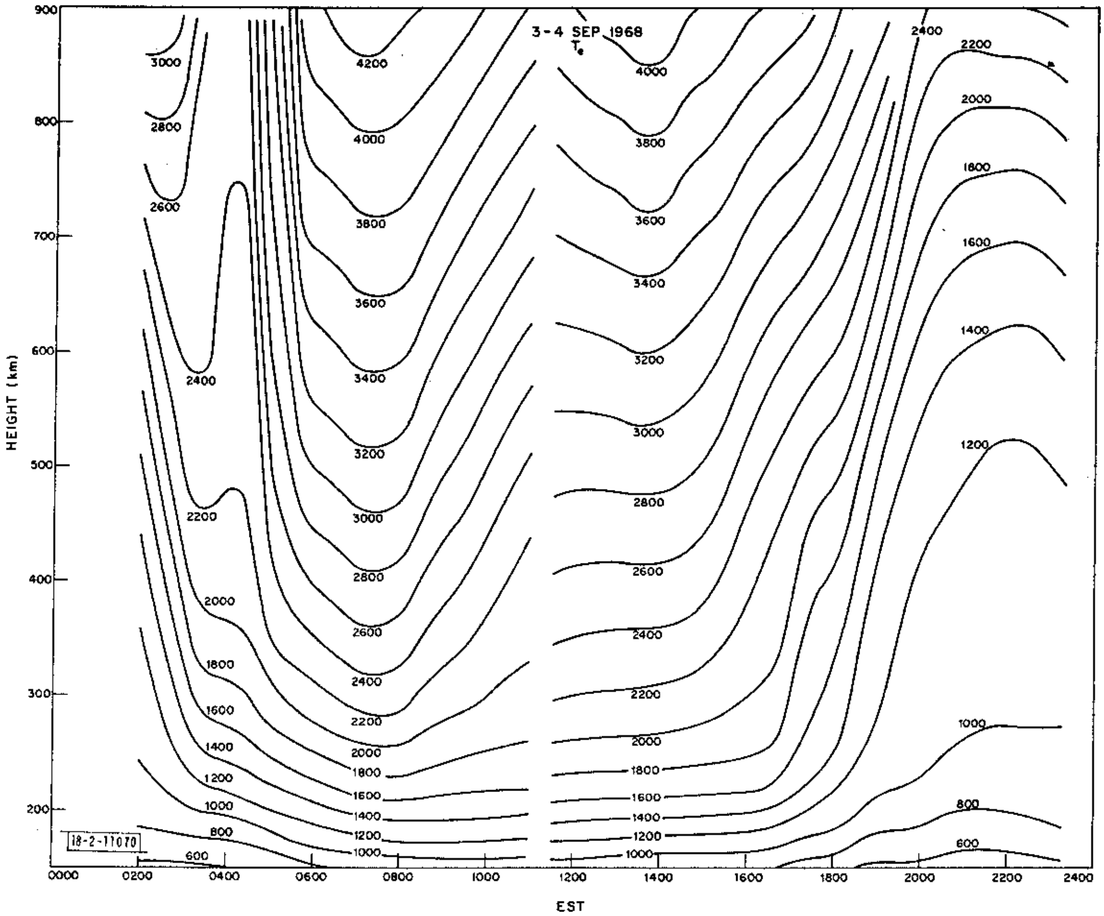

(e)

Fig. 5(a–s). Continued.

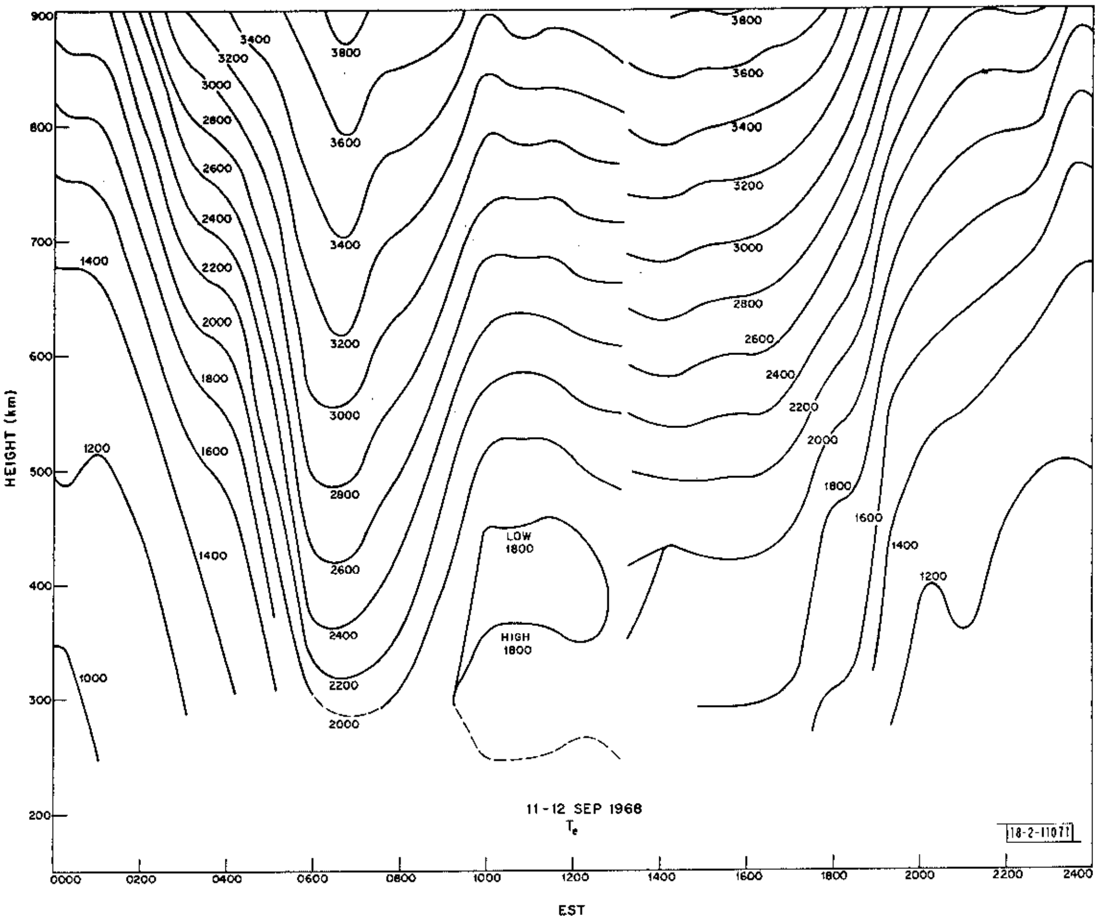

(f)

Fig. 5(a–s). Continued.

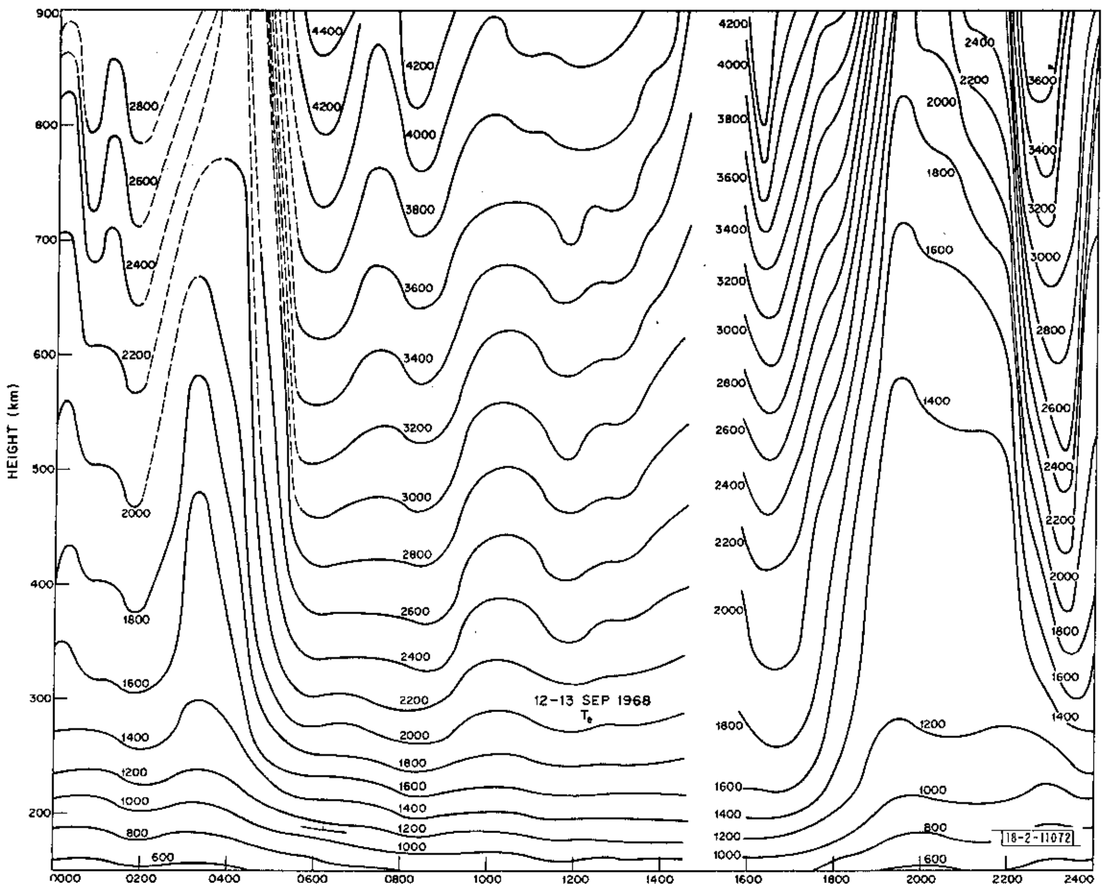

(g)

Fig. 5(a-s). Continued.

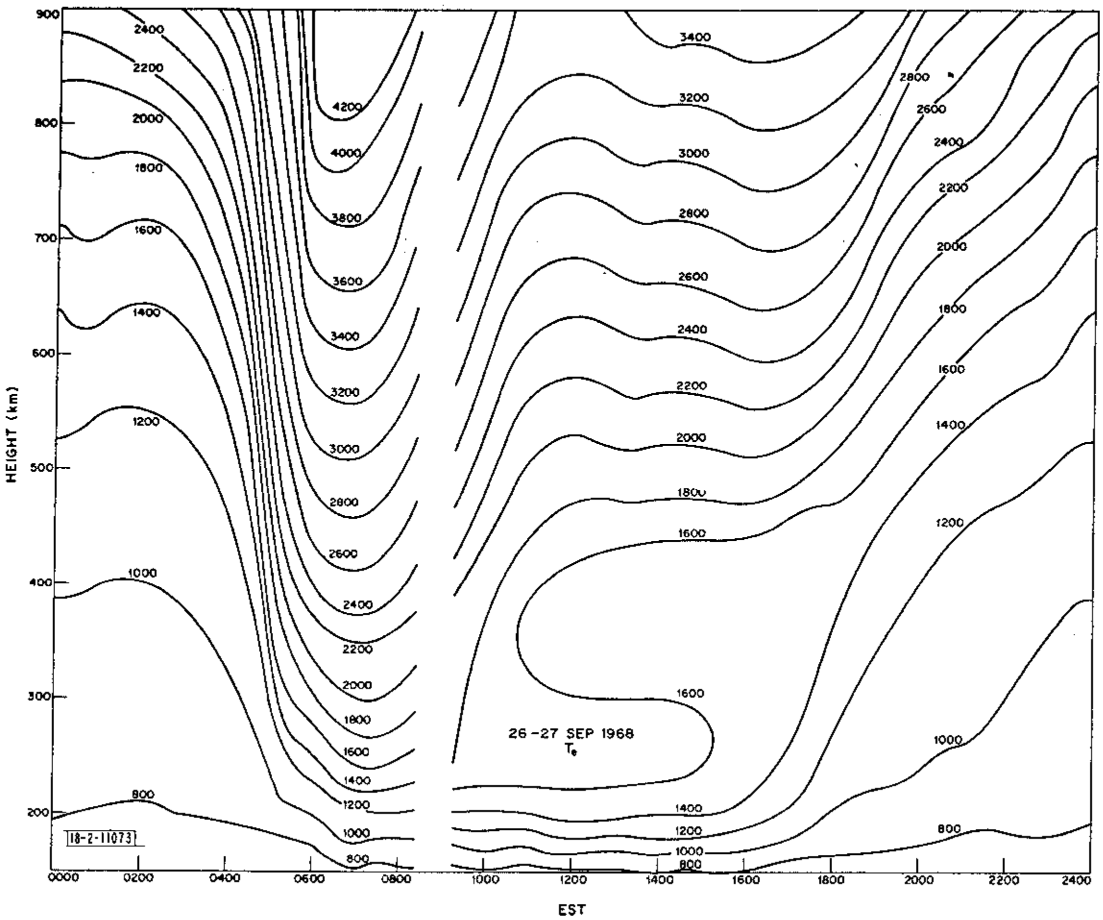

(h)

Fig. 5(a–s). Continued.

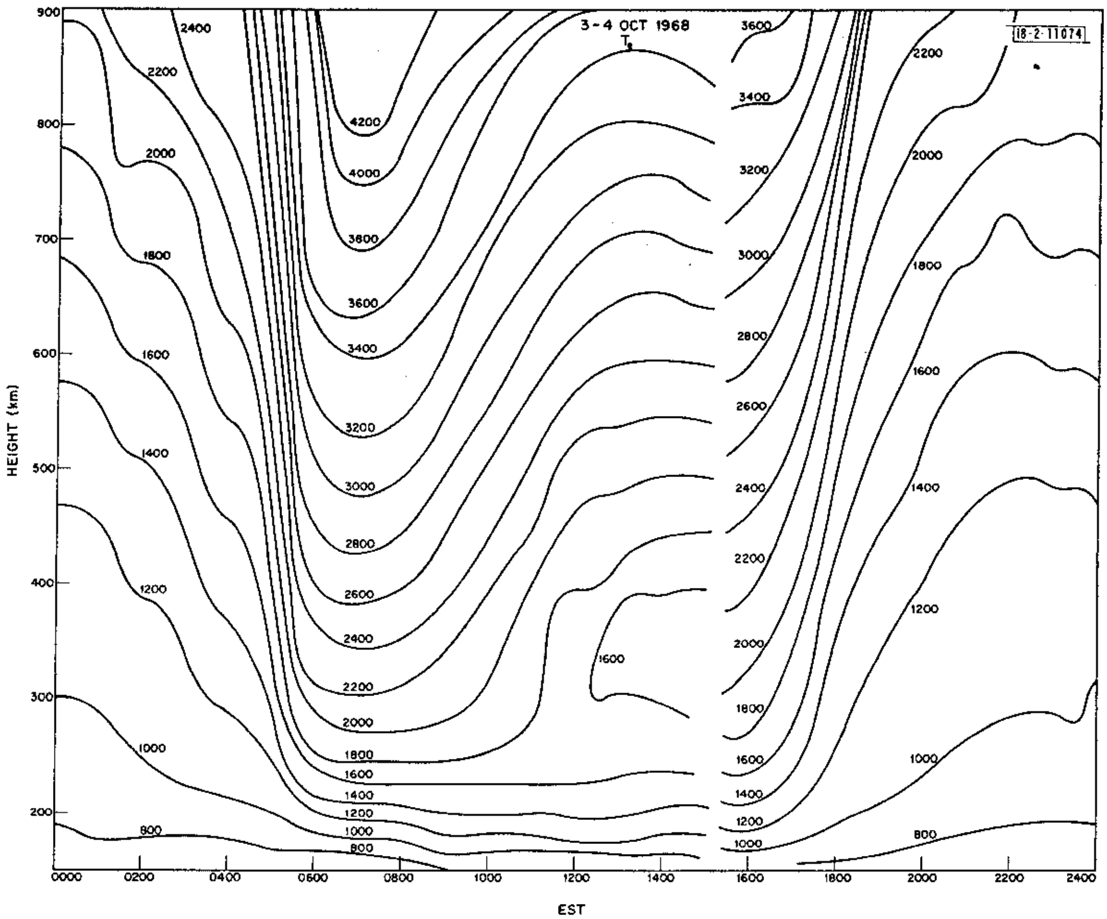

(i)

Fig. 5(a–s). Continued.

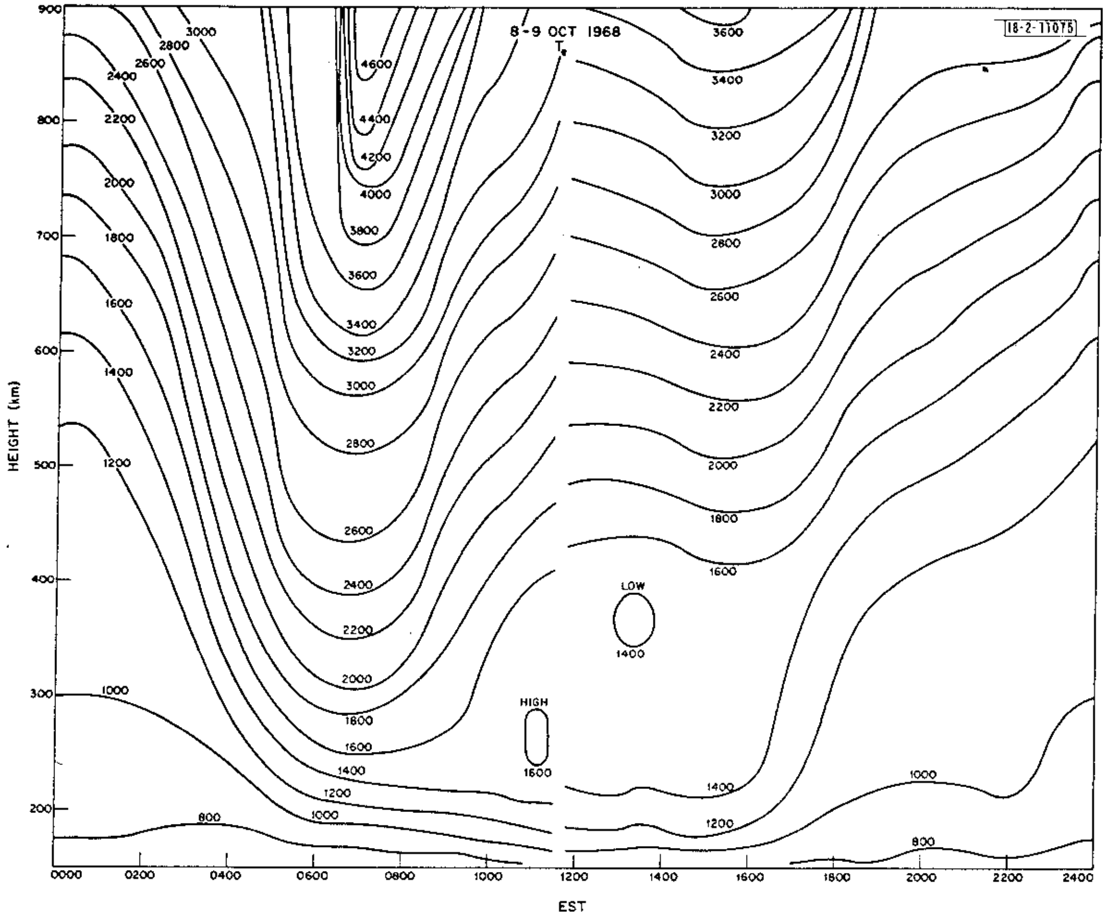

(j)

Fig. 5(a-s). Continued.

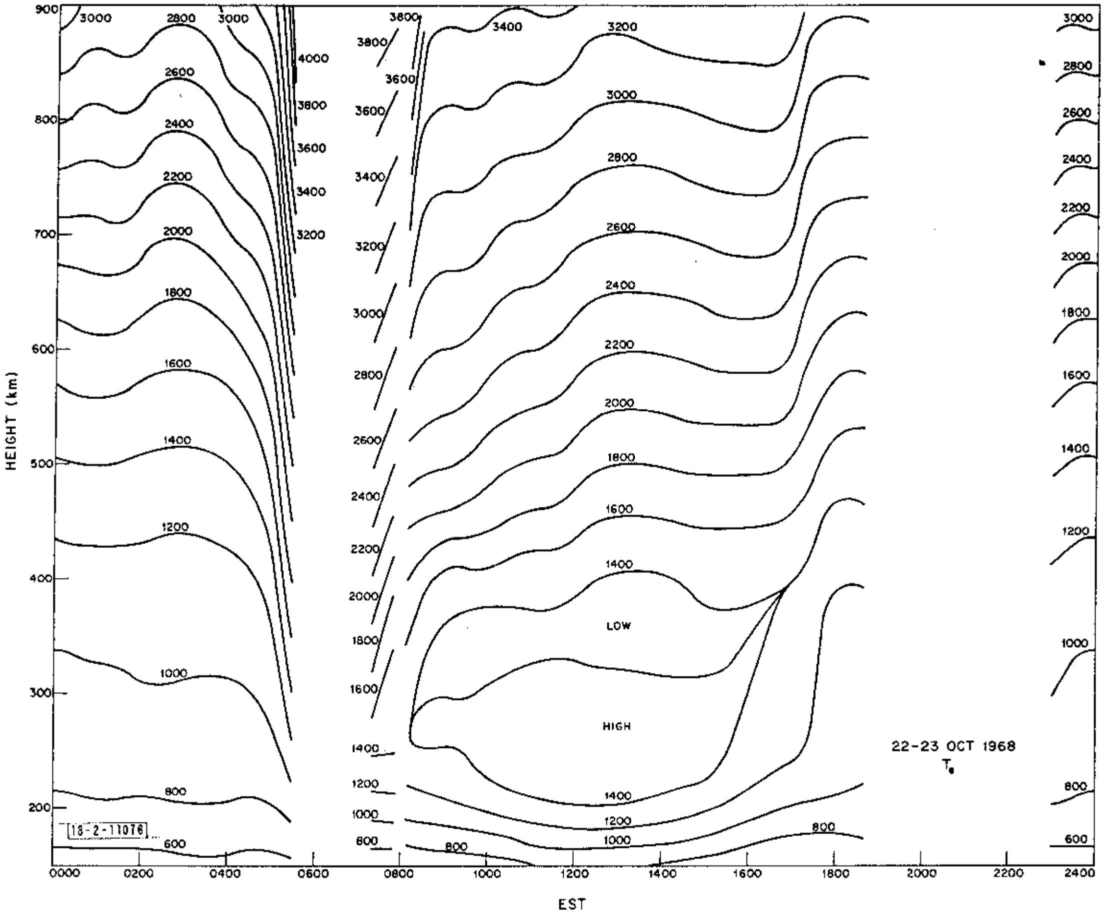

(k)

Fig. 5(a–s). Continued.

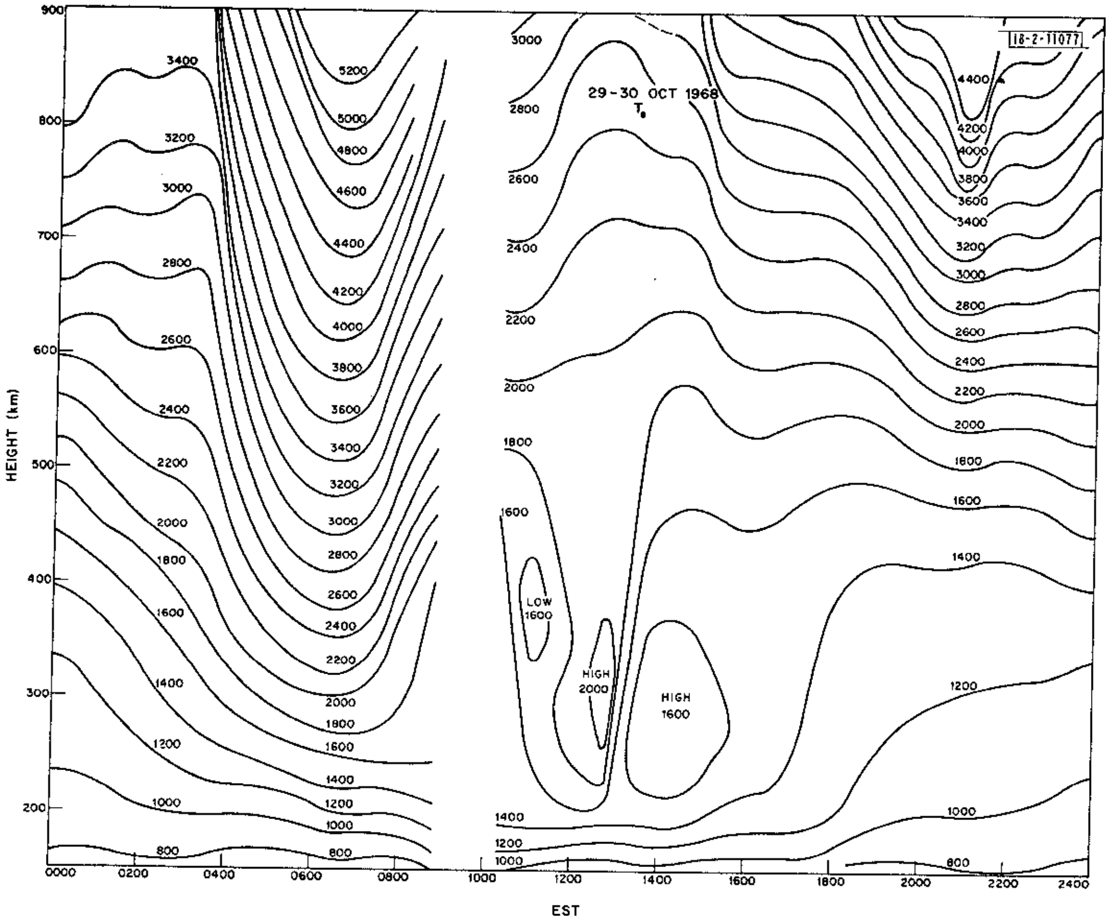

(l)

Fig. 5(a–s). Continued.

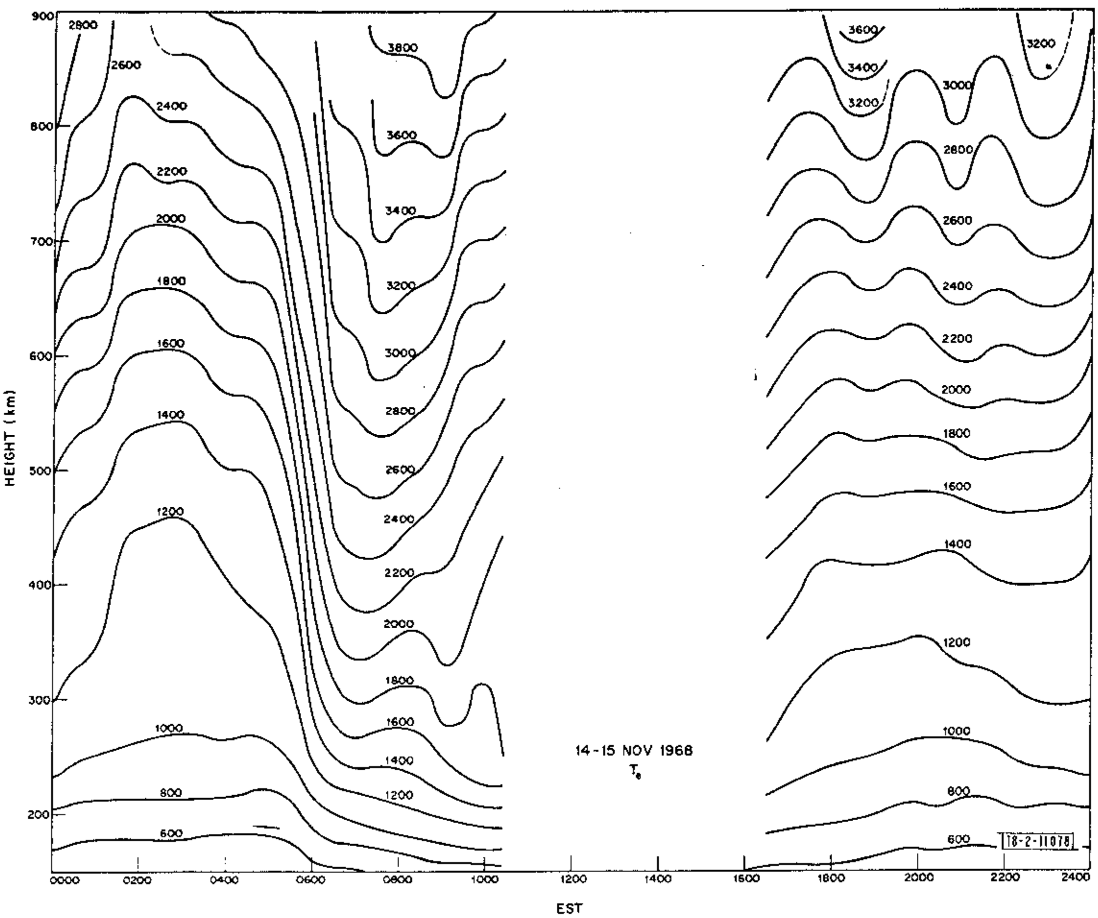

(m)

Fig. 5(a-s). Continued.

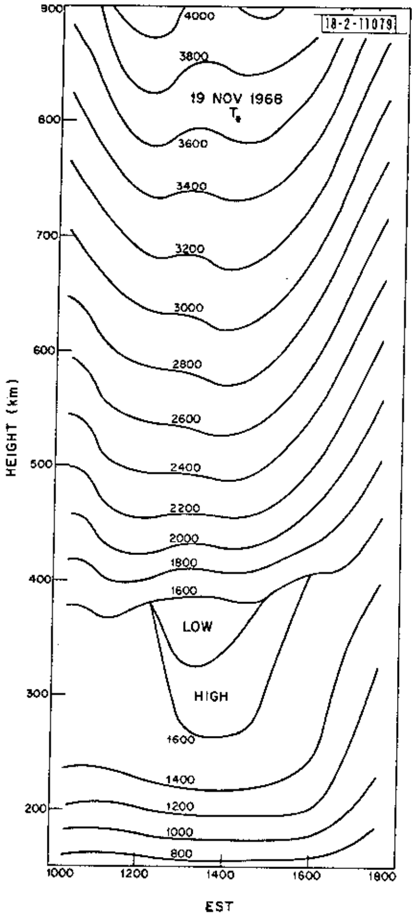

(n)

Fig. 5(a–s). Continued.

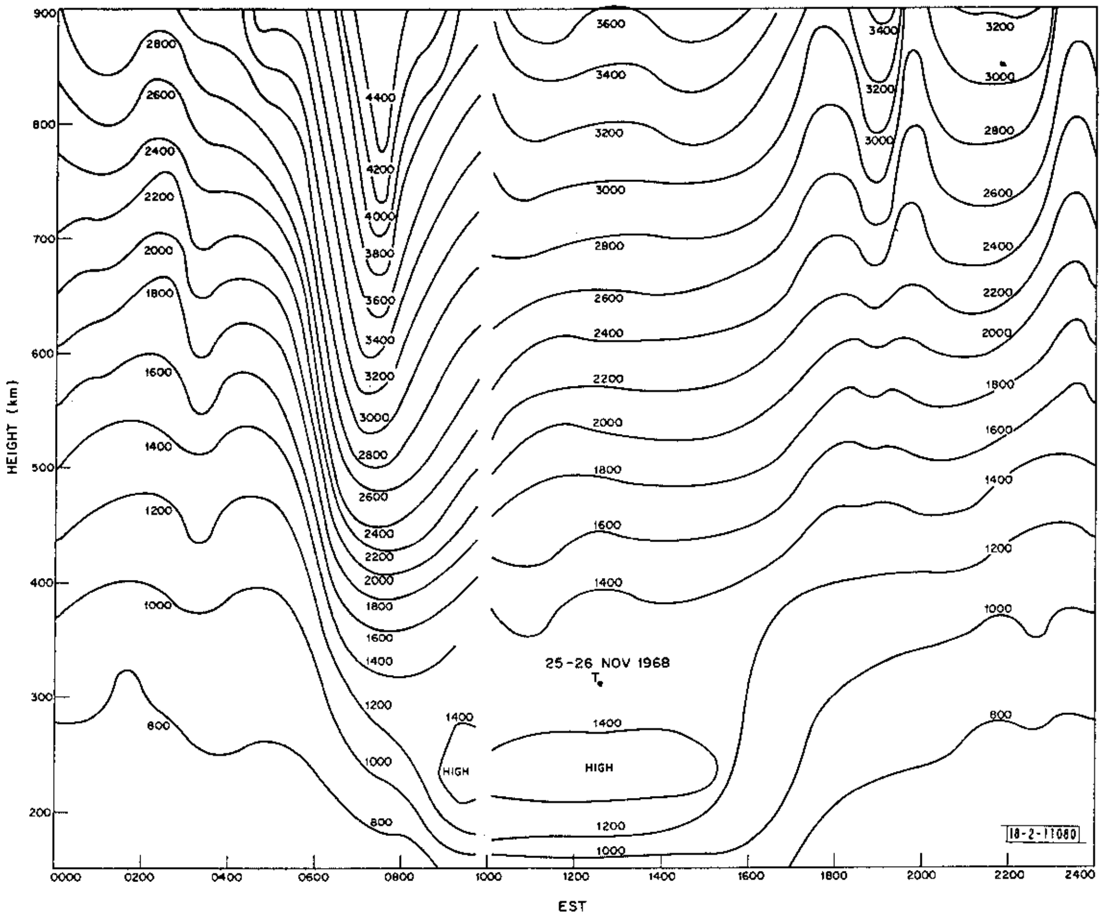

(o)

Fig. 5(a–s). Continued.

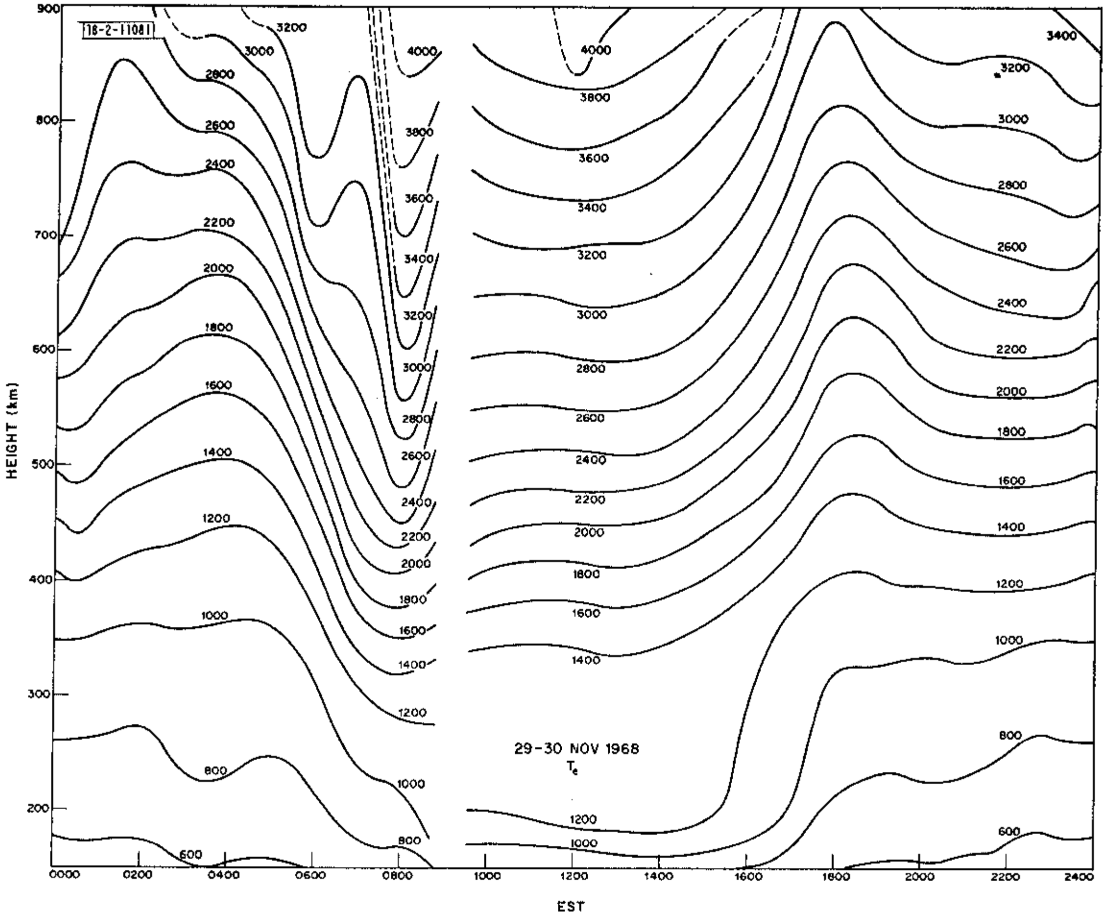

(p)

Fig. 5(a–s). Continued.

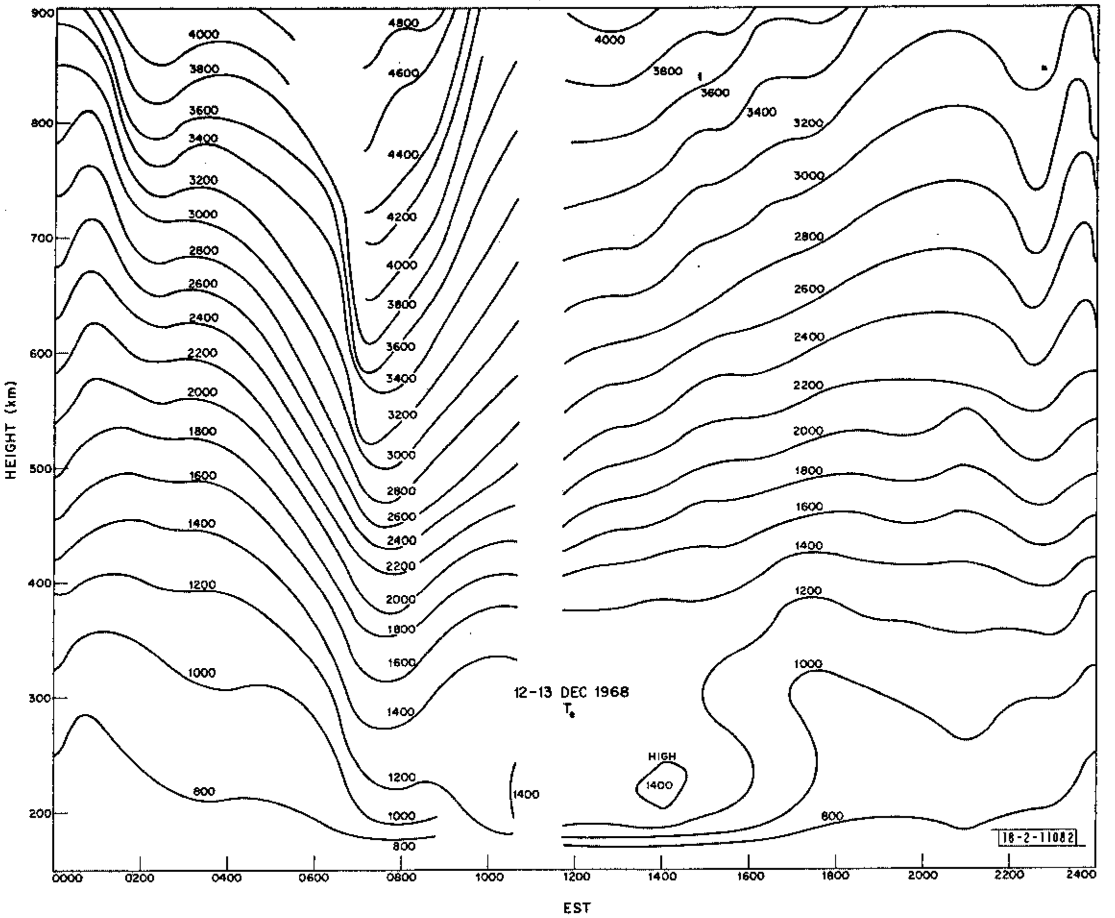

(q)

Fig. 5(a-s). Continued.

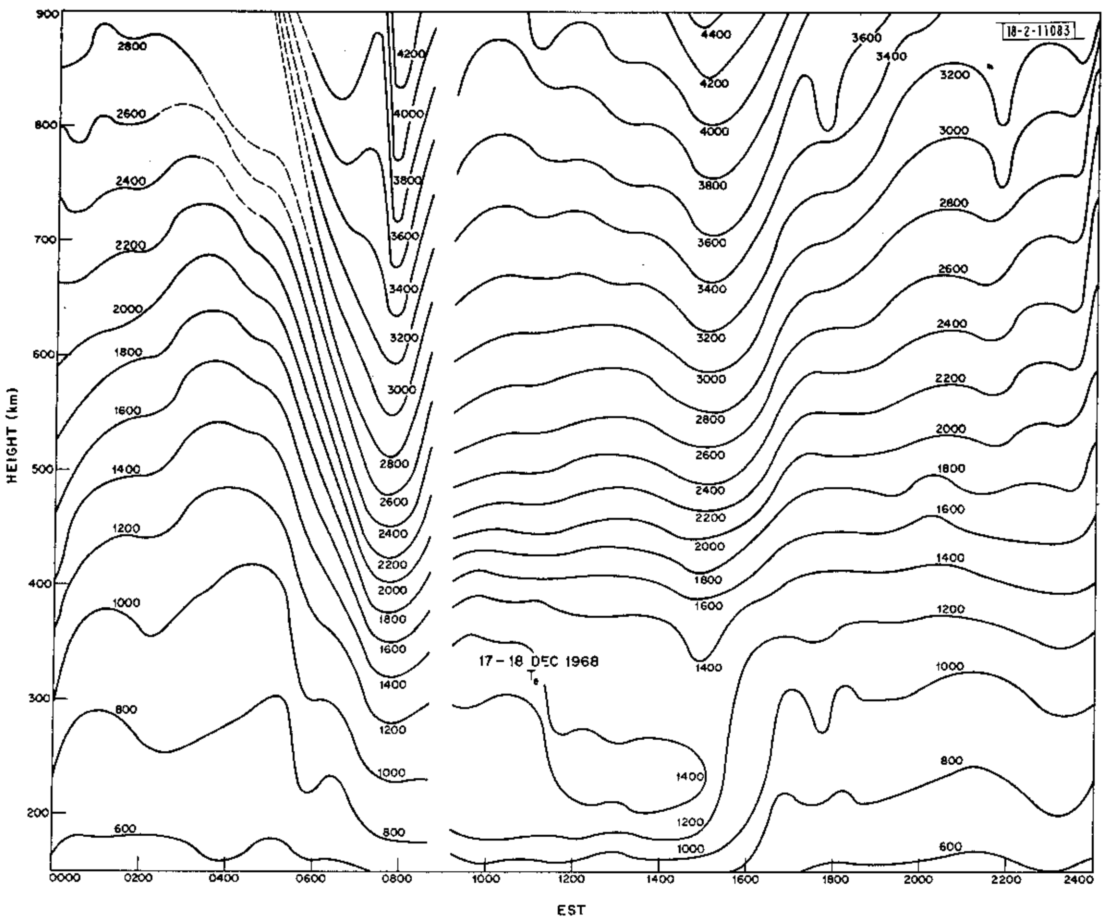

(r)

Fig. 5(a–s). Continued.

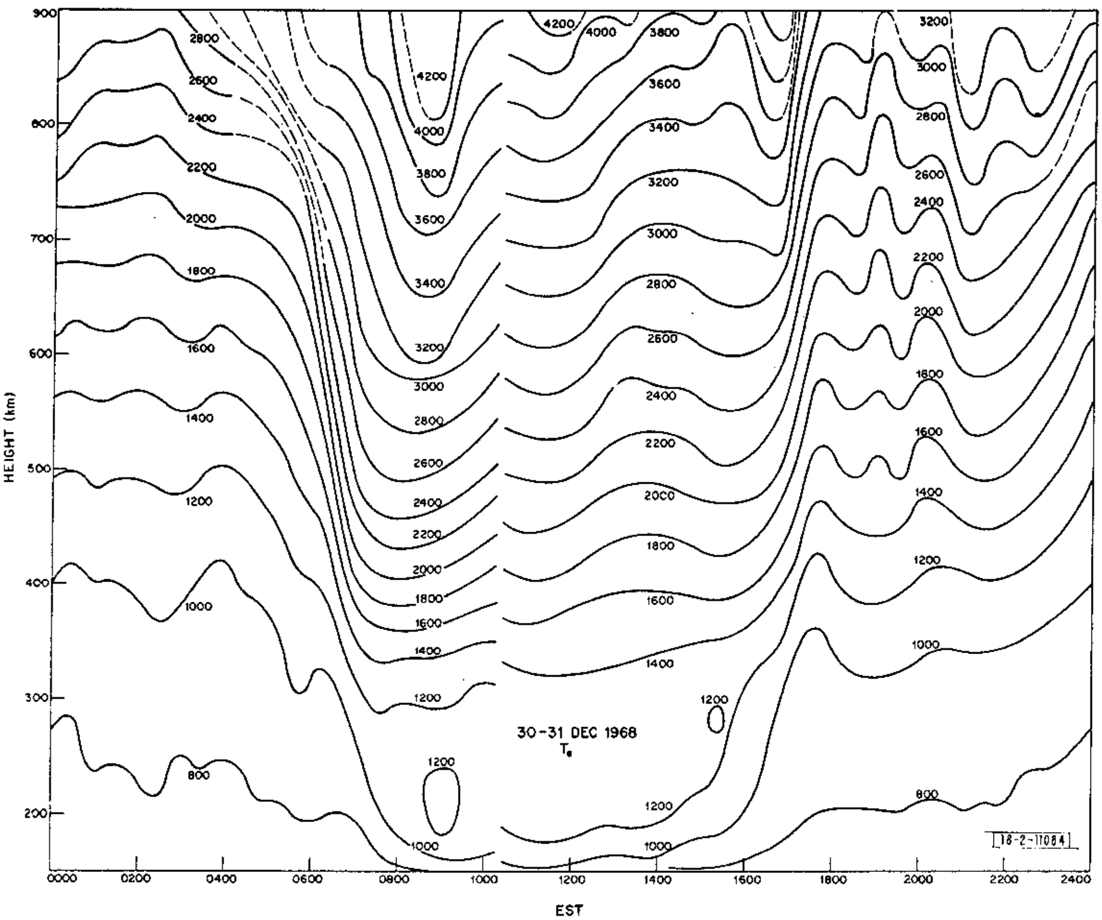

(s)

Fig. 5(a-s). Continued.

There is a large increase in temperature at all levels at sunrise that is followed by a period lasting until sunset when the temperature remains essentially constant with time. At sunset, the temperature decreases, albeit less rapidly than the corresponding increase at sunrise. The nighttime temperatures are much lower than those observed during the day and usually exhibit a shallow minimum near midnight. Examples of this behavior are presented in Figs. 4(b) through (d).

In winter, the variation both with altitude and time is frequently more complex. At night, the temperature remains high owing to the heating of the magnetosphere by photo-electrons escaping from the conjugate ionosphere which then remains sunlit. Thus, the lowering of the electron temperature following local sunset in winter is usually arrested near 2000, and the temperature may then increase as the density continues to decrease [see Figs. 4(a), 4(b)]. At sunspot minimum, the temperature is usually found to decrease after midnight in association with the early morning density increase. This phenomenon can be seen most clearly for 23-24 January [Fig. 4(b)] and somewhat less markedly on several days toward the end of the year [Figs. 5(p) through (s)]. These nocturnal temperature variations tend to cause the temperature increase that occurs at sunrise to appear much more pronounced than the decrease at sunset. In summer, the two usually are of comparable amplitude.

Yet another feature of the winter behavior is the appearance, during portions of the day, of a temperature minimum at an altitude somewhat above $h_{max}F2$, i.e., typically 350 km. This feature can be seen in Figs. 4(a), 4(d), 4(e) and Figs. 5(e) through (h), 5(o), 5(q) through (s). This minimum is produced by strong local cooling of the electron temperature which occurs whenever the electron density at this altitude is particularly high. Previously,[5] we reported that a local electron density $N_e \geq 10^6$ el/cm^3 at 300 km appeared to be the necessary condition for the development of this temperature minimum. A somewhat better statement, based on the present results, might be that the local density at the height of the minimum should exceed about $7\text{-}8 \times 10^5$ el/cm^3 depending somewhat on the exact altitude.

This temperature minimum has been observed on days that, based on the diurnal variation of the density, would be classed as "summer." Examples are provided by 25-26 April, 23-24 May [Figs. 4(g), 4(h)] and 11-12 September [Fig. 5(f)]. Thus, this feature should be associated with the above density condition rather than season. Owing to the annual variation in the density, the condition is reached more often in winter than summer, and at Millstone only encountered during years near sunspot maximum.[4,5,12]

The electron temperature appears to be a sensitive indicator of abnormal behavior. The very high values observed on 16-17 January beginning near 0230 [Fig. 4(a)], we believe are associated with the motion of the mid-latitude trough over Millstone.[12] Similarly, the high temperatures following sunrise on 26-27 March [Fig. 4(e)] are believed to be associated with the negative phase of the ionospheric storm then in progress. In part, the higher temperatures result from lower than normal densities, but in some storms large heat fluxes from the protonosphere also contribute.[10] These fluxes are presumed to be produced by the decay of ring current particles through ion-cyclotron damping – the same process that appears to be responsible for nighttime mid-latitude red arcs.[21] An impressive example of nocturnal heating, probably caused by this process is provided by the results for 12-13 September [Fig. 5(g)] during the period 2200-2400. The large temperature increase occurring at this time does not appear to be associated with particularly low electron densities [Fig. 3(g)] as would be the case when the trough lies overhead, but with high E-region densities that occur when there is precipitation of ionizing particles.

In general, the results for 1968 appear to contain fewer instances of anomalous temperature behavior than 1967, despite the increase in sunspot level and magnetic activity. We believe that this simply reflects the fact that, by chance, fewer of the days of observation were magnetically disturbed.

C. Ion Temperature

Ion temperature results for the period July through December are presented in Figs. 6(a) through (s) as isotherms at 100°K intervals as functions of height and time. The ion temperature reaches a nearly isothermal level between 250 and 350 km, and this gives rise to the erratic fluctuation in the height of the isotherm(s) in this interval [e.g., Figs. 6(r), 6(s)]. Below about 350 km, the ion temperature is largely governed by the thermal coupling with neutral particles. Thus, the ion temperature is usually only slightly greater than the neutral temperature and exhibits a similar diurnal variation. Thus, the ion temperature at these levels usually reaches a shallow maximum in the afternoon and a minimum just before sunrise.

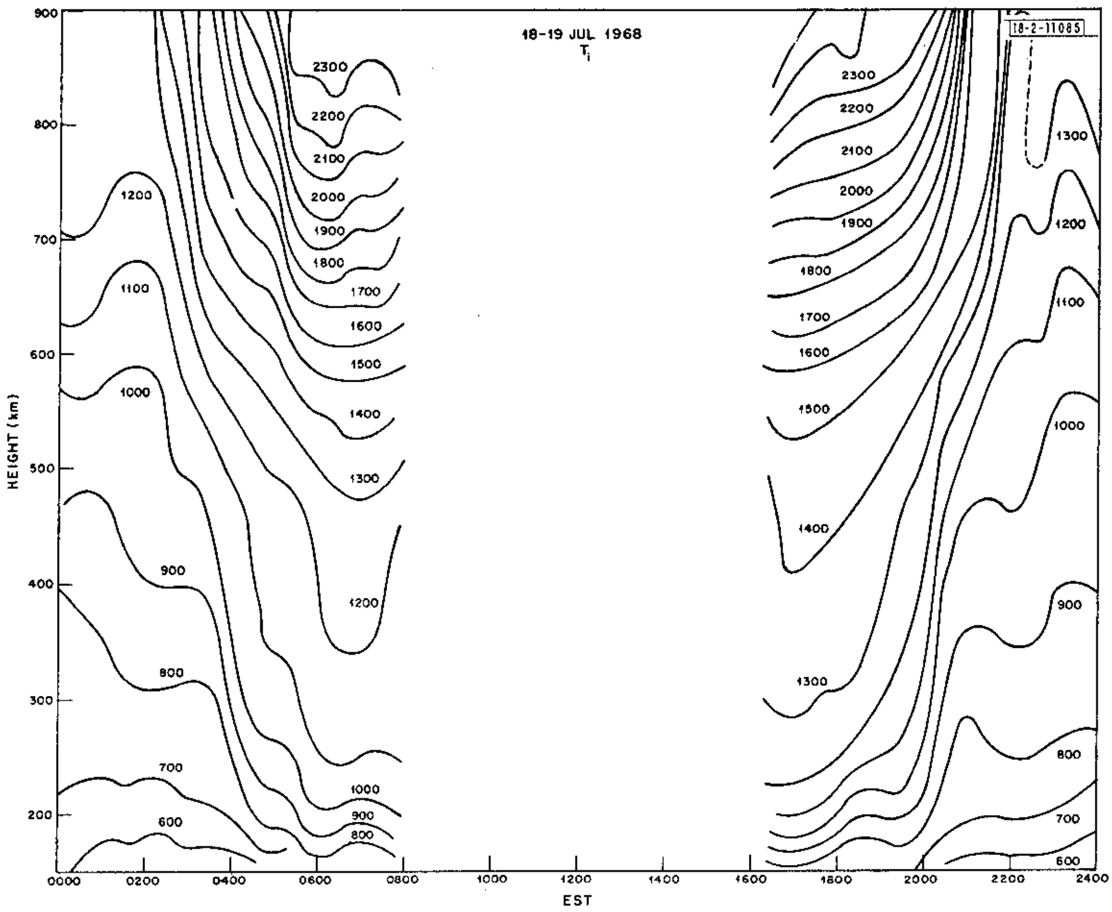

(a)

Fig. 6(a–s). Contour diagrams of constant ion temperature (in 100°K steps) as functions of height and time gathered during the last six months of 1968.

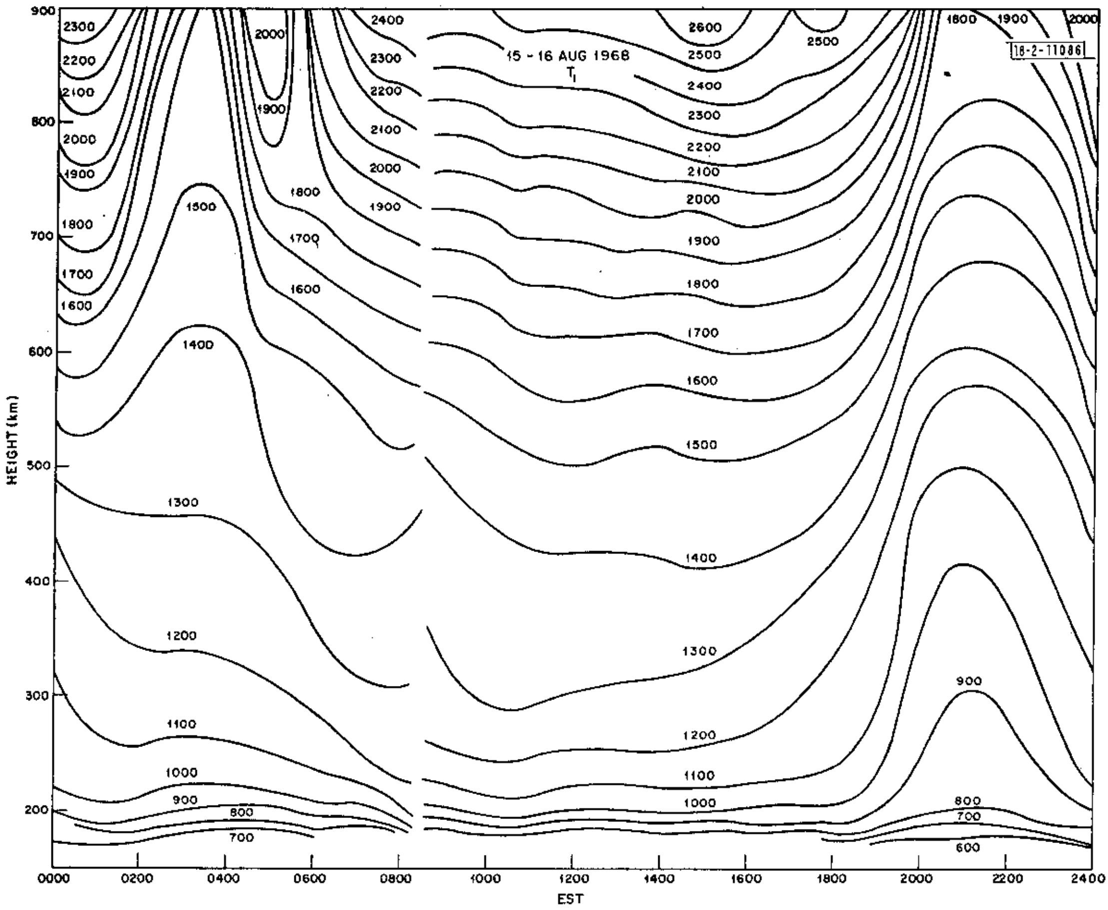

(b)

Fig. 6(a–s). Continued.

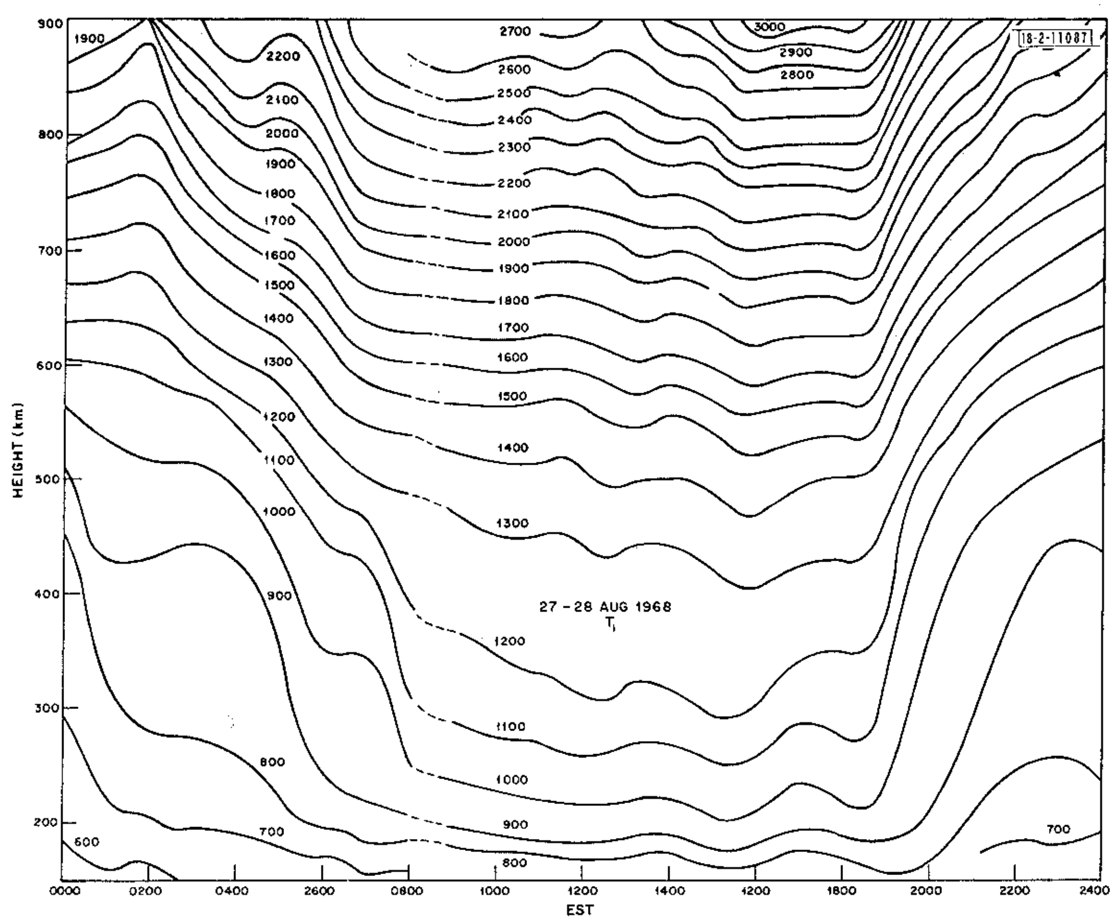

(c)

Fig. 6(a–s). Continued.

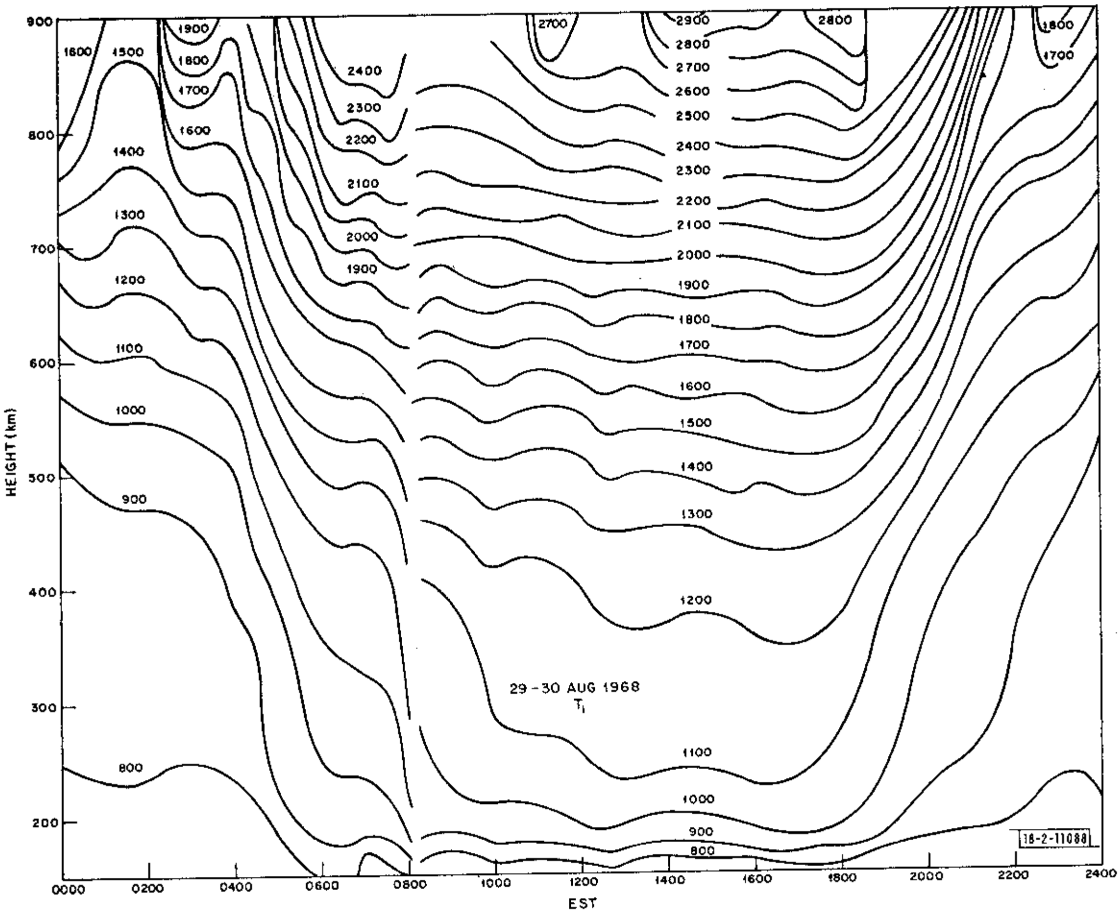

(d)

Fig. 6(a–s). Continued.

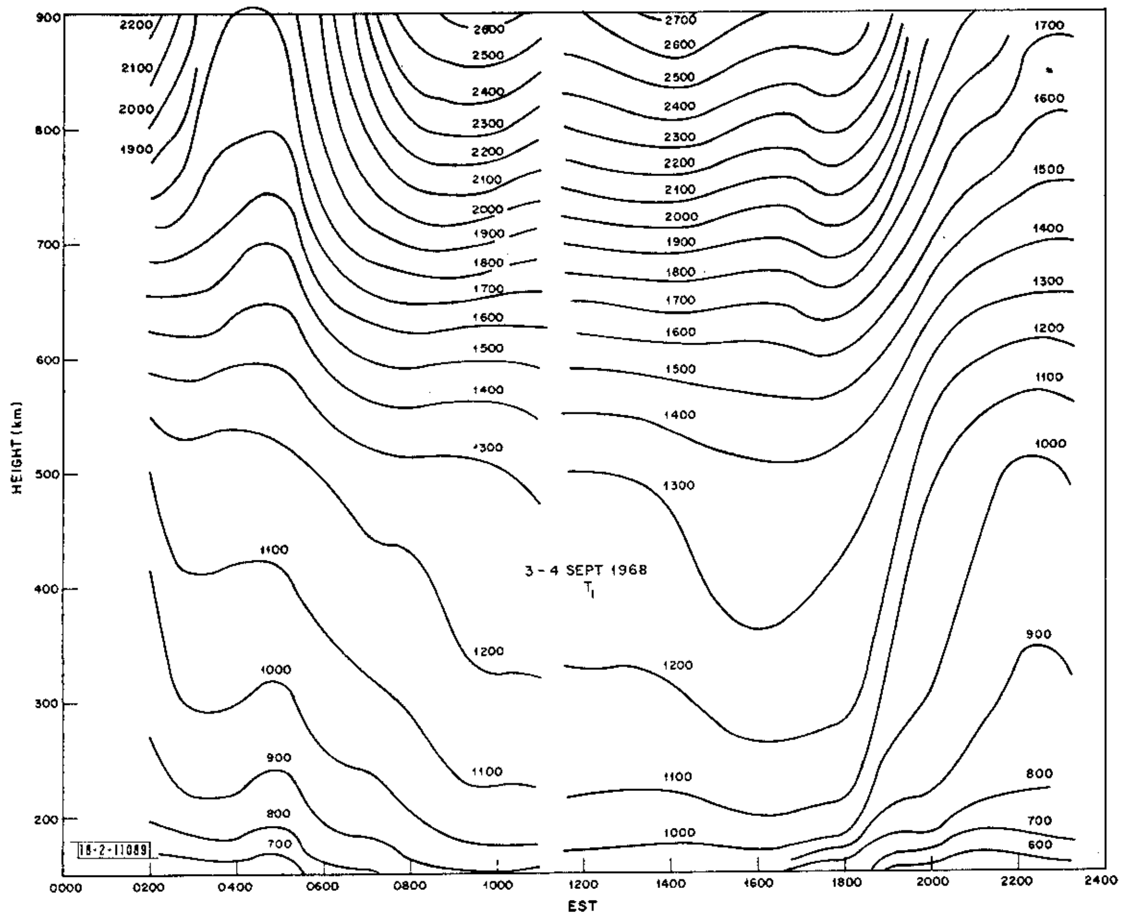

(e)

Fig. 6(a-s). Continued.

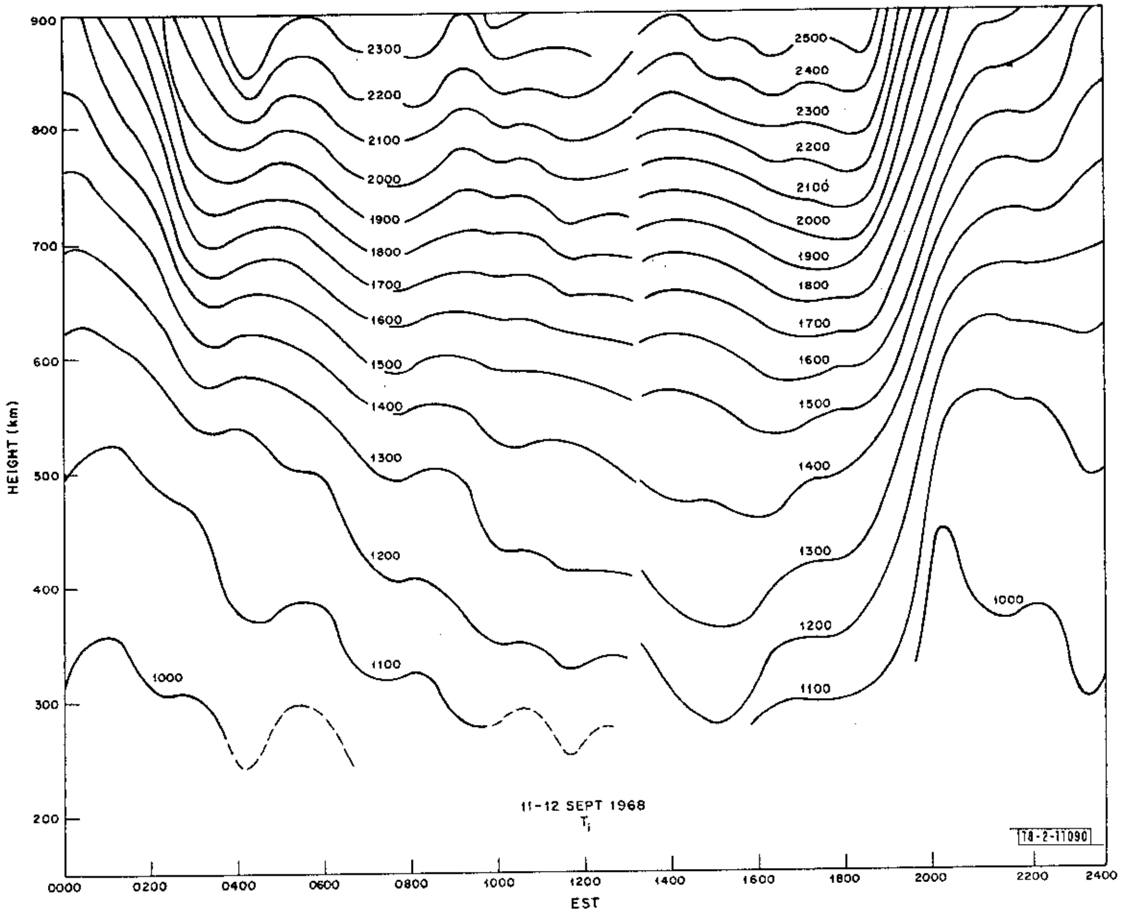

(f)

Fig. 6(a–s). Continued.

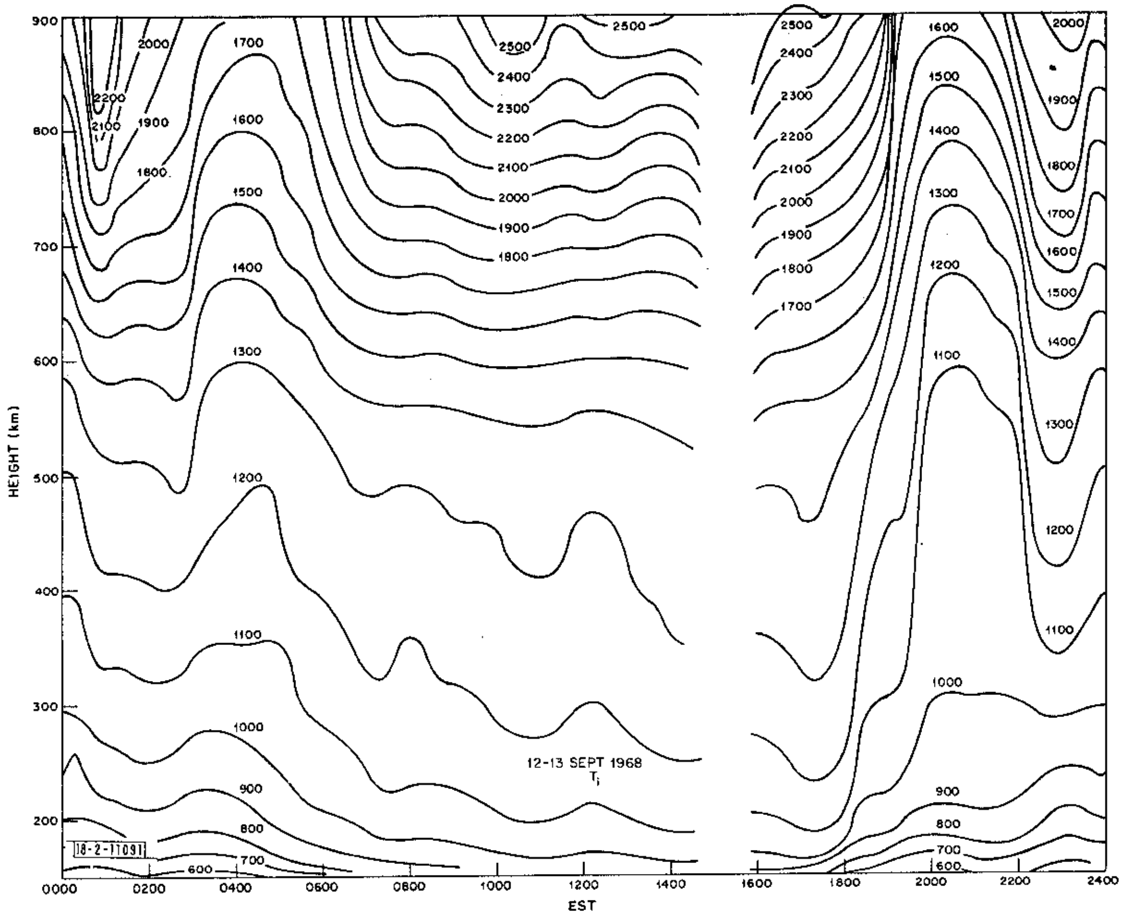

(g)

Fig. 6(a–s). Continued.

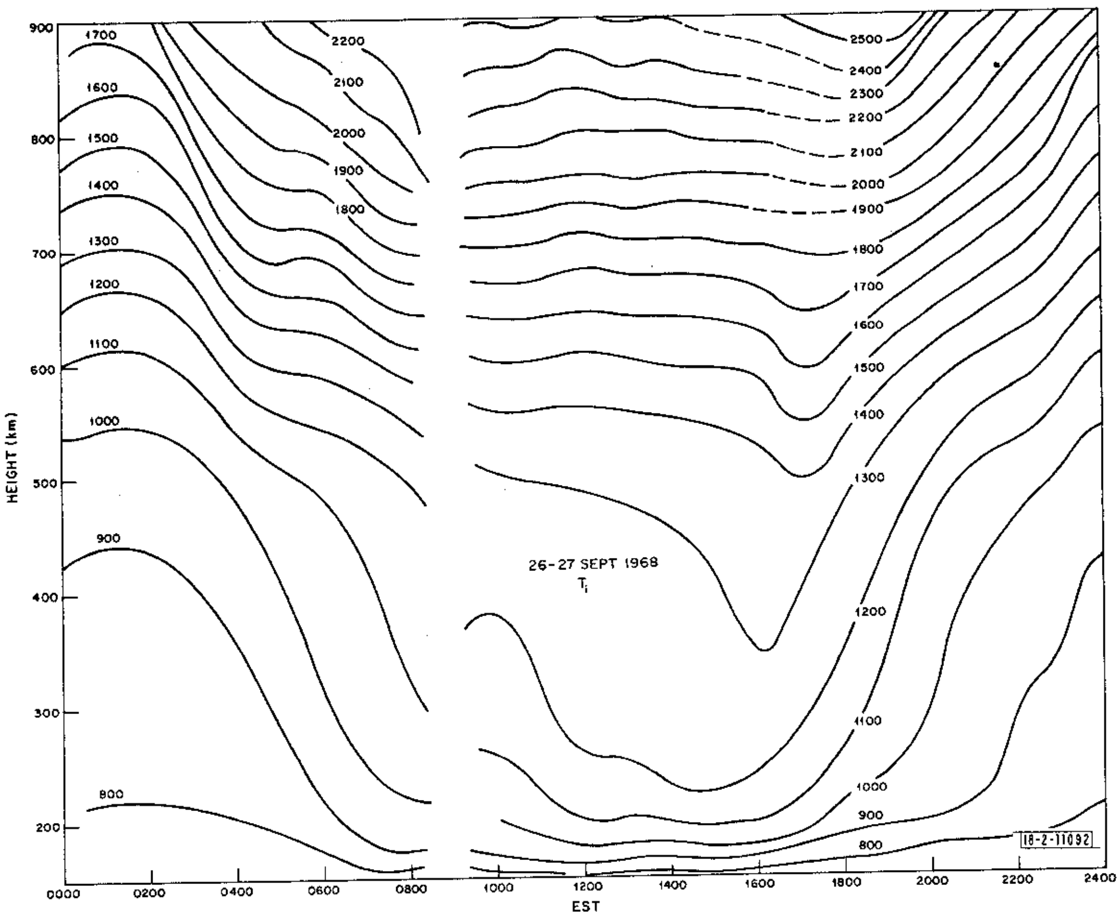

(h)

Fig. 6(a-s). Continued.

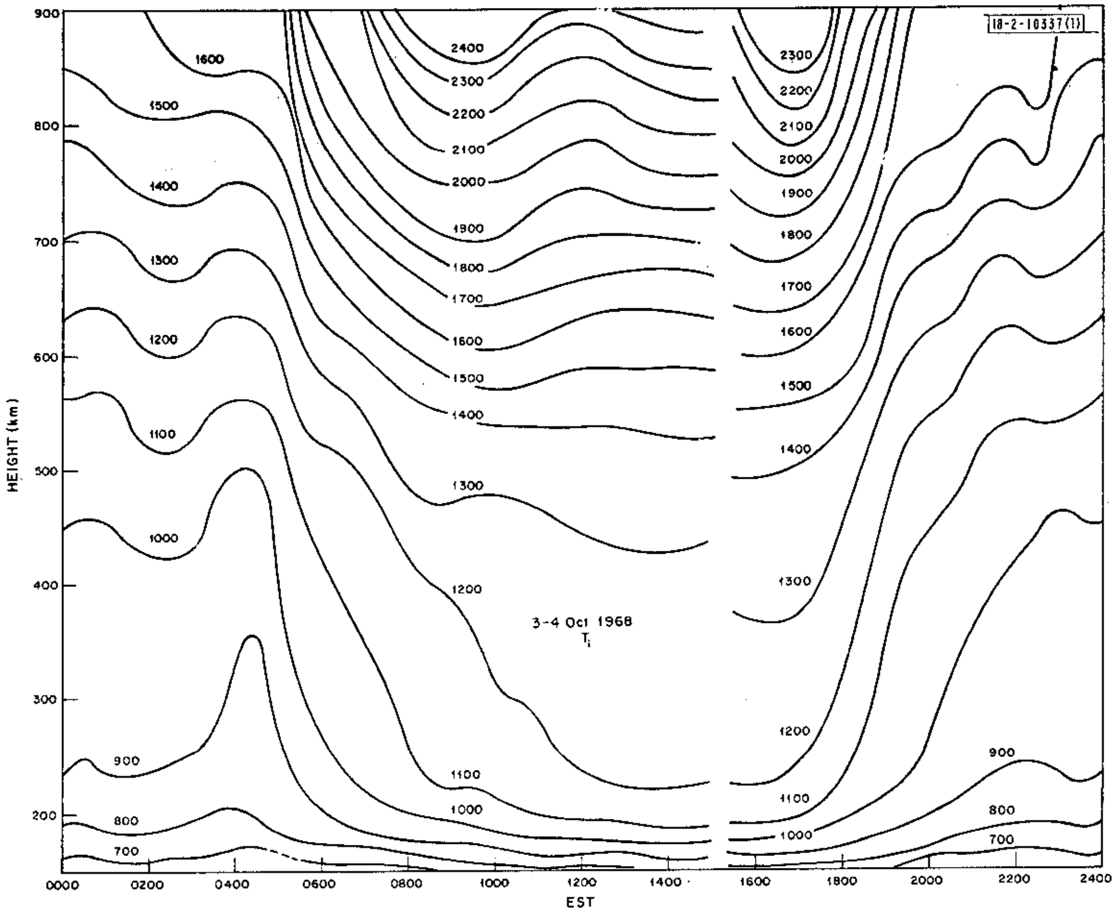

(i)

Fig. 6(a–s). Continued.

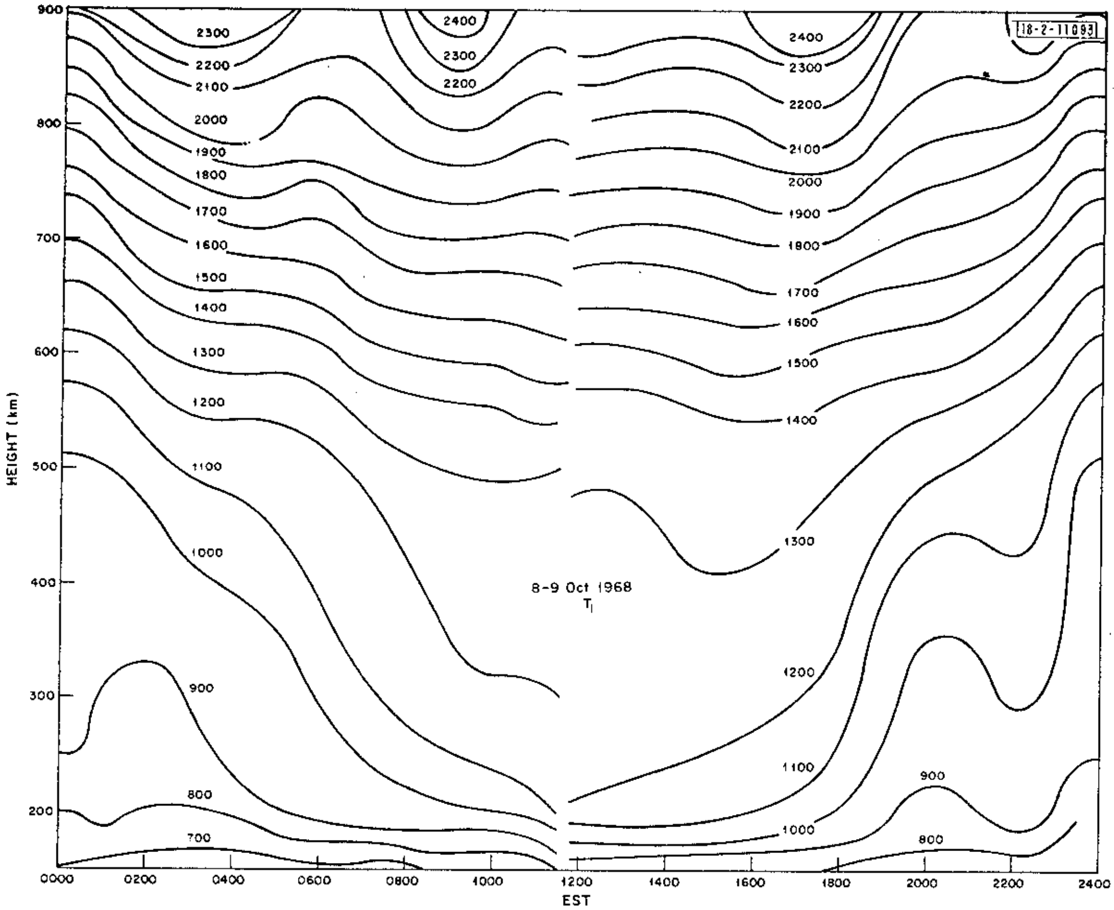

(j)

Fig. 6(a–s). Continued.

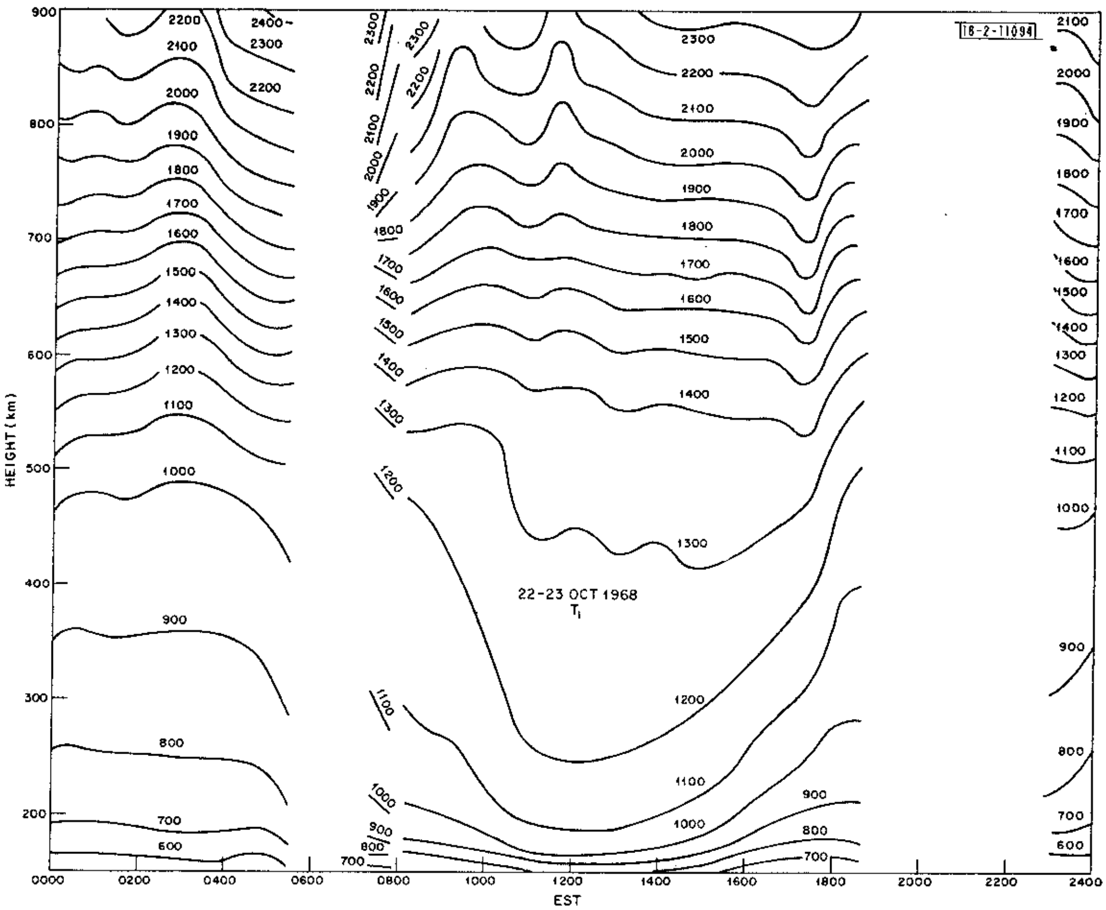

(k)

Fig. 6(a-s). Continued.

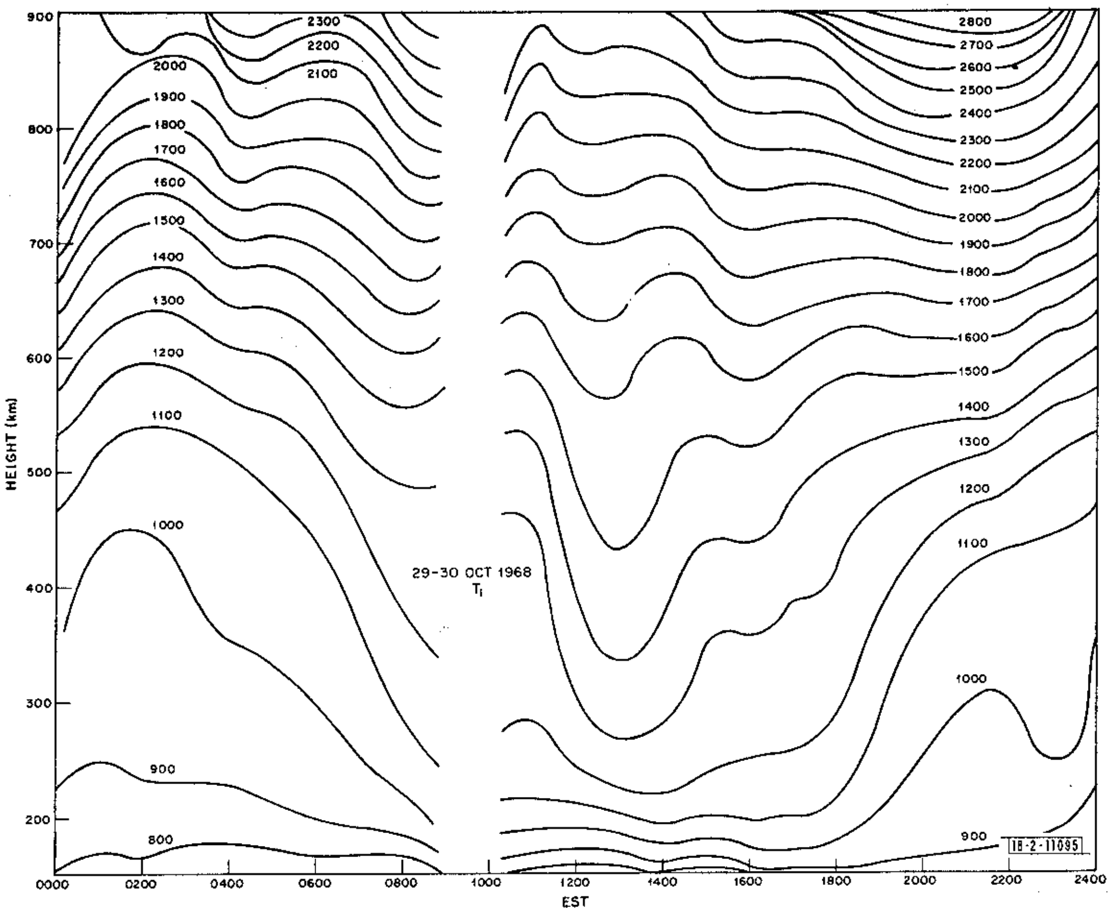

(l)

Fig. 6(a–s). Continued.

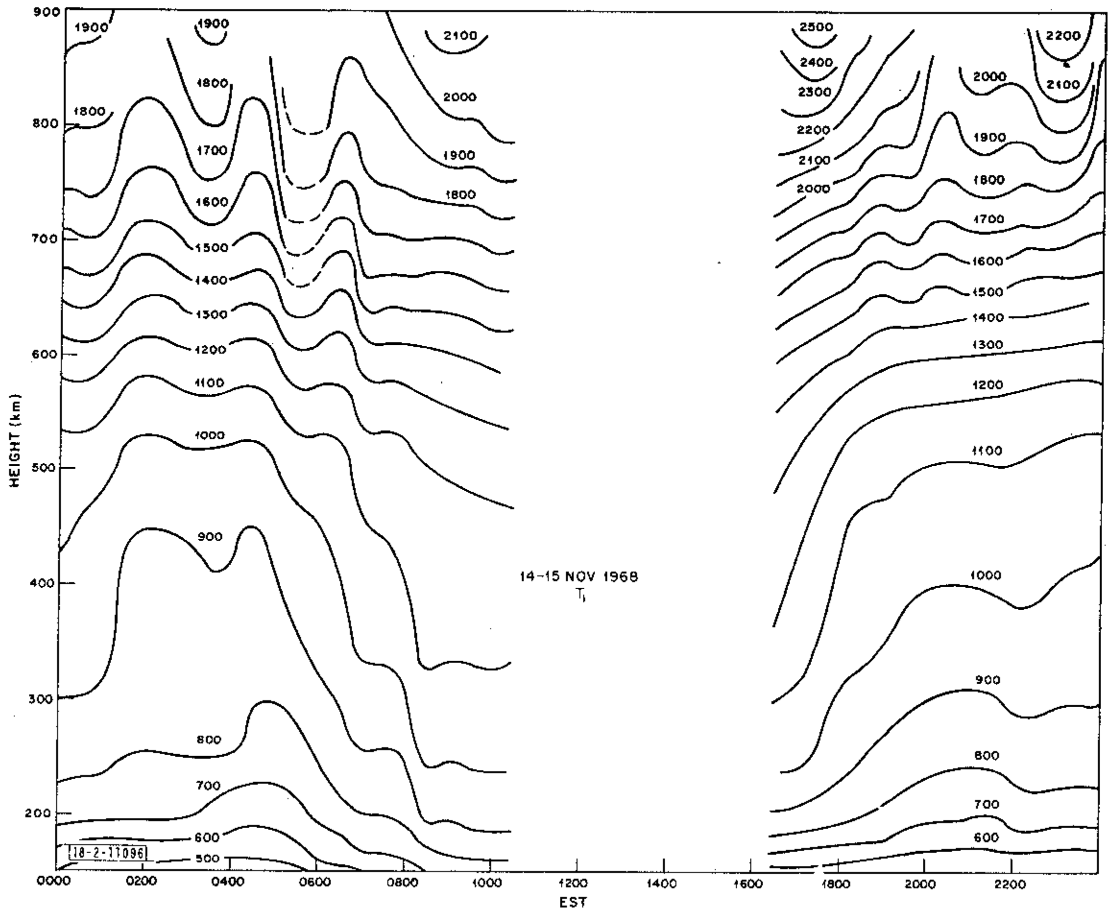

(m)

Fig. 6(a–s). Continued.

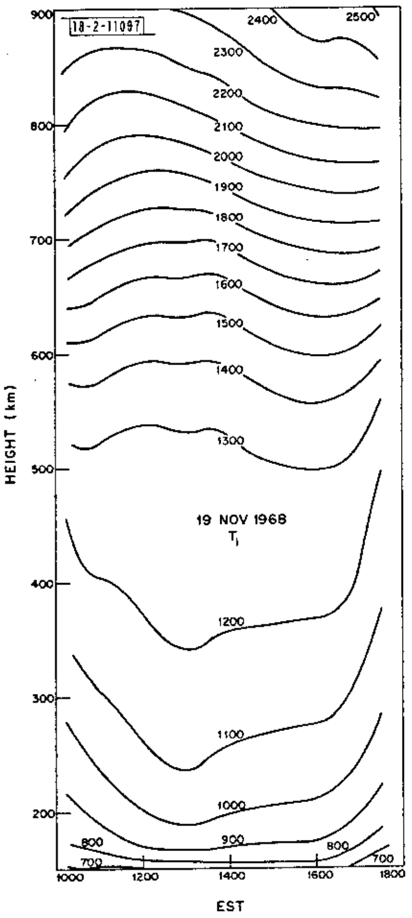

(n)

Fig. 6(a–s). Continued.

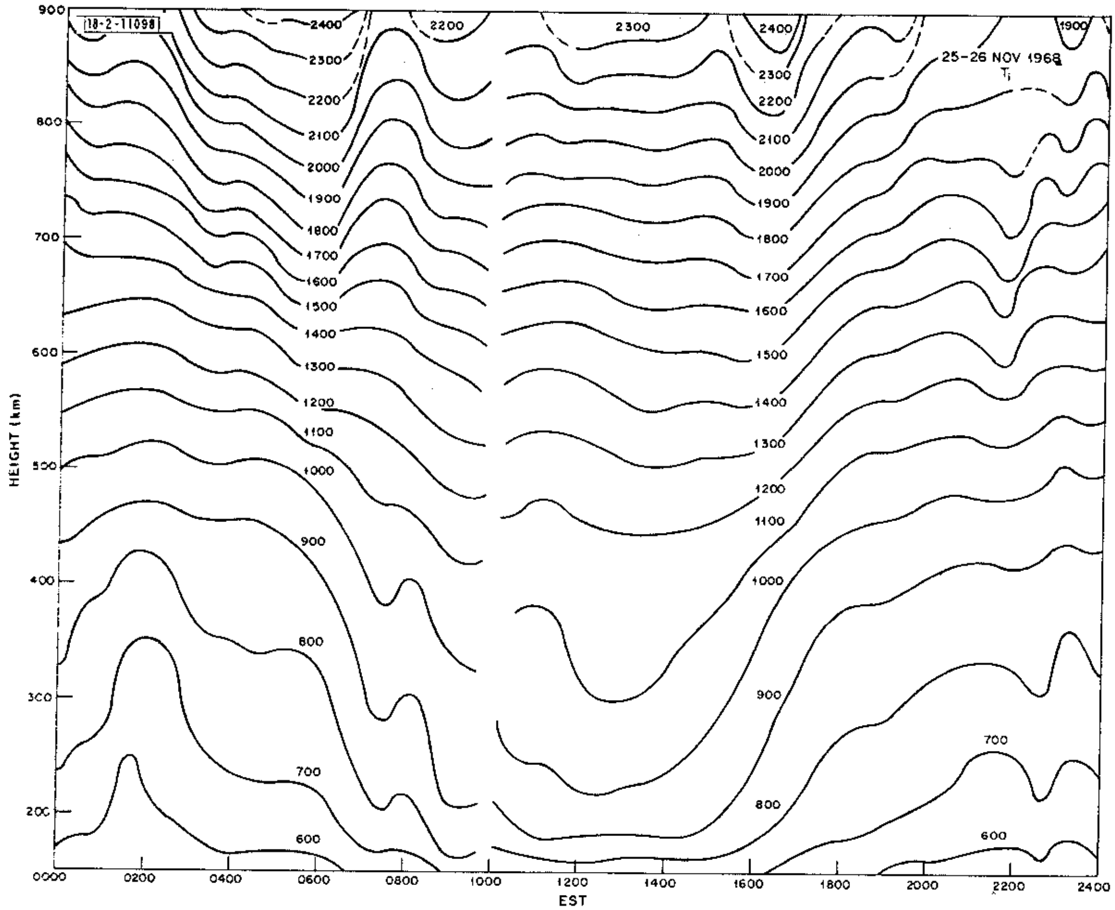

(o)

Fig. 6(a–s). Continued.

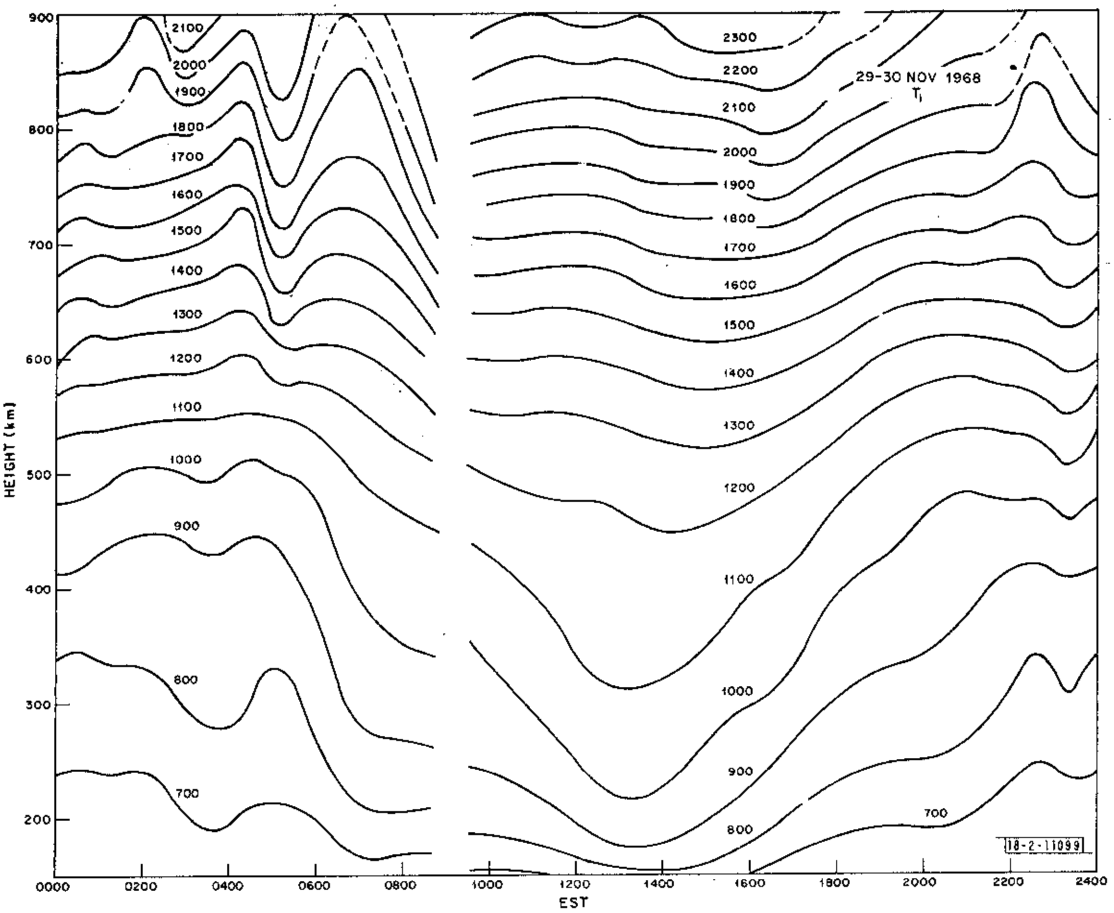

(p)

Fig. 6(a-s). Continued.

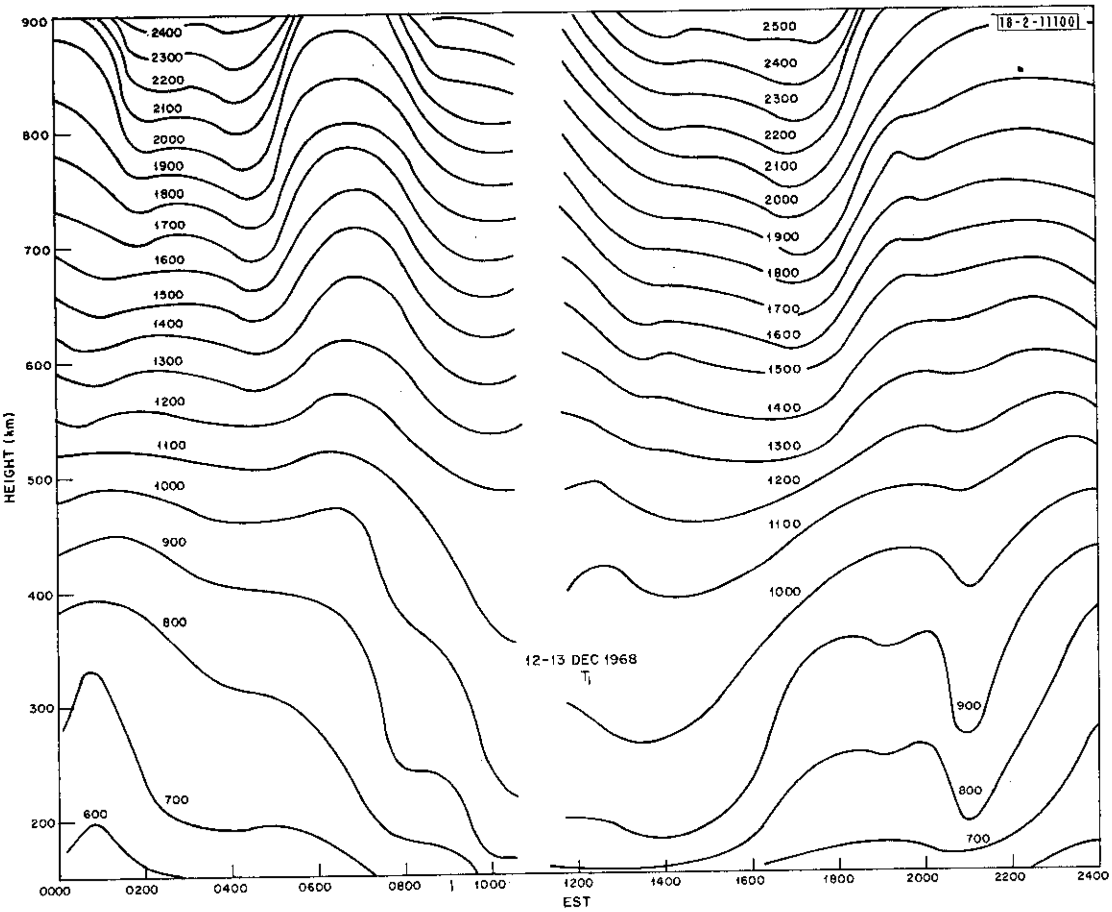

(q)

Fig. 6(a–s). Continued.

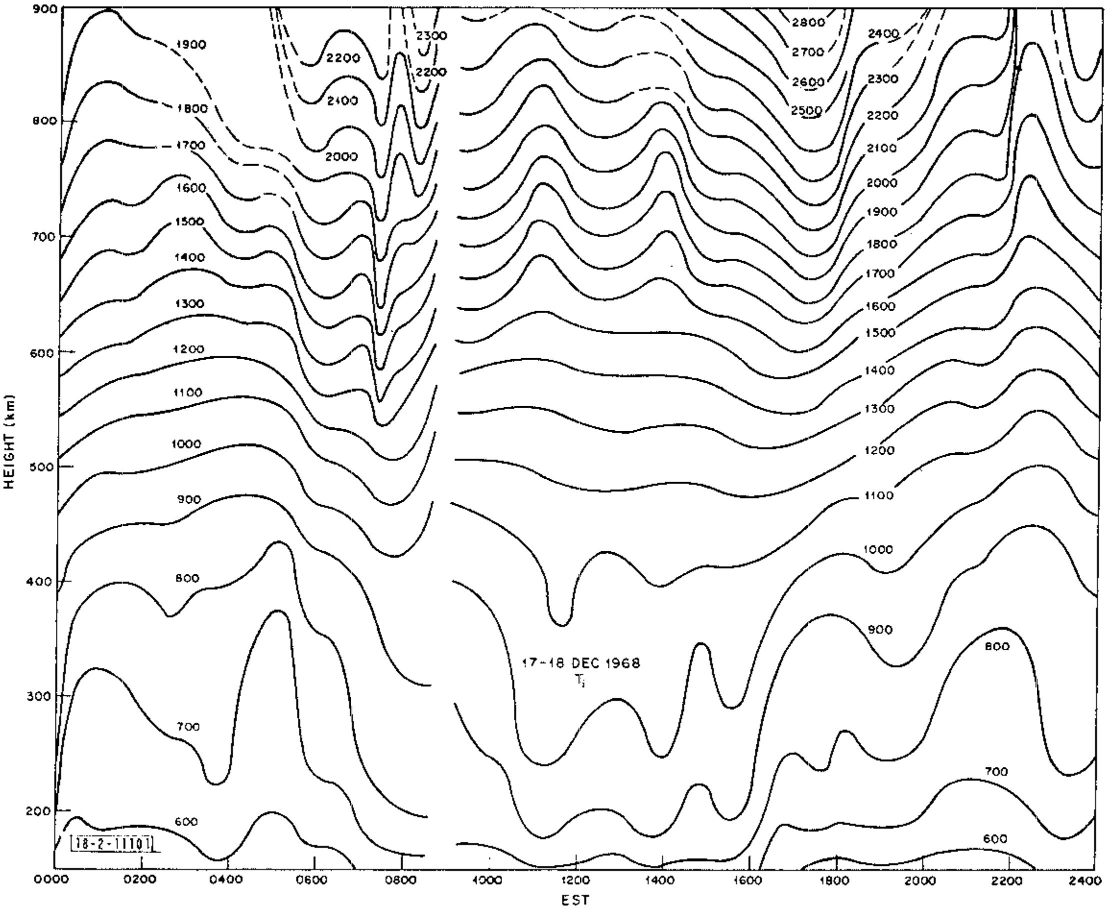

(r)

Fig. 6(a–s). Continued.

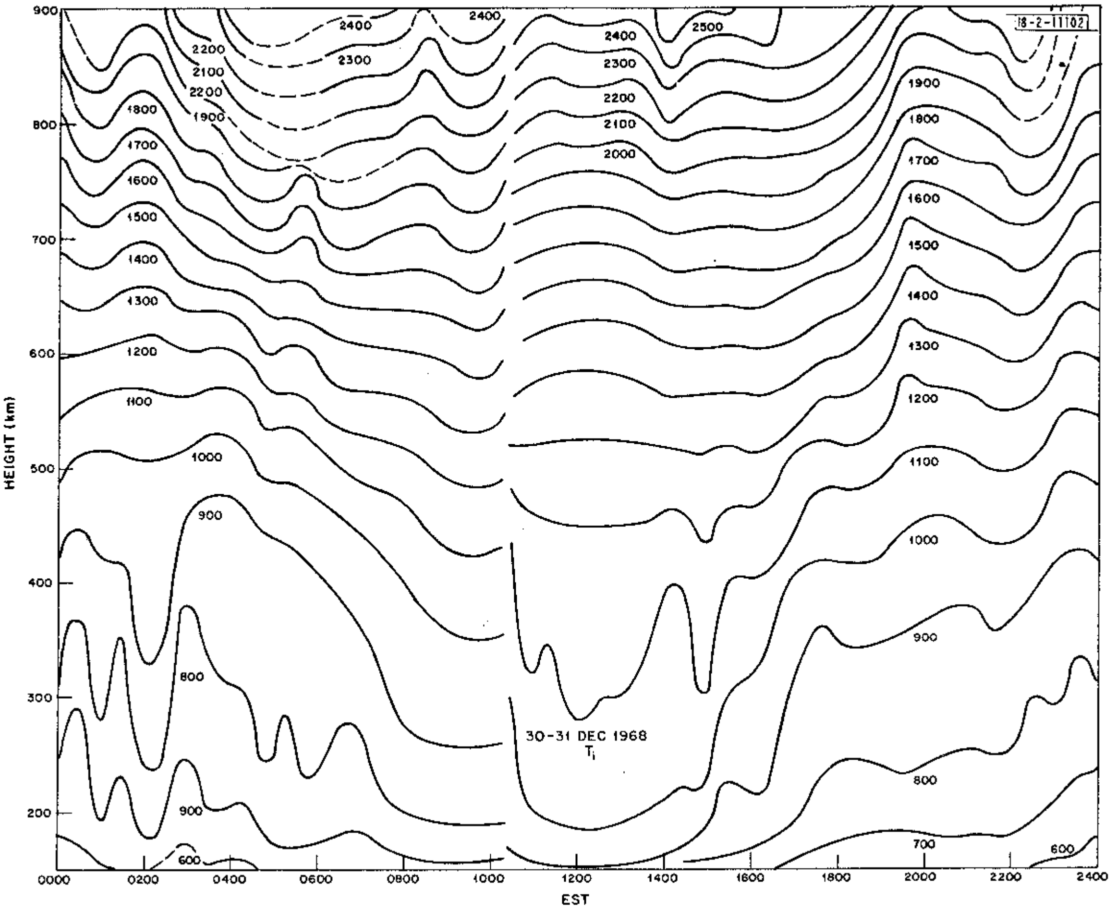

(s)

Fig. 6(a–s). Continued.

Above about 400 km altitude, T_i increases rapidly and converges toward the electron temperature. At these altitudes, the ions are heated by Coulomb encounters with electrons, and their temperature tends to follow changes in electron temperature. Thus, the increase and decrease in temperature at sunrise and set can be quite marked [e.g., Figs. 6(b) through (d)] and instances of nocturnal heating can be recognized [e.g., Fig. 6(g)].

D. Average Temperature Profiles

At sunspot minimum, it was found that for large portions of the day and the night the electron and ion temperatures did not vary appreciably.[1-3] Owing to the poor quality of some of the results, this encouraged the construction of average temperature curves in an attempt to better define the variation with altitude. Two averages were constructed, viz., daytime (1000-1500 EST) and nighttime (2100-0300 EST). As sunspot maximum was approached, the justification for averaging the results was reduced, yet the practice was continued as it provided a useful way of detecting seasonal and sunspot cycle trends.[22] These average temperature curves were constructed for the data gathered prior to July 1968 and are shown in Figs. 7(a) through (i); thereafter, this work was discontinued.

The curves shown in Figs. 7(a) through (i) were obtained in the manner employed previously,[5] i.e., by computing the average of the electron temperatures read (at 100 km intervals) off the original curves obtained in these two time intervals. Several of the winter daytime curves [e.g., Figs. 7(a), 7(d), 7(e)] clearly show the temperature minimum that then develops.

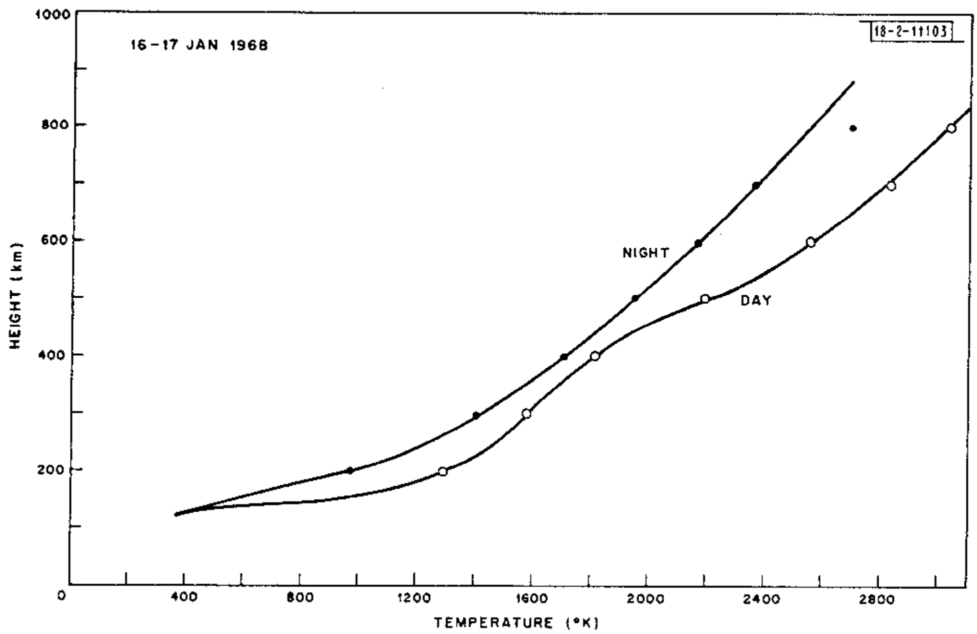

(a)

Fig. 7(a-i). Average daytime (1000-1500 EST) and nighttime (2100-0300) electron temperatures vs altitude observed during the first six months of 1968.

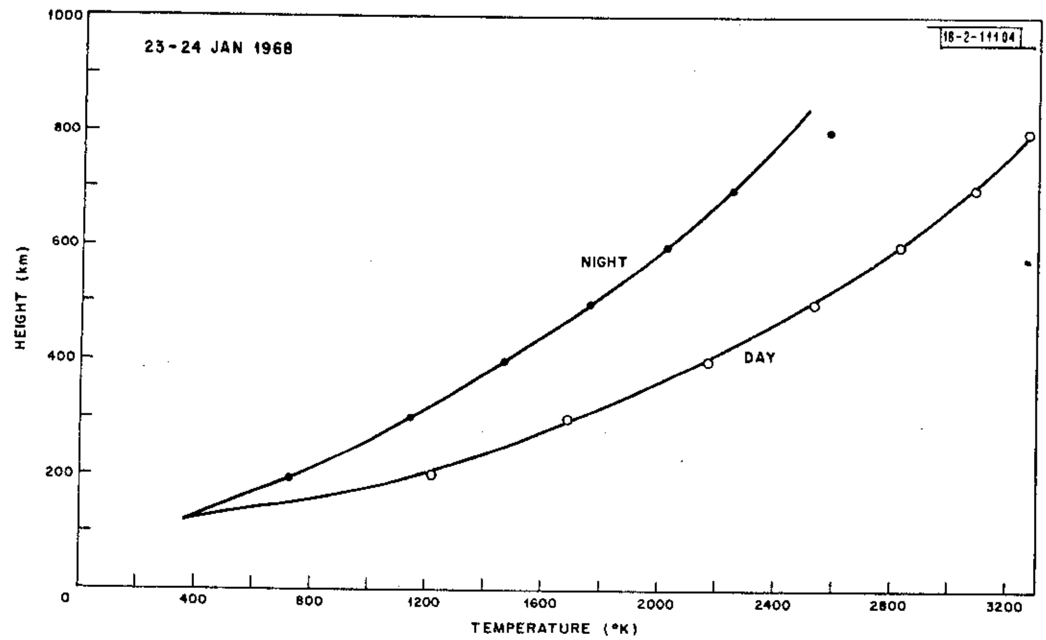

(b)

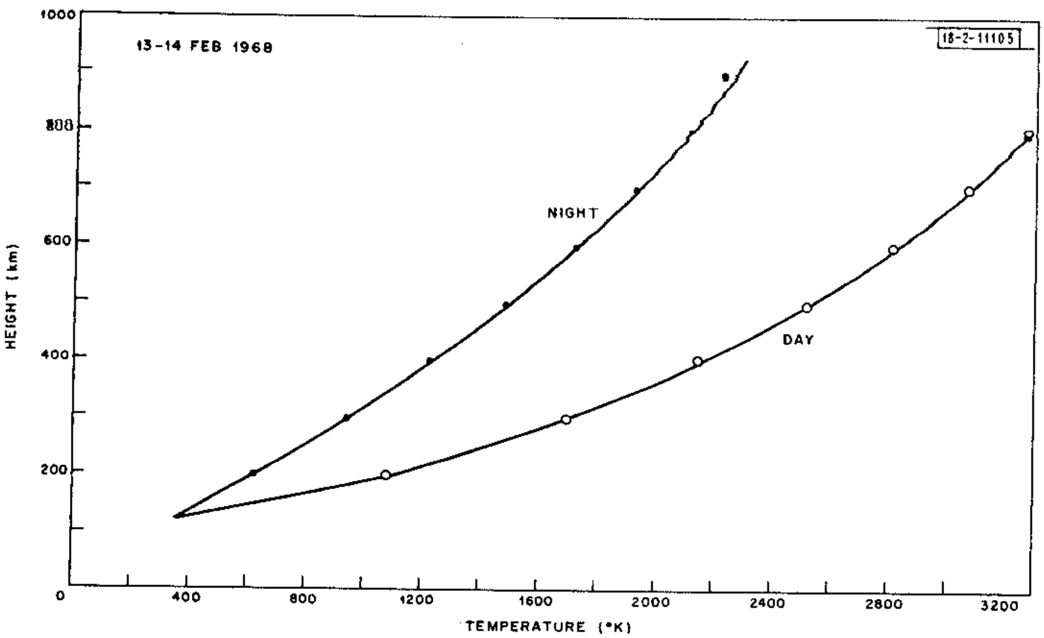

(c)

Fig. 7(a-i). Continued.

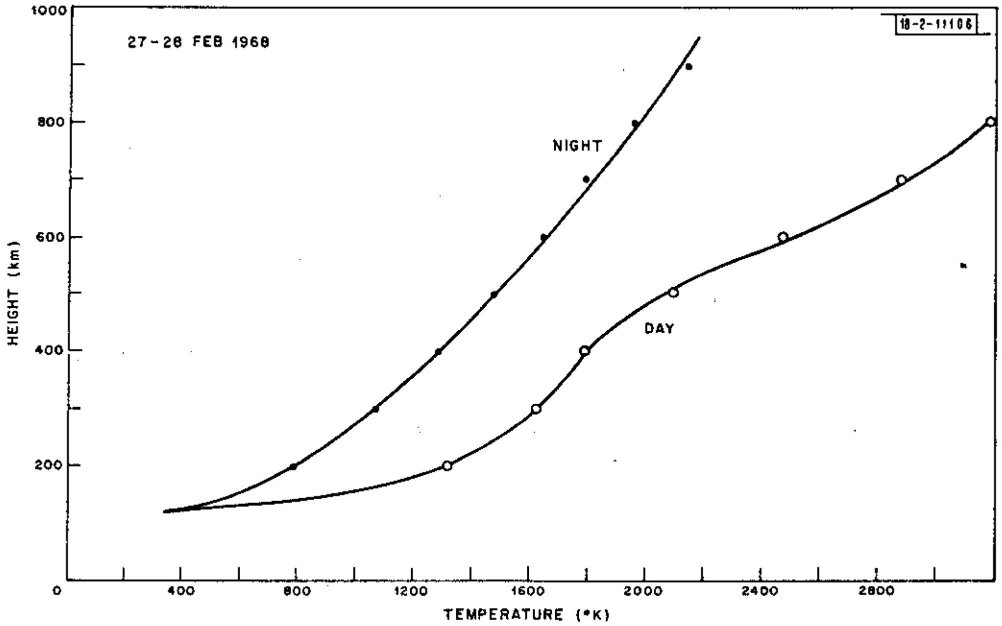

(d)

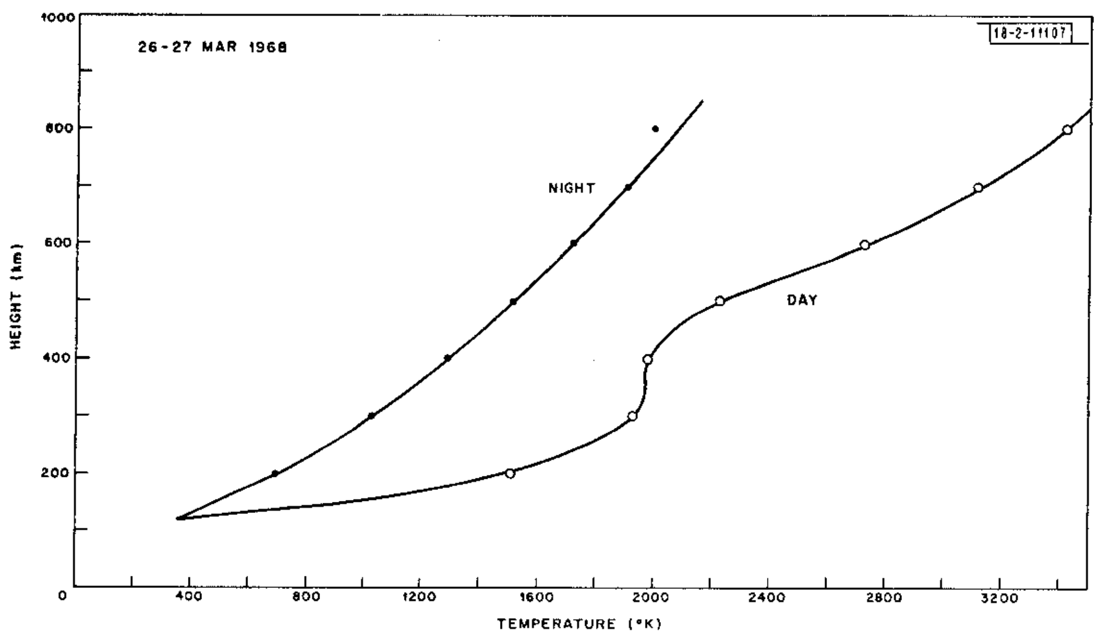

(e)

Fig. 7(a-i). Continued.

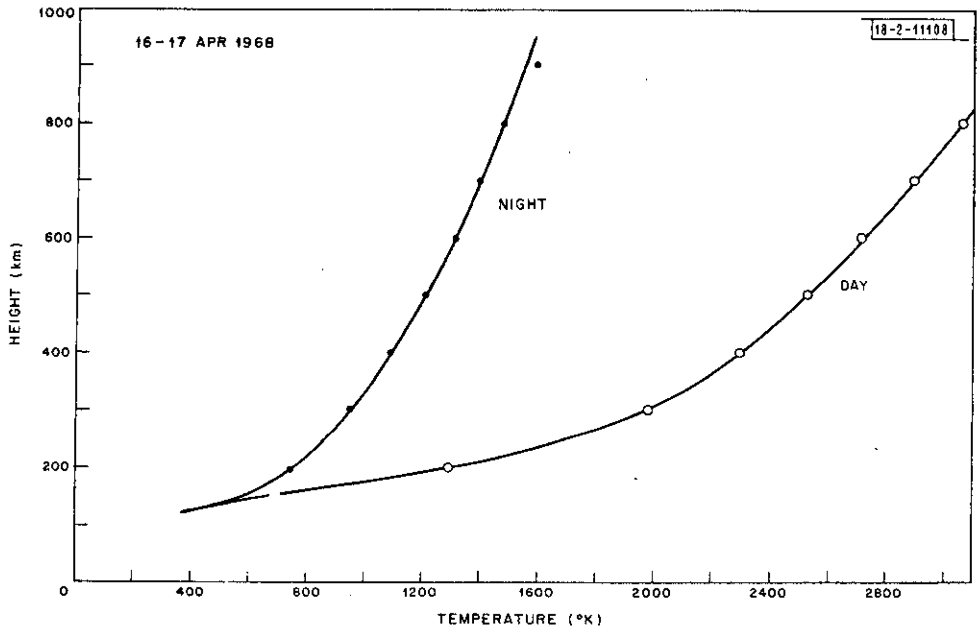

(f)

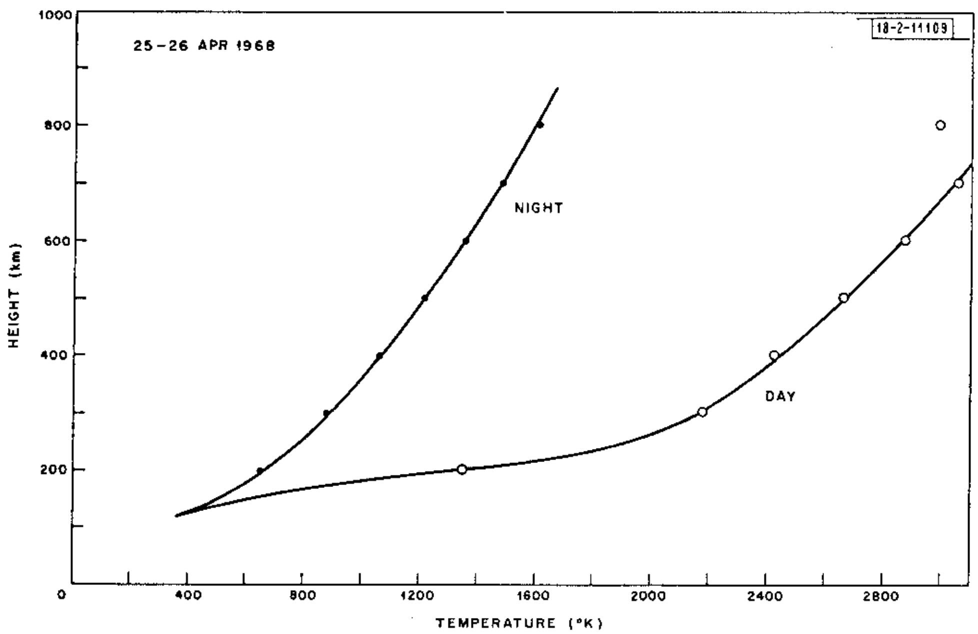

(g)

Fig. 7(a-i). Continued.

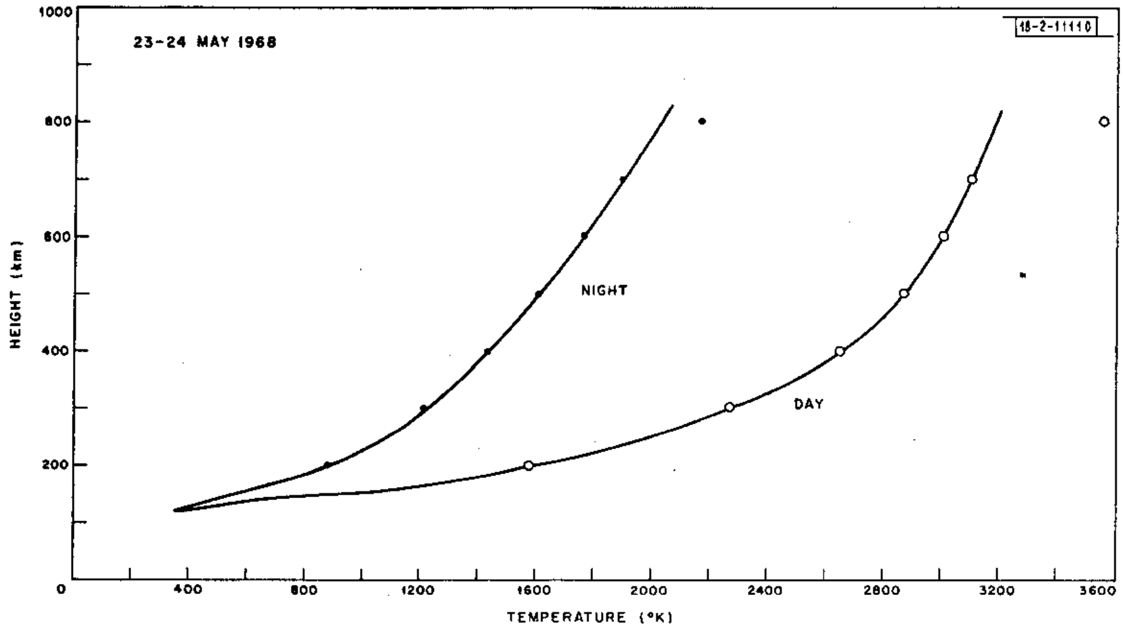

(h)

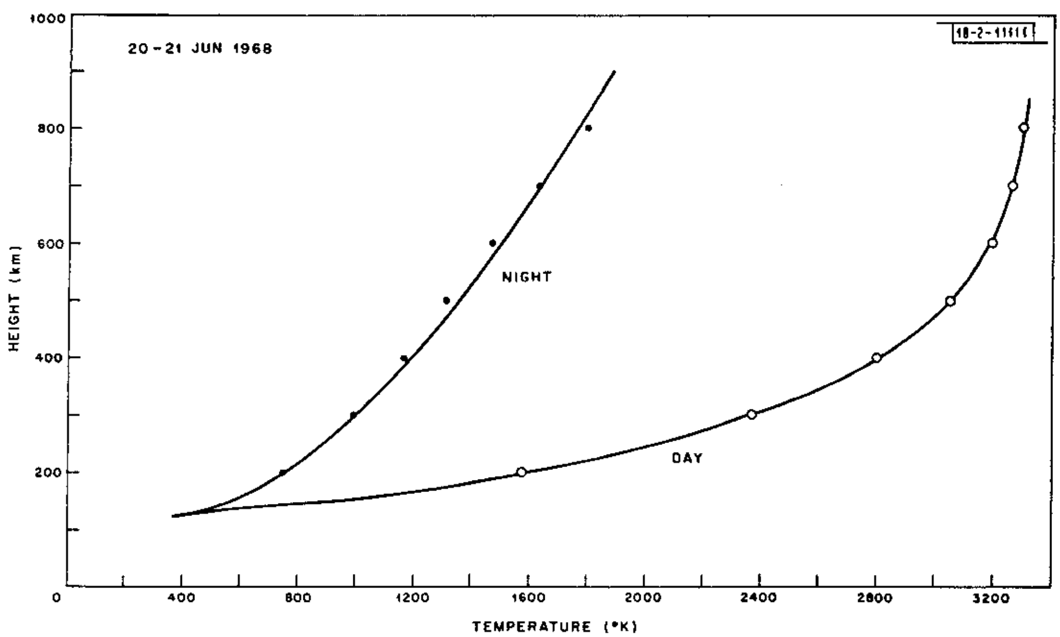

(i)

Fig. 7(a-i). Continued.

E. Seasonal Variations

The seasonal variations that may be inferred from these results have been discussed previously.[22] Thus, for example, the nighttime winter temperatures are high, as noted above, as a result of photoelectron heating of the magnetosphere by the conjugate ionosphere. This may be seen in Figs. 8 and 9, which represent different attempts to present seasonal trends. In

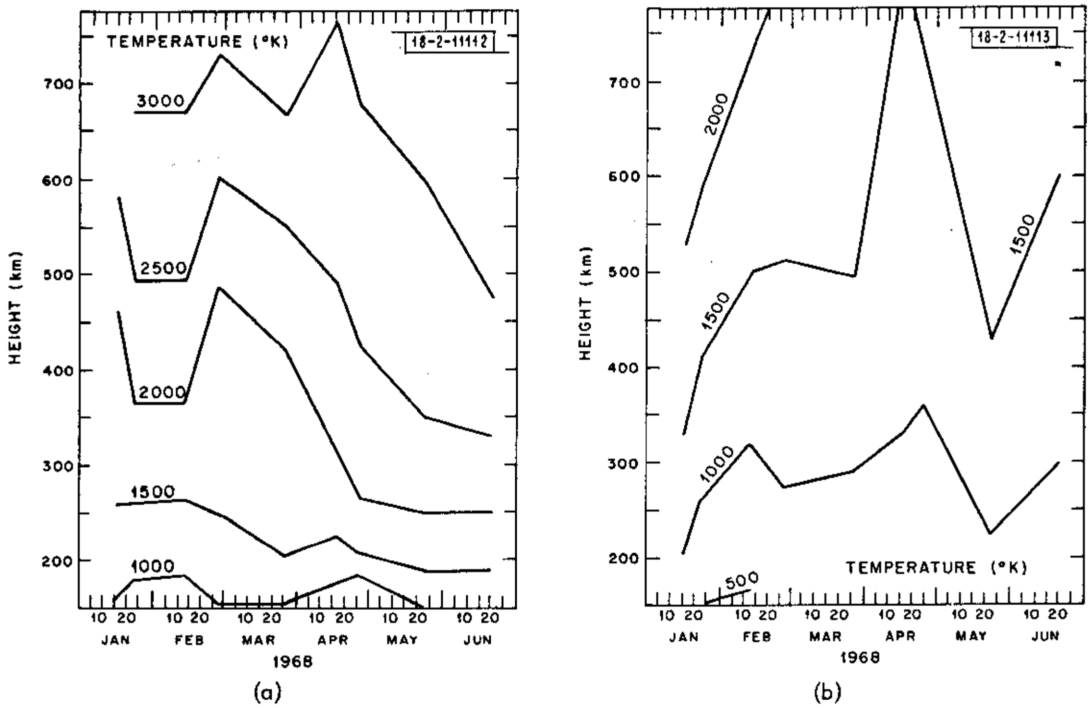

Fig. 8(a-b). Contour diagrams of average electron temperature (in 500°K steps) vs height and months for the first six months in 1968; (a) daytime (1000-1500 EST), (b) nighttime (2100-0300 EST).

Figs. 8(a) and 8(b), contours are drawn of electron temperature at 500°K intervals as a function of height and month for the daytime (1000-1500 EST) and nighttime (2100-0300 EST) averages (Fig. 7). In Figs. 9(a) and (b), the electron temperature at 300 and 500 km is plotted as a function of month.

Figures 8(a) and 9(a) show that the daytime temperatures are larger in summer than winter. This variation is much less pronounced near sunspot minimum[22] and, in large part, is introduced by the appearance of the temperature minimum near 350 km altitude chiefly in the winter months.

F. Magnetospheric Heat Fluxes

The positive temperature gradient in Fig. 7 at altitudes above 500 km implies the existence of a heat flux from the magnetosphere. The magnitude of the flux has been computed from the average temperature difference over the height intervals 500-600, 600-700 and 700-800 km via

$$G_p = 7.7 \times 10^5 \, T_e^{5/2} \, \frac{dT_e}{dh} \, \sin^2 I \, \mathrm{eV/cm^2/sec} \quad .$$

These independent estimates were then averaged and are plotted in Figs. 10(a) and (b).

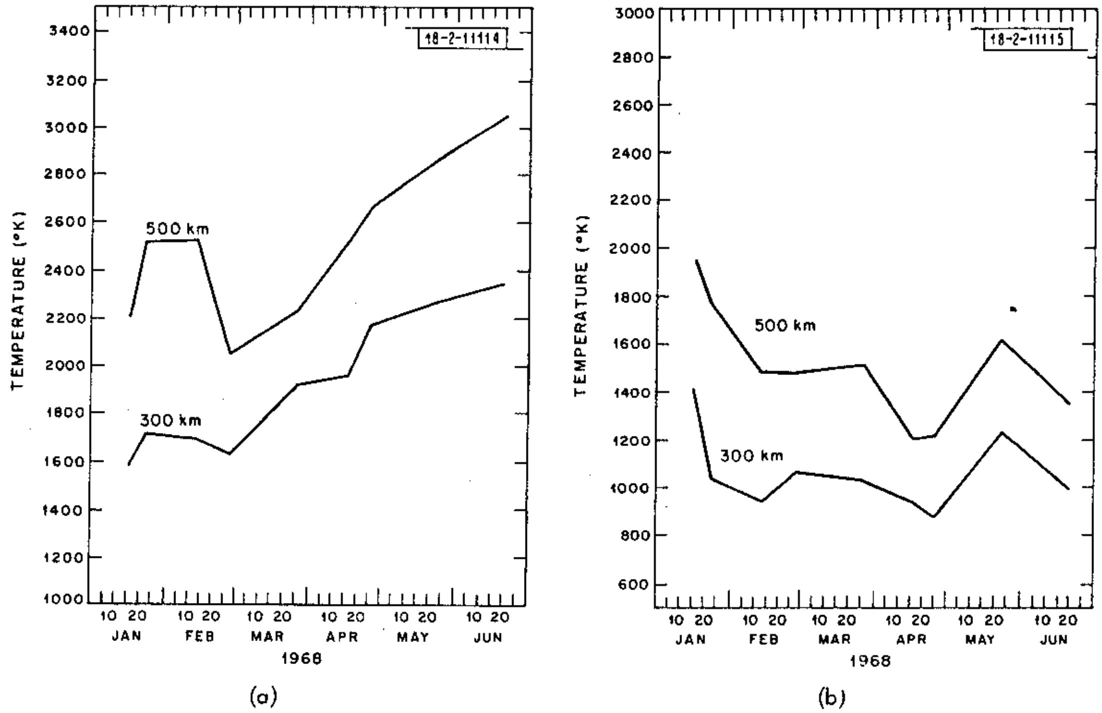

Fig. 9(a-b). Average electron temperature at 300 and 500 km altitude vs month for the first six months in 1968; (a) daytime (1000-1500 EST), (b) nighttime (2100-0300 EST).

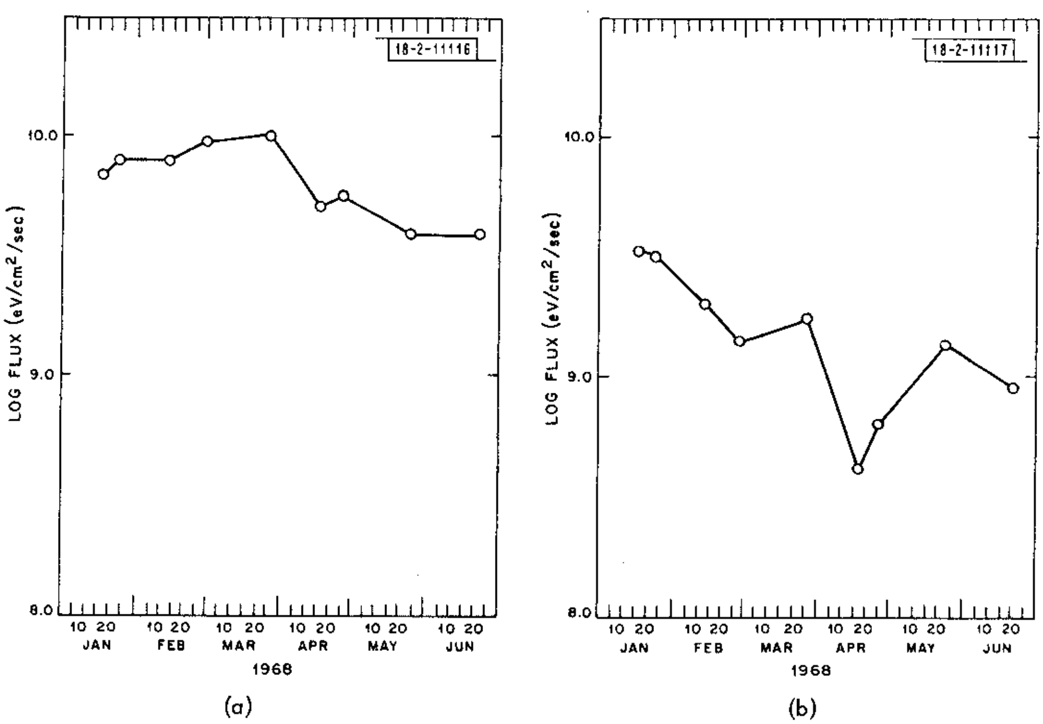

Fig. 10(a-b). Magnetospheric heat flux computed from the temperature curves in Fig. 7; (a) daytime (1000-1500 EST), (b) nighttime (2100-0300 EST).

At night the heat flux is considerably larger in winter than in summer [Fig. 10(b)] and this can be accounted for in terms of the conjugate heating of the magnetosphere, provided that the opacity of the field tube is quite high. This appears to be necessary in order to account for nighttime fluxes which are only a factor of 2 smaller than those observed during the day.

During the day, on the other hand, the flux tends to be larger in winter than summer [Fig. 10(a)], and this is contrary to expectation. This behavior has been observed in previous years as indicated in Table IV which summarizes the mean seasonal values of the daytime average heat fluxes

TABLE IV

AVERAGE DAYTIME (100-1500) PROTONOSPHERE HEAT FLUXES (10^9 eV/cm^2/sec)

Year	Summer (April-September)	Winter (January-March, October-December)
1964	3.66 ± 1.06	5.16 ± 1.28
1965	2.03 ± 0.57	3.23 ± 0.88
1966	3.74 ± 1.56	4.42 ± 1.11
1967	5.08 ± 1.42	7.74 ± 3.33
1968*	4.64 ± 0.74	8.81 ± 1.79

* First six months only.

observed each year since 1964 (Ref. 22). It is clear that the summer fluxes are lower than those observed in winter despite the fact that the temperature (and, therefore, the thermal conductivity) is higher. There is also a clear trend of increasing values as sunspot maximum is approached. This is illustrated in Fig. 11 where the fluxes given in Table IV are plotted against time together

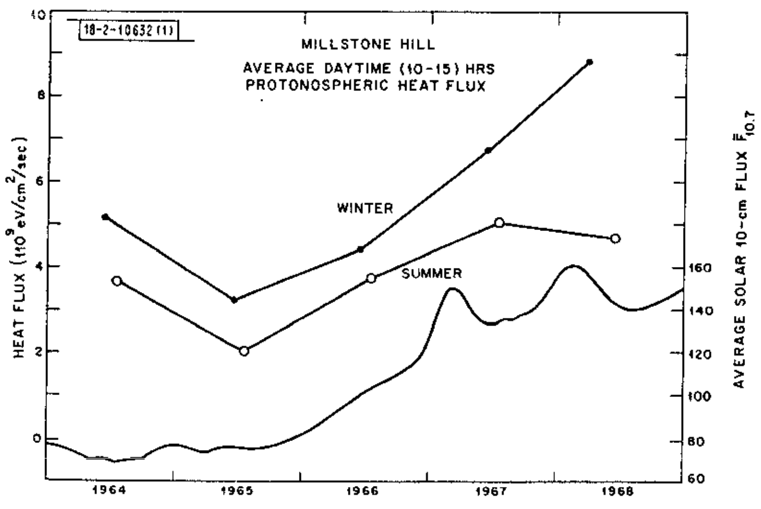

Fig. 11. Variation of the average winter (January-March, October-December) and summer (April-September) daytime average (1000-1500 EST) magnetospheric heat flux since 1964. Also shown in the solar radio flux at 10.7 cm wavelength averaged over three solar rotations, $\bar{F}_{10.7}$.

with the solar flux at 10.7 cm, averaged over three solar rotations, $\overline{F}_{10.7}$. It can be seen that the large winter values in 1967 and 1968 appear to be associated with peaks in the solar flux (Fig. 11).

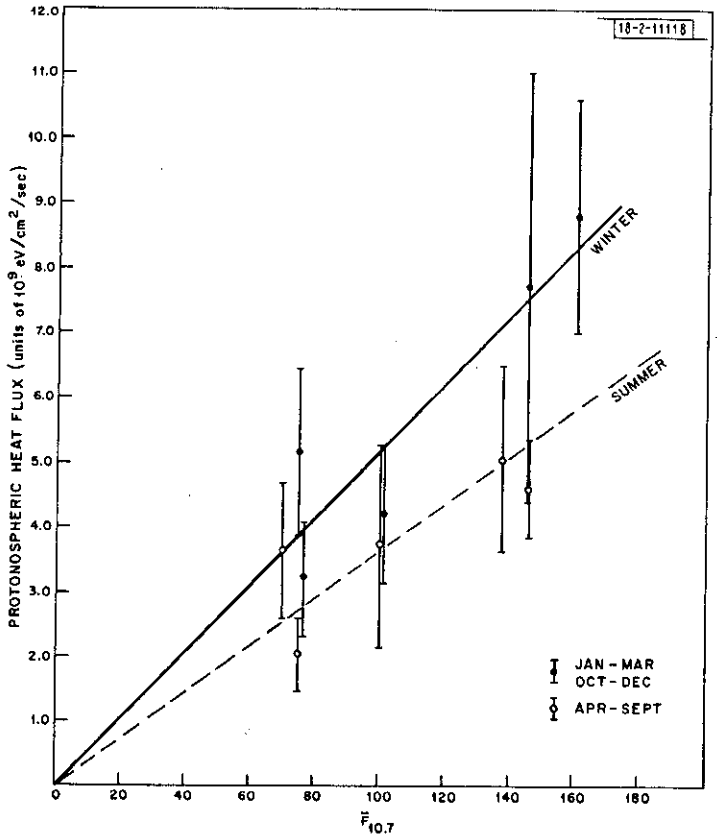

Fig. 12. Dependence of seasonal average heat fluxes (Fig. 11) on $\overline{F}_{10.7}$ for summer and winter.

As a quantitative test of the dependence of the average annual daytime heat flux on changes in solar radiation, we have plotted the values given in Table IV as functions of the mean solar flux $\overline{F}_{10.7}$ when averaged over the same 6 month periods (Fig. 12). Although the results are somewhat spread, it seems that both summer and winter days obey a simple linear dependence of the form

$$G_p = a\overline{F}_{10.7}$$

where

$$a_{summer} = 3.65 \times 10^7 \text{ eV/cm}^2\text{/sec/flux unit, and}$$

$$a_{winter} = 5.4 \times 10^7 \text{ eV/cm}^2\text{/sec/flux unit} \quad .$$

Reasons for the possible summer to winter difference have been considered. It appears that the annual variation in the F-region temperature is not capable of causing more heat to flow to the colder (winter) hemisphere to the extent necessary to explain these results.[22] Possibly the photoelectron production and/or escape is different in the two hemispheres as a consequence of changes in the composition of the neutral atmosphere and this can account for the difference.

IV. SUMMARY

Incoherent scatter synoptic studies of F-region electron densities, electron and ion temperatures were made at the Millstone Hill Field Station for periods of 24 hours approximately twice per month in 1968 (Table II). During the first six months, the data were gathered and reduced in a manner established in June 1965 that has been described previously.[3] Unfortunately, the method of measuring the spectra of the signals introduced distortion rendering the determination of the ion temperature uncertain, and these data have not been included in this report. Beginning in July 1968, a new data-processing system was put into operation that provided complete real-time processing of the signals and obviated the need for recording the received signals on magnetic tape for later processing. The implementation of this new system has been described elsewhere.[16] It was found that the new system was capable of detecting small frequency shifts in the spectra of the signals caused by drifts in the plasma.[16-18] However, we have not attempted to include drift velocity measurements in this report as a satisfactory method of presenting the data in a useful and compact fashion has not been found.

1968 was the peak of the current sunspot cycle. Despite this, a greater amount of magnetically disturbed conditions appears to have been encountered for the measurements made in 1967 (Ref. 5). We attribute this simply to the fact that most of the days chosen for observation in 1968 fell during magnetically quiet periods. The results gathered in 1968 confirm that the characteristic "summer" and "winter" behavior identified at near sunspot minimum[2,3] persists through sunspot maximum, albeit confined to magnetically quiet periods.

Several recognizable departures from the quiet day behavior have been identified.[4,5] These include both the positive and negative phases of magnetic storms. Elsewhere, we have proposed that there are two separate mechanisms that can give rise to increases of electron density during the positive phase.[19] Cases in which the increase is irregular and persists for a large part of the day appear to be caused by lifting of the F-layer brought about by thermospheric neutral winds blowing toward the equator in response to auroral heating of the atmosphere. The density and velocity observations for 29-30 October 1968 are consistent with this explanation.[19] Another cause of positive phase increases appears to be a redistribution of ionization in the dusk sector caused by the penetration of magnetospheric electric fields inside the plasmasphere.[15,19,20] These events appear to give rise to a single density increase occurring near 1700 LT coincident with an increase in the local total magnetic field and the start of a substorm.

Marked decreases in F-region electron density are found usually on the second day of the magnetic storm and at night when the mid-latitude trough moves southward to occupy a position over Millstone. Instances of this behavior were common in 1967, but were seen only once each in 1968. The mid-latitude trough appears to have been present overhead on 17 January and low daytime F-region densities were encountered on 27 March during a minor magnetic storm.

The electron temperature results have been employed to study the average heat flux from the magnetosphere into the ionosphere during the daytime. We find that the flux appears linearly related to the 10.7 cm solar flux averaged over 3 solar rotations, $\overline{F}_{10.7}$ with a dependence of $\sim 5.4 \times 10^7$ eV/cm^2/sec/flux unit in winter, and $\sim 3.65 \times 10^7$ eV/cm^2/sec/flux unit in summer. Satisfactory reasons for this difference have not been found.

ACKNOWLEDGMENTS

W. A. Reid, R. F. Julian and L. B. Hanson were largely responsible for the modifications to the radar equipment and associated software that resulted in the large improvement in the quality of the measurements achieved during 1968. The new data-analysis computer program was the work of R. F. Julian and J. K. Upham (Azrex Corporation). The author is indebted to these individuals and to L. A. Carpenter, R. J. Cicerone (both of the University of Illinois), A. Beauregard, J. H. McNally and others at the Millstone Hill Field Station for assistance in gathering these data. Thanks are also due to Mrs. L. Bill, and Mrs. A. Freeman and Miss F. Angier who assisted with the preparation of the figures.

REFERENCES

1. J. V. Evans, "Ionospheric Backscatter Observations at Millstone Hill," Technical Report 374, Lincoln Laboratory, M.I.T. (22 January 1965), DDC AD-616607.
2. __________, "Millstone Hill Thomson Scatter Results for 1964," Technical Report 430, Lincoln Laboratory, M.I.T. (15 November 1967), DDC AD-668436.
3. __________, "Millstone Hill Thomson Scatter Results for 1965," Technical Report 474, Lincoln Laboratory, M.I.T. (18 December 1969), DDC AD-707501.
4. __________, "Millstone Hill Thomson Scatter Results for 1966," Technical Report 481, Lincoln Laboratory, M.I.T. (15 December 1970), DDC AD-725742.
5. __________, "Millstone Hill Thomson Scatter Results for 1967," Technical Report 482, Lincoln Laboratory, M.I.T. (22 July 1971).
6. __________, Planet. Space Sci. 13, 1031 (1965), DDC AD-616607.
7. __________, J. Geophys. Res. 70, 1175 (1965), DDC AD-614310.
8. __________, Planet. Space Sci. 15, 1387 (1967).
9. __________, J. Geophys. Res. 75, 4083 and 4815 (1970), DDC AD-714447.
10. __________, J. Atmos. Terr. Phys. 32, 1629 (1970), DDC AD-716057.
11. __________, Planet. Space Sci. 18, 1225 (1970), DDC AD-716056.
12. __________, Planet. Space Sci., in press (1973).
13. __________, and L. P. Cox, J. Geophys. Res., 75, 159 (1970), DDC AD-703492.
14. L. P. Cox and J. V. Evans, J. Geophys. Res. 75, 6271 (1970), DDC AD-722911.
15. J. V. Evans, J. Geophys. Res. 77, 2341 (1972).
16. __________, R. F. Julian and W. A. Reid, "Incoherent Scatter Measurements of F-Region Density, Temperatures, and Vertical Velocity at Millstone Hill," Technical Report 447, Lincoln Laboratory, M.I.T. (6 February 1970), DDC AD-706863.
17. __________, R. A. Brockelman, R. F. Julian, W. A. Reid and L. A. Carpenter, Radio Science 5, 27 (1970).
18. L. A. Carpenter and S. A. Bowhill, "Investigation of the Physics of Dynamical Processes in the Topside F-Region," University of Illinois Aeronomy Report 44 (15 September 1971).
19. J. V. Evans, J. Atmos. Terr. Sci., 35, 593 (1973).
20. M. D. Papagiannis and M. Mendillo, Planet. Spac Sci. 19, 503 (1971).
21. J. M. Cornwall, F. V. Coroniti and R. M. Thorne, J. Geophys. Res. 76, 4428 (1971).
22. J. V. Evans, "Seasonal and Sunspot Cycle Variations of F-Region Electron Temperatures and Protonsopheric Heat Fluxes," J. Geophys. Res., 78, 2344 (1973).

DOCUMENT CONTROL DATA – R&D

(Security classification of title, body of abstract and indexing annotation must be entered when the overall report is classified)

1. ORIGINATING ACTIVITY *(Corporate author)* Lincoln Laboratory, M.I.T.	2a. REPORT SECURITY CLASSIFICATION Unclassified 2b. GROUP None
3. REPORT TITLE Millstone Hill Thomson Scatter Results for 1968	
4. DESCRIPTIVE NOTES *(Type of report and inclusive dates)* Technical Report	
5. AUTHOR(S) *(Last name, first name, initial)* Evans, John V.	
6. REPORT DATE 23 January 1973	7a. TOTAL NO. OF PAGES 7b. NO. OF REFS
8a. CONTRACT OR GRANT NO. F19628-73-C-0002 b. PROJECT NO. 7X263304D215 c. d.	9a. ORIGINATOR'S REPORT NUMBER(S) Technical Report 499 9b. OTHER REPORT NO(S) *(Any other numbers that may be assigned this report)* ESD-TR-73-55
10. AVAILABILITY/LIMITATION NOTICES Approved for public release; distribution unlimited.	
11. SUPPLEMENTARY NOTES None	12. SPONSORING MILITARY ACTIVITY Office of the Chief of Research and Development Department of the Army

13. ABSTRACT

This report summarizes the results for the electron density distribution, electron and ion temperatures in the F-region obtained during 1968 using the Millstone Hill (42.6°N, 71.5°W) Thomson (incoherent) scatter radar system. These data, for the height interval approximately 200 to 800 km, were gathered over 24-hour observing periods, roughly twice per calendar month. The time required to obtain a complete electron density and temperature profile over this height interval was usually 30 minutes.

During 1968 the apparatus employed to measure the frequency spectrum of the reflected signals vs altitude, which in turn yields the estimates of the electron and ion temperatures, was rebuilt permitting the measurements at all altitudes to be made in real time, and with greater accuracy than heretofore. In addition, the new spectrum analyzer permitted the first measurements at Millstone Hill of the vertical drift of the plasma. These results, which are difficult to condense into summary form, are not included in the report.

The density and temperature results show that the separate clear patterns of summer and winter diurnal behavior, recognized at sunspot minimum, can still be discerned at sunspot maximum on all but very disturbed days. A number of disturbance patterns observed previously were again detected in 1968, albeit on fewer occasions than in 1967. Apparently, by chance, the days selected for observation in 1968 contained fewer instances of magnetic disturbance than in 1967.

The average heat flux from the magnetosphere has been investigated. While there appears to be a clear dependence on solar flux (as defined by the 10.7-cm radio emission), there remains a summer-to-winter variation of 5 to 7 that cannot be easily explained.

14. KEY WORDS

Millstone radar	electron density	temperature effects
F-region	ionospheric scatter	spectrum analyzers
diurnal variations	seasonal variations	